CHO CELL MEDIA OPTIMIZATION AND ITS APPLICATION IN THE BIOPHARMACEUTICAL INDUSTRY

by

Wanyue Cui

A dissertation submitted in partial fulfillment of the requirements
for the Doctor of Philosophy Degree
State University of New York
College of Environmental Science and Forestry
Syracuse, New York
April 2023

Department of Chemical Engineering

Approved by:
Shijie Liu, Major Professor
Gregory McGee, Chair, Examining Committee
Bandaru V. Ramarao, Department Chair
Valerie A. Luzadis, Dean, The Graduate School

Acknowledgments

Five years passed by quickly. Looking back at my Ph.D. study, I find this is my most precious experience and knowledge full of self-encouragement, effort, confidence, research, and growth. I still clearly remember my mood when I solved and overcome every difficulty.

First, I would like to thank my funders, the SUNY-ESF Department of Chemical Engineering and Bristol-Myers Squibb Company. They provide excellent theoretical education and good practice in biopharmaceutical industry. I want to express my utmost gratitude and heartful thanks to my advisor -- Dr. Shijie Liu, who taught me what earning a doctoral degree truly means. He provided excellent supervision and help during my five years of Ph.D. study. My supervisor at BMS -- Dr. Jianlin (Jim) Xu, led me into the biopharmaceutical industry and taught me a lot in the past five years. I always feel lucky to meet knowledgeable and patient mentor like Dr. Liu and Dr. Xu. I also want to express sincerely thank my Bristol-Myers Squibb advisors, Dr. Jianlin Xu, Dr. Jianfa Ou, Dr. Shun Zheng, and Dr. Emily Rittershaus, the expert in the process development area, who coached me with the knowledge and skills. The mentorship and training I received from Dr. Liu, Dr. Xu and Dr. Ou, Dr. Zheng and Dr. Rittershaus are invaluable and lifelong benefits.

I thank my lab mates, Yutong Xiang, Yaoyao Wang, Jinglei Xie, Jianfei Wang, Jiaqi Huang, Julian Tucci, Guoyu Dong, and Wei Dai. Thanks to my ESF colleagues, Mr. David Kiemle, Yuxuan Wang, Anindita Paul, Linjing Jia, Anqi Ji and Fnu Kalyani Ananthakrishnan. Thanks to my BMS colleagues, Dr. Yawen Tang, Dr. Erik Vandermark, Dr. Yuxiang Zhao, Phong Luu, Bryanne Zonghi, Alexander Williams, and Christopher Oliveira, for their support on the experiments.

I would also like to offer my profound thanks to my committee and chair: Dr. Shijie Liu, Dr. Jinalin Xu, Dr. Deepak Kumar, Dr. Chang Geun Yoo, Dr. Bandaru Ramarao and Dr. Gregory McGee, who spent their precious time and effort in reading this work and provide helpful

comments.

Finally, I want to acknowledge my parents' consistent support and inspiration. They are the best parents I could ever dream of, and I would dedicate all my love and achievements to them.

Table of Content

List of Figures

List of Tables

Abbreviations

CHO: Chinese hamster ovary

DoE: Design of Experiment

SBD: Superlative box design

RSM: Response surface methodology

CTLA-4: Cytotoxic T-lymphocyte-associated antigen-4

DMEM: Dulbecco's modification of Eagle's medium

FBS: Fetal bovine serum

NMR: Nuclear Magnetic Resonance

ELISA: Enzyme-linked immunosorbent assay

ANOVA: Analysis of variance

AA: Amino acid

LC–MS/MS: Liquid chromatography-mass spectrometry

EEM: Excitation-emission matrix

NMR: Nuclear magnetic resonance

NIR: Near-infrared fluorescence spectroscopy

PCA: Principal Component Analysis

PLS: Partial Least Squares

PARAFAC: Multi-way parallel factor analysis

N-PLS: N-way partial least squares

PARAFAC: Parallel factor analysis

GLU: Glutamic acid

ASP: Aspartic acid

HIS: Histidine

LYS: Lysine

MET: Methionine

TYR: Tyrosine

SER: Serine

ARG: Arginine

LEU: Leucine

PHE: Phenylalanine

PRO: Proline

THR: Threonine

VAL: Valine

ASN: Asparagine

ILE: Isoleucine

TRP: Tryptophan

PCC: Pearson correlation coefficient

RT: Room temperature

PBS: Phosphate-buffered saline

Abstract

W. Cui. CHO Cell Media Optimization and its Application in the Biopharmaceutical Industry, 139 pages, 17 tables, 46 figures, 2023. ACS style dissertation used.

In modern industrial applications, media cost pressure, market demands, and the development of process analytical technology challenge the media development for Chinese Hamster Ovary cell culture manufacturing. However, the solubility of powder media and cold room stability of liquid media is still challenging for preparing highly concentrated media. Cell culture media development aims to use process analytical technology tools to evaluate the media quality and deeply understand the media change under different preparation conditions and storage duration. This dissertation consists of six chapters. First, a brief introduction about this dissertation. Second, the impact of preparation pH and temperature on amino acid stability of highly concentrated cell culture feed media was presented. Then, the characterization of cell culture media under different treatment conditions by EEM, Raman, and FTIR in PCA and PARAFAC was investigated, and the cell culture performance was subsequently investigated. The sixth chapter showed the optimization of adaptation parameters from adhesion cell culture in serum-containing media to suspension in chemically defined media by superlative box design was shown. And finally, a summary and outlook were made based on the above six chapters.

Key Words: Chinese Hamster Ovary cell, media optimization, cell culture, Process Analytical Technology, principal component analysis

W. Cui
Candidate for the degree of Doctor of Philosophy, April 2023
Shijie Liu, Ph.D.
Department of Chemical Engineering
State University of New York, College of Environmental Science and Forestry,
Syracuse, New York

Chapter 1: Introduction

An increasing number of evidence suggest that cell culture performance and quality could be affected by medium preparation conditions. Chapter 2 examined if adjusting the preparation pH or temperature could resolve the issues with media precipitation. Also examined if an elevated preparation pH could maintain solubility when basal powder and AA concentrations were further increased. Chapter 2 describes the medium preparation parameters to improve AA stability and mitigate precipitation issues. The result suggests that increasing pH and preparation temperature could prevent feed media precipitation during storage.

The stability of amino acids (AAs) in a highly concentrated cell culture medium is affected by medium preparation and storage conditions. Variability in the concentration of medium components including AAs can influence cell culture performance and product quality attributes. In this report, we evaluated the impact of preparation pH, preparation temperature, and storage temperature on the stability of 16 AAs in a highly concentrated cell culture feed medium. Optimizing the medium pH enabled an increase in the initial feed medium concentration by 30% plus 3.9 g/L tyrosine with no observed precipitation after 28 days. Up to 6.0 g/L tyrosine can be supplemented in the medium at ~pH 10 without precipitation. Moreover, preparing the medium at 40-50°C prevented precipitation during storage at 4-8°C. A slight negative impact on AA stability during this high-temperature preparation was observed, but this impact was negligible relative to the AA degradation observed during extended storage of media prepared at 37°C. The optimal preparation pH and temperature allowed the concentrated medium to be stored at 4-8°C with minimal AA degradation and without precipitation. These discoveries were further supported by principal component analysis of AA profile similarity before and after storage at different pH and temperature conditions. This study describes the medium preparation parameters to improve AA

stability and mitigate precipitation issues. The optimization strategy will facilitate the development of robust cell culture production processes.

Before cell culture media are used, judging whether their quality is fit is essential for cell growth and protein production. In chapter 3, Raman spectroscopy was used to compare and ascertain the quality of the cell culture medium under different treatment conditions and different storage conditions. Different initial pH treatment, different initial temperature treatment, dark/light storage conditions, different temperature storage conditions are selected as the influencing factors. Storage temperature was found to have the most notable effect on the cell culture medium. The amino acid concentration results confirmed the accuracy of Raman spectroscopy. Therefore, Raman-based method combined with principal component analysis can be used to monitor the quality of the cell culture media, to speculate and judge the treatment conditions and storage conditions in order to minimize the differences between batches and ensure uniform product quality. This simple and inexpensive way of monitoring and judging samples is worthy of implementation.

In chapter 4, excitation-emission matrix spectroscopy was used to monitor fluorescent molecules' characteristics in cell culture medium. We used principal component analysis (PCA) and parallel factor analysis (PARAFAC) models to analyze cell culture medium under different storage conditions. The comparison of fluorescence spectra showed subtle differences, and the peak ratio revealed the influence of pH and the similarity of the same culture medium. A positive relationship between the two is obtained by studying the medium's intensity at a specific excitation-emission position with the temperature increases.

Simultaneously, the PCA model and PARAFAC model were used to explore the correlation between fluorescent molecules and storage conditions and determine the relative optimal storage

conditions for cell culture medium. Also, chapter 4 compared the properties of fluorescent molecules under different storage conditions and evaluated the effect of storage conditions on cell culture medium.

Chapter 5 compared Raman, EEM and FTIR by PCA to evaluate the cell culture media quality. After that, the Raman and FTIR data were used to build two screen models for media quality evaluation. Cell culture performance results also validated the use of PAT tools.

A new design of experiments – superlative box design (SBD), was adopted to optimize the adaptation of Chinese hamster ovary cells from adhesion culture to serum-free suspension culture in chapter 6. It is a general trend to use a serum-free medium instead of a serum-containing medium. The advantage of serum-free medium (chemically defended) is that it does not contain unknown components and avoids safety issues. SBD requires fewer experiments while ensuring a sufficient number of experiments and uniformity in the distribution of experiments amongst all the factors. Six factors were considered in this experimental design with 43 runs plus three more repeating center runs. The cell line was adapted to serum-free media by gradually reducing serum, and from adherent to suspension by rotating at various speeds in a shake flask. Response surface methodology was applied to find the optimum condition. The optimized cell density reached 7.02×10^5 cells/mL, calculated by the quadratic model.

Experiments validated the predicted cell adaptation with the maximum cell density. Three suspension runs were selected randomly to perform in the bioreactor to validate cell stability and production homogeneity. This study provides an efficient method to transfer adherent cells to suspension cells and is the first to successfully use SBD and establish a parameter quadratic optimization model.

Chapter 2: Impact of preparation pH and temperature on amino acid stability of highly concentrated cell culture feed media

Short title: Impact of cell culture medium preparation on amino acid stability

This chapter was adapted from the author's publication in J Chem Technol Biotechnol (J Chem Technol Biotechnol 2022; 97: 2078-2086) with modifications.

2.1 Introduction

Process intensification is pursued to improve process yield and alleviate resource constraints during the production of monoclonal antibodies.[1] Concentrating media represents one process intensification method capable of improving titer and product quality.[2, 3] During medium optimization, the concentration of nutrients such as vitamins, cofactors, metabolic substrates, amino acids, inorganic ions, and trace elements are adjusted to support cell growth and protein synthesis.[4] For instance, McCoy developed a 5-fold concentrated medium system with various supplements that was stabilized by the addition of pyruvate and sodium carbonate.[2] In another example, Chinese hamster ovary (CHO) cell perfusion media were developed from a fed-batch platform by increasing the concentration of basal powder, rebalancing amino acids, and eliminating unnecessary components.[5] Mixing different commercial feed supplements to improve cell culture performance represents another optimization strategy.[6]

Although increasing medium concentration can improve cell culture performance, these formulations can also result in medium instability, such as precipitation, discoloration, and nutrient degradation. Medium color changes can result from variations to the pH and levels of media components, such as bicarbonate, pyruvate, and AAs.[2] Oxidation is a leading cause of degradation, which can be alleviated by optimizing preparation and storage temperatures.[7] Additionally, pH is

another factor that can impact media stability and cell culture performance.[8] Amino acid stability represents another crucial aspect of media composition.[9, 10] Through deamination, amino acids and proteins slowly release ammonium ions.[11] For example, L-glutamine decomposes to form cyclic pyrrolidonecarboxylic acid and ammonia.[12, 13] After weeks of storage, these changes could accrue and negatively affect cell culture performance.[14] A long shelf life could significantly improve the flexibility of the manufacturing schedule. Still, there are limited publications on how nutrient levels change during storage, and more importantly, how preparation conditions impact long-term medium stability.[15]

Here, we investigated the impact of highly concentrated cell culture media final preparation pH, preparation temperature, and storage temperature conditions on media quality by examining AA profiles. A panel of 16 amino acids including glutamic acid (GLU), aspartic acid (ASP), histidine (HIS), lysine (LYS), methionine (MET), tyrosine (TYR), serine (SER), arginine (ARG), leucine (LEU), phenylalanine (PHE), proline (PRO), threonine (THR), valine (VAL), asparagine (ASN), isoleucine (ILE), and tryptophan (TRP) was tested by ultra-performance liquid chromatography to provide an insight into complex feed medium quality. This panel includes all essential AAs and some important nonessential AAs. Tested conditions for the final preparation pH range from 7.0 to 10.0 over 28 days of storage. The AA stability is characterized by the relative amount in solution. The change of concentration was caused by physical precipitation or degradation. AA concentration could also be reduced by nonenzymatic reaction with other components such as glucose. This reaction is grouped as degradation here to simplify the discussion. Precipitation from the medium was observed under some conditions – in these instances, AA profiles of the precipitates were also examined. Media were treated at temperatures between 40 to 50°C to examine the impact of temperature during medium preparation. Two

statistical methods, principal component analysis (PCA) and Pearson correlation coefficient (PCC), were applied to determine media preparation conditions that best preserved AA stability and to identify AAs sensitive to these preparation conditions.[16] This study could provide insight on developing highly concentrated media for process intensification, extending media shelf life based on stability profile, and ultimately achieving a more robust cell culture production process.

2.2 Materials and Methods

2.2.1 Materials

BMS's in-house feed medium was used in this study. The highly concentrated proprietary medium was designed to provide complex nutrients for mammalian cell culture processes. All other reagents and consumables were provided by Fisher Scientific (Pittsburgh, PA) unless otherwise specified.

2.2.2 Medium preparation

A general medium preparation process begins with preheating the water to 30-40°C and maintaining that temperature until the major components are dissolved. Basal powders, glucose, AAs, and other components are added in a defined order. Intermediate pH is then adjusted to facilitate powder dissolution. Finally, the preparation pH of the medium is adjusted again before filtration. Only the final preparation pH was evaluated in this study. Therefore, final pH and preparation pH are used interchangeably.

To examine the impact of the preparation pH on media stability, the medium was prepared at a 5 L scale in glass containers as pooled material, adjusted to pH 7.8 as a control, then split into aliquots prior to the final filtration step. The pH of the aliquots (final preparation pH) was adjusted

to 7.0, 7.4, 7.8, 9.0, and 10.0 immediately with 10N NaOH or 5N HCl solution. Medium samples were then filtered and aliquoted to 125 mL sterile plastic containers and stored at either room temperature (RT) or at 4-8°C.

In the preparation temperature study, pooled material was prepared at 37°C at a 5L scale in a glass container. The filtered medium was aliquoted into sterile 500 mL plastic containers and further treated at 37°C (control), 40°C, 45°C, or 50°C in an incubator for 3 hours, respectively, to mimic the actual preparation duration. Treated samples were sterilely aliquoted to 125 mL plastic containers and stored at different temperatures (RT and 4-8°C) and for different durations (14 and 28 days). Precipitation was apparent in the control sample stored at 4-8°C as early as 20 days, while all other samples remained homogeneous over the whole study.

To further improve medium concentration, feed medium was prepared with 30% more basal powder and supplemented with either 0, 2.4 g/L, 3.9 g/L, or 6 g/L tyrosine from a 100 mg/mL stock solution. Final pH was adjusted by the addition of 0, 2 mL/L, and 20 mL/L extra 10N NaOH solution. Samples were filtered, stored at RT, and inspected daily for homogeneity.

2.2.3 Sample storage

Media were aliquoted and covered with foil to protect them from light. Samples were collected on days 0, 14, and 28 and stored at -80°C. Samples were thawed at 36.5°C, mixed, and subjected to AA analysis.

2.2.4 Precipitation collection and treatment

The precipitate was separated and collected through gravity settlement, then resuspended in Phosphate-buffered saline (PBS). 10N NaOH solution was added slowly with constant mixing

until the precipitate fully dissolved. The final volume of the resuspended material corresponded to 50% of the original medium volume for AA analysis.

2.2.5 Instrumentation and data collection

AA analysis was performed on an AccQ•Tag Ultra RP column (130Å 1.7 µm, 2.1 mm 100 mm) using a Waters Acquity ultra-performance liquid chromatography (UPLC, Shimadzu Scientific Instruments, Columbia, MD) system equipped with a TUV and a PDA detector. Data were collected and processed with empower chromatography software. Samples were derivatized with AccQ•Tag Ultra reagent following the manufacturer's procedure and diluted as needed before injection. A gradient elution program was developed internally with a 10.2min period at 43°C and 0.7 mL/min flow rate. Four mobile phases were used: (A) AccQ•Tag Ultra eluent A, (B) 10:90 AccQ•Tag eluent B - MilliQ water, (C) water, and (D) AccQ•Tag eluent B.

2.2.6 Data analysis

Data normalization was done in Microsoft Excel. PCA and PCC were performed using SAS 9.4 (SAS Institute Inc. Cary, NC, USA) with a 95% confidence level for significance.

2.3 Results

2.3.1 Amino acid stability during storage at different temperatures

The effect of storage temperature on the stability of AAs in feed medium was evaluated over 28 days. Under control conditions, the medium was prepared at a final pH of 7.8 and a temperature of 37°C. As shown in **Fig. 2.1(A)**, AA degradation was reduced when the medium was stored at 4-8°C relative to the RT treatment. At RT, almost half of the AAs degraded by more than 20% after 14 days. The normalized concentrations of ASP and LYS were lower than 0.7, while

those of eight AAs were between 0.7 and 0.8, and six AAs were higher than 0.8. Conversely, all AAs remained at a relatively high concentration at 4-8°C. As storage extended to 28 days [**Fig. 2.1(B)**], severe precipitation was observed in samples stored at 4-8°C, reducing most AAs to <40% of their initial levels. Precipitation was not observed during storage at RT, although AAs levels continued to decrease from day 14 to day 28. To reduce AA degradation and prevent precipitation during extended storage, we optimized the feed medium final preparation pH and preparation temperature as described in the following sections.

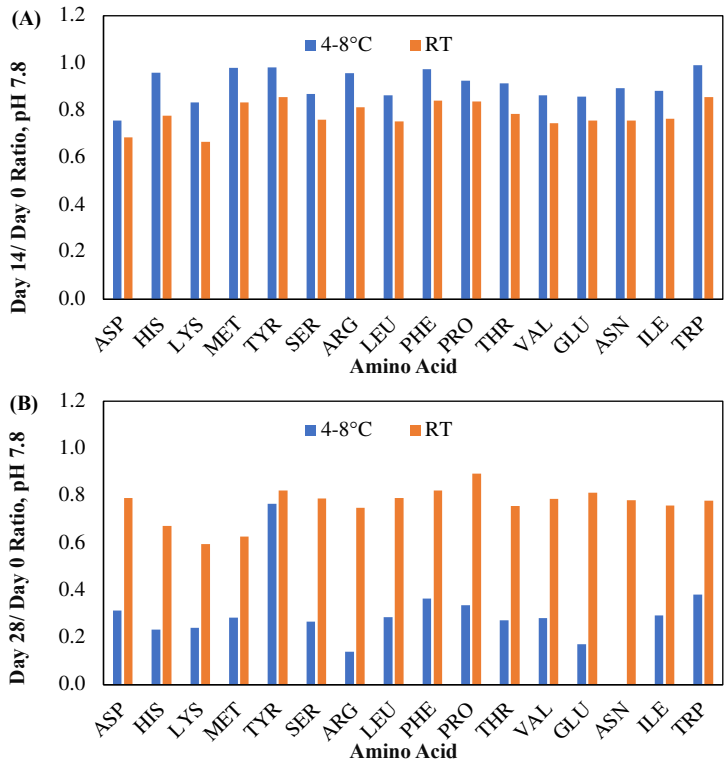

Figure 2.1. Effect of storage temperature on AA stability in feed medium at pH 7.8. (A) The ratio of AA concentrations on day 14 vs day 0. (B) The ratio of AA concentrations on day 28 vs day 0. Blue bar: 4-8°C storage; Orange bar: RT storage.

2.3.2 Optimization of final preparation pH to improve medium stability

The effect of varying pH values (7.0, 7.4, 9.0, and 10.0) relative to the control pH of 7.8 on AA stability was examined (**Fig. 2.2**). When media were stored at 4-8°C, samples prepared at pH 7.0 and 10.0 exhibited the greatest changes to AA stability through two different mechanisms. (1) Increased precipitation was observed for samples prepared at a pH of 7.0 relative to the control condition, alongside a 5%-18% reduction for most AAs, except for ASP, which remained similar to the control. In contrast, the sample prepared at pH 7.4 had slightly higher AAs than that of the control due to less precipitation. (2) No precipitation was observed for the sample prepared at pH 10.0, but increased AA degradation was apparent, with a maximum of 9% extra degradation compared to the control. The sample prepared at pH 9.0 also showed no precipitation and a similar AA profile to that of the control.

Storage	pH	ASP	HIS	LYS	MET	TYR	SER	ARG	LEU	PHE	PRO	THR	VAL	GLU	ASN	ILE	TRP
4-8°C	7.0	0.99	0.86	0.93	0.90	0.86	0.93	0.82	0.95	0.88	0.89	0.90	0.93	0.94	0.91	0.89	0.89
	7.4	1.11	1.01	1.14	1.05	1.03	1.05	1.04	1.06	1.03	1.06	1.06	1.06	1.10	1.07	1.05	1.03
	9.0	1.11	0.98	1.03	0.99	1.02	1.08	1.02	1.08	1.02	1.05	1.04	1.07	1.05	1.05	1.08	1.02
	10.0	0.95	0.91	0.98	0.93	0.91	0.94	0.93	0.93	0.92	0.96	0.96	0.93	1.01	0.97	0.93	0.92
RT	7.0	1.16	1.14	1.16	1.11	1.10	1.09	1.01	1.11	1.10	1.08	1.10	1.10	1.12	1.14	1.11	1.10
	7.4	1.23	1.12	1.24	1.13	1.13	1.19	1.13	1.20	1.13	1.14	1.14	1.20	1.17	1.17	1.21	1.13
	9.0	1.15	1.05	0.92	1.05	1.05	1.11	1.03	1.09	1.06	1.11	1.07	1.07	1.07	1.12	1.04	1.04
	10.0	1.16	0.78	0.83	1.05	1.00	1.11	0.94	1.04	1.03	1.09	1.09	1.04	1.14	1.13	0.99	0.98

Figure 2.2. Change of AAs after 14 days under different final preparation pH and storage temperatures. AA concentrations are normalized by pH 7.8 under the same storage condition. The relative increase and decrease are coded by gradient blue and red color, respectively. P: precipitation was observed in samples stored at 4-8°C with pH 7.0, 7.4, and 7.8. All other conditions remained free of precipitation after 14 days.

Samples stored at room temperature exhibited no signs of precipitation, but AA degradation was readily apparent. Samples prepared at pH 7.0 and pH 7.4 exhibited slower degradation than the control. For example, the levels of ASP and LYS were 16%-23% and 16%-24% higher, respectively. Samples prepared at pH 9.0 and stored at RT showed a similar AA profile to the control and to those stored at 4-8°C. Samples prepared at pH 10.0 showed more HIS and LYS degradation (22% and 17%) than the control. Therefore, pH 9.0 is the optimal final preparation pH for the evaluated feed media to prevent precipitation without significant degradation.

Fig. 2.3 illustrates our attempts to further optimize the medium concentration using different final preparation pH values while avoiding precipitation. A 1.3x feed medium was prepared with 30% more component powder at each preparation step. Different masses of tyrosine were also supplemented into the medium. With 0 to 2.4g/L supplemental tyrosine, both 1x and 1.3x feed medium samples remained homogeneous for up to 20 days. The addition of 3.9g/L tyrosine caused precipitation soon after medium preparation. This precipitation was slightly delayed by increasing the preparation pH to 8.5 and held for 20 days with a preparation pH of 9.8. Similarly, 1x feed medium prepared at pH 9.8 remained homogeneous over the experimental period with 6.0g/L tyrosine.

NaOH ml/L	Tyrosine g/L	Feed 1x			Feed 1.3x		
		Day 1	Day 7	Day20	Day 1	Day 7	Day20
0 (pH7.8)	0						
	2.4						
	3.9						
	6.0						
2 (pH8.5)	0						
	2.4						
	3.9						
	6.0						
20 (pH9.8)	0						
	2.4						
	3.9						
	6.0						

Figure 2.3. Stability of concentrated feed medium with various tyrosine addition. The final pH was adjusted by adding 0, 2, and 20mL/L NaOH solution (10M). Tyrosine was added to targeted concentration using 100mg/mL stock solution, followed by final quantity sufficient (Q.S.). Samples were store at RT. The red grid indicates timing of precipitation first observed.

Appearance provides additional information on media stability (**Fig. 2.4**). For example, color change in a highly concentrated feed medium can be caused by iron-mediated tryptophan oxidation.[17] After 28 days of storage at RT, media prepared at a pH of 7.8, 9.0, and 10.0 exhibited a light amber, dark amber, and reddish-brown color, respectively [**Fig. 2.4(A), (B), and (C)**]. Precipitation was observed for medium prepared at a pH of 7.8 and stored at 4-8°C, while samples prepared at pH 9.0 or 10.0 remained homogenous when stored at the same temperature [**Fig. 2.4(D) and (E)**]. All samples stored at 4-8°C showed a golden yellow appearance regardless of their final preparation pH.

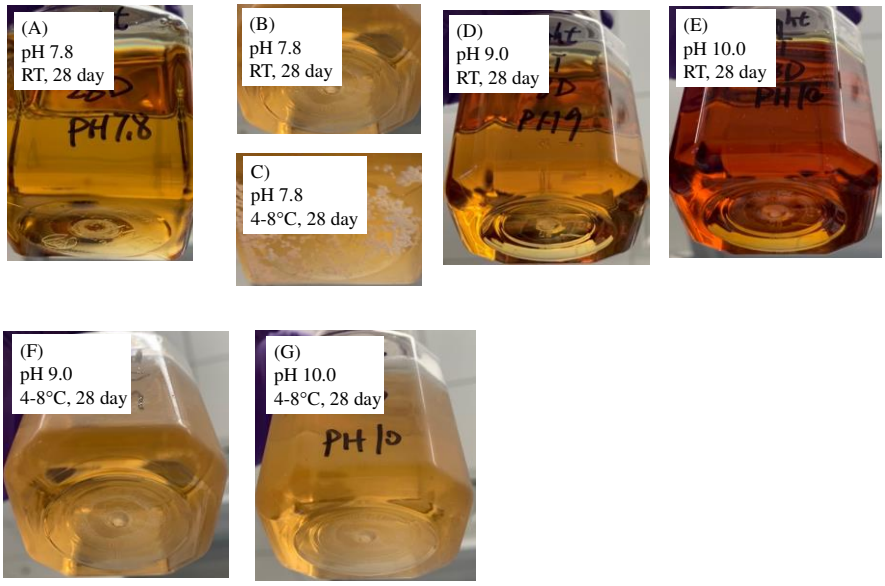

Figure 2.4. Feed medium appearance after 28 days at different final preparation pH and storage temperatures. No precipitation was observed at RT storage for all pH conditions (A, B, D, E). pH 9.0 and pH 10.0 prevented precipitation formation over 28 days at 4-8°C (C vs. F and G). 4-8°C storage condition significantly reduced the color formation at pH 9.0 and pH 10.0 (D and E vs. F and G).

In summary, we present a preparation pH optimization strategy to improve medium stability. The concentration of basal powder and AAs could be increased from the control condition by escalating preparation pH (**Fig. 2.3**), while storage at 4-8°C slows down AA degradation caused by high pH.

2.3.3 Characterization of feed media precipitate

Fig. 2.5 demonstrates the composition changes to the precipitates formed at different preparation pH and storage times. When stored at 4-8°C, AA precipitation was observed between days 7 and 14 by visual examination. Precipitation increased at more acidic pH values when

quantified on day 14 [**Fig. 2.5(A)**]. PHE was the most enriched AA in the precipitate, while HIS, TYR, and ARG were the least abundant. More AA precipitation was observed between 14 and 28 days, with similar profiles for samples prepared among pH 7.0, pH 7.4, and pH 7.8 [**Fig. 2.5(B)**]. All tested AAs were present in the precipitate, accounting for 12%-41% of the respective initial concentrations. HIS, PHE, and TRP were the most enriched components of the precipitate. This precipitation process is visualized in **Fig. 2.5(C)**. White particles were observed at the bottom of the bottle for all the samples prepared at the three pH levels in 14 days storage at 4-8°C. Visual inspection suggested that precipitation further accelerated between days 14 and 28.

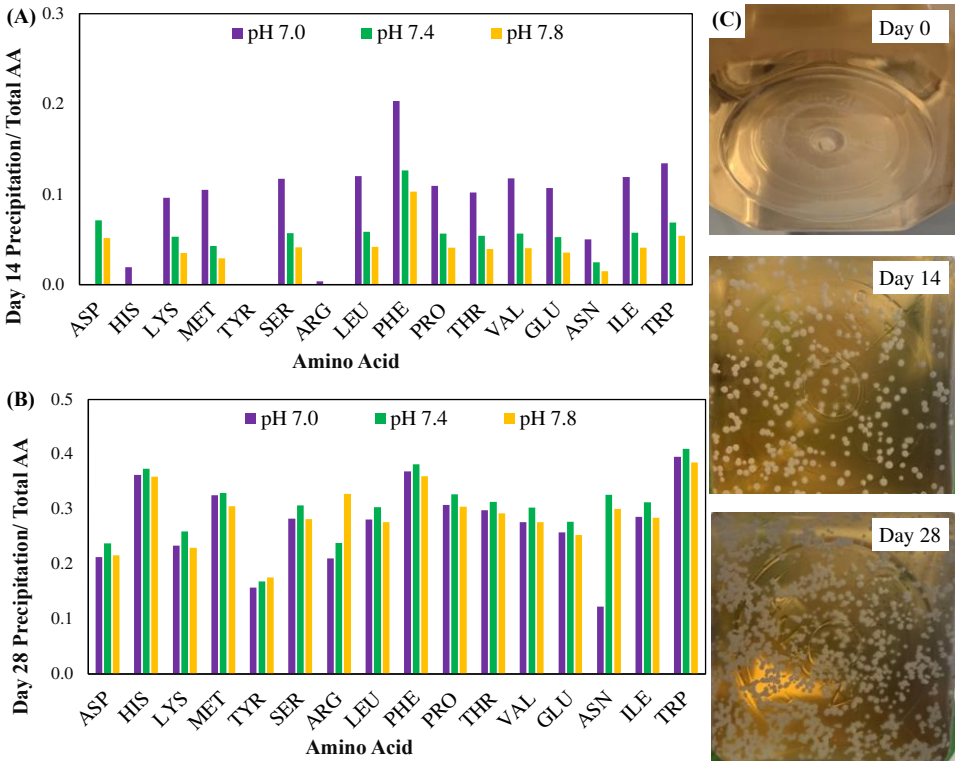

Figure 2.5. Precipitation composition analysis and formation process. Feed medium was stored at 4-8°C for (A) 14 days and (B) 28 days. Precipitation was collected through gravity settlement and redissolved to 50% of the original volume before measurement. All AA values are normalized by the respective concentrations in the feed medium on day 0 (defined as total concentration). Purple bar: pH 7.0, green bar: pH 7.4, yellow bar: pH 7.8. Through visualization, the precipitation process

was accelerated between days 14 and 28 (C).

2.3.4 Optimizing preparation temperature to mitigate feed precipitation

After 14 days of storage at RT, AAs remained between 71% to 95% of the day 0 concentrations at all tested conditions, as shown in **Fig. 2.6(A)**. Unsurprisingly, the normalized AA concentration negatively correlated with increasing treatment temperatures. After 28 days of storage at RT, AAs decreased to 50% to 89% of the initial concentrations, as shown in **Fig. 2.6(B)**. Consistent with **Fig. 2.1**, LYS had the most degradation. Different treatment temperatures did not reduce AA degradation during storage.

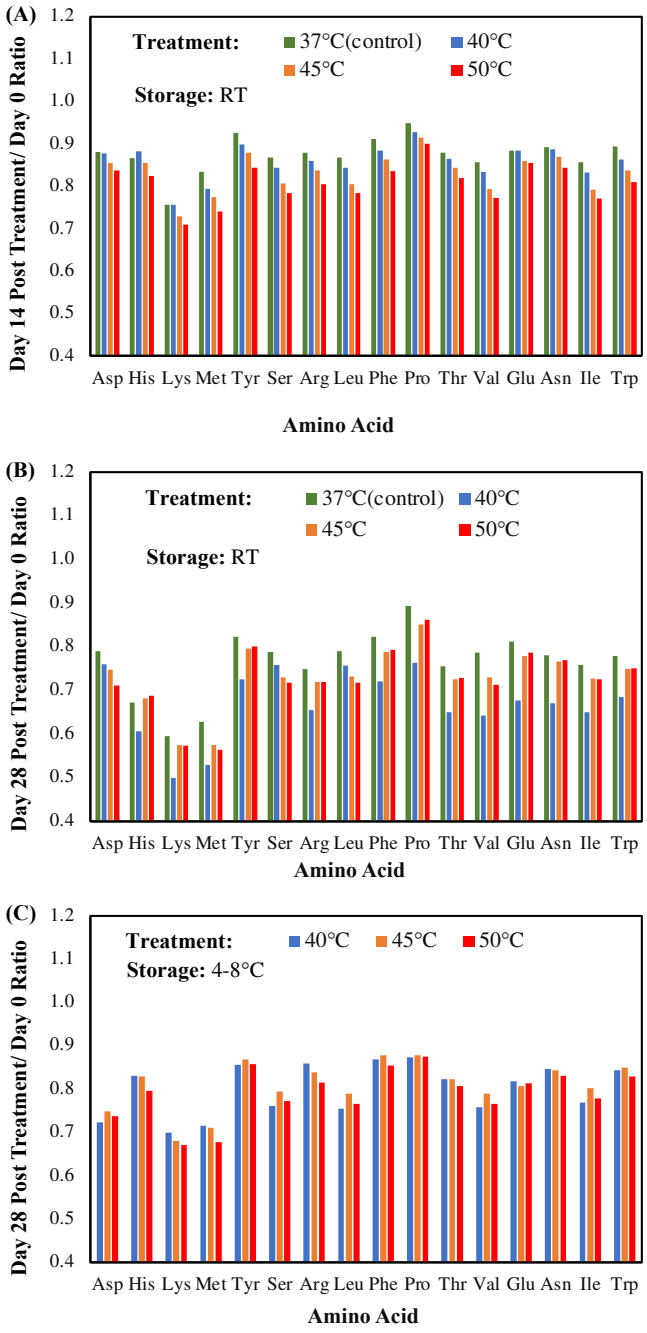

Figure 2.6. Impact of different treatment temperatures on AA profile. Post-filtration medium samples (pH 7.8) were aliquoted and treated at 37°C (control), 40°C, 45°C, and 50°C for 3h, then stored at room temperature for (A) 14 days and (B) 28 days, and (C) at 4-8°C for 28 days. Samples were subjected to AA analysis. Post-treatment AA change on day 0 was smaller than assay variance (±5%). AA values of day 14 and day 28 data are normalized by day 0 value.

However, elevated treatment temperatures mitigated the precipitation observed by visual examination when media was stored at 4-8°C. Storage at 4-8°C was implemented to slow down AA degradation. After 28 days of storage at 4-8°C, AA remained 67% to 88% of initial concentrations [**Fig. 2.6(C)**]. Like **Fig. 2.6(B)**, the treatment at 40°C, 45°C, and 50°C had no significant impact on AA concentration, compared to the 37°C control condition. By visual examination (**Fig. 2.7**), media samples treated at 40-50°C showed similar coloration as the control condition. These data indicate that elevated preparation temperatures had a negligible impact on AA stability and appearance of the tested medium.

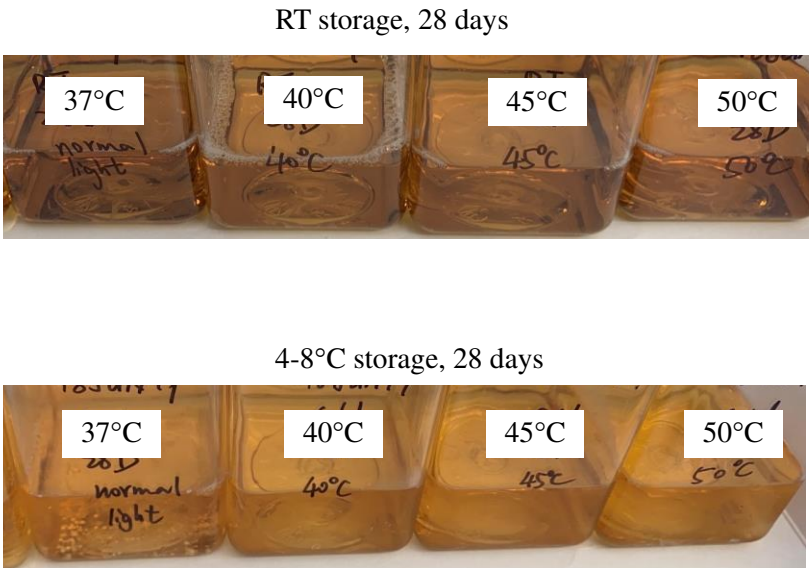

Figure 2.7. Impact of different treatment temperatures on medium appearance. Post filtration medium samples (pH 7.8) were aliquoted and treated at 37°C (control), 40°C, 45°C, and 50°C for 3h, followed by storage at RT and 4-8°C for 28 days. Treatment temperature had an insignificant impact on coloring compared to the impact of storage temperature. Precipitation was only observed at 37°C treatment 4-8°C storage. Treatment at 40-50°C prevented precipitation during storage.

Medium samples were collected after final filtration for a 3h treatment at different temperatures. Consistent with **Figures 2.4 and 2.5**, precipitation was observed with samples treated at 37°C (**Fig. 2.7**), indicating that simply extending the preparation time does not improve medium stability. However, we observed that media incubated at 40-50°C showed no signs of precipitation after 28 days of storage at 4-8°C.

2.3.5 Systematic evaluation of AA profiles by PCA and PCC

PCA reduces the dimensionality caused by many variables, namely 16 AAs in this case, provides a systematic data review, and identifies which conditions are responsible for the variability [18]. Data from **Figures 2.1, 2.2, 2.5, and 2.6** were grouped into three datasets for PCA. **Table 2.1** shows the top five components, corresponding eigenvalues (or the magnitude of each component), and proportion. Components that explain >90% of the variance are considered principal components. Consistent with the results discussed above (Second section), the variance of dataset 1 is mainly caused by precipitation. It corresponds to the first component, accounting for 89% of AA variation. Degradation played a secondary effect, accounting for 8% of AA variation. Datasets 2 and 3 identify one principal component (PC), reflecting that degradation accounts for 95% and 93% of the AA variation, respectively.

Table 2.1. Principal component analysis based on final preparation pH, storage temperature, and preparation temperature. Components that explain >90% of the variance are considered as principal components for analysis.

Data set	Component	Eigenvalue	Proportion	Cumulative
1. Different pH & stored in cold room	1	14.18	0.89	0.89
	2	1.34	0.08	0.97
	3	0.20	0.01	0.98
	4	0.14	0.01	0.99
	5	0.06	0.00	1.00
2. Different pH & stored at RT	1	15.19	0.95	0.95
	2	0.43	0.03	0.98
	3	0.22	0.01	0.99
	4	0.07	0.00	0.99
	5	0.04	0.00	1.00
3. Different treatment temperature	1	14.81	0.93	0.93
	2	0.58	0.04	0.96
	3	0.35	0.02	0.98
	4	0.15	0.01	0.99
	5	0.05	0.00	1.00

Note:

Dataset 1 and dataset 2 are analyzed separately because they have a different mechanism for amino acid change (e.g., precipitation and degradation).

Fig. 2.8 plots the samples based on their similarity. As shown in **Fig. 2.8(A)**, samples were clearly distinguished before and after 14 days of storage at 4-8°C. Driven by precipitation and

degradation, various preparation pHs led to the data scattering in PCA plots. Replicated samples did not always precipitate on the same day, resulting in a relatively large deviation. The day 14 pH 9.0 sample was the closest match to the day 0 sample, consistent with Figures 1 and 2. Data points in **Fig. 2.8(B)** are clustered into three groups: day 0 samples, day 14 pH 7.0 and 7.4, and day 14 pH 7.8-10.0. These clusters are mainly distinguished by degradation on component 1. **Fig. 2.8(C)** presents the similarity of samples prepared at different temperatures. Day 0 samples showed a similar component 1 and 2 values as day 14 storage at RT samples. However, samples stored at RT drifted away from the day 0 values after 28 days, while samples stored for the same length of time at 4-8°C remain close to the day 0 samples. Consistent with the last section, the data indicates that the high-temperature treatment leads to an early but minimal increase in AA degradation and prevents precipitation during extended storage.

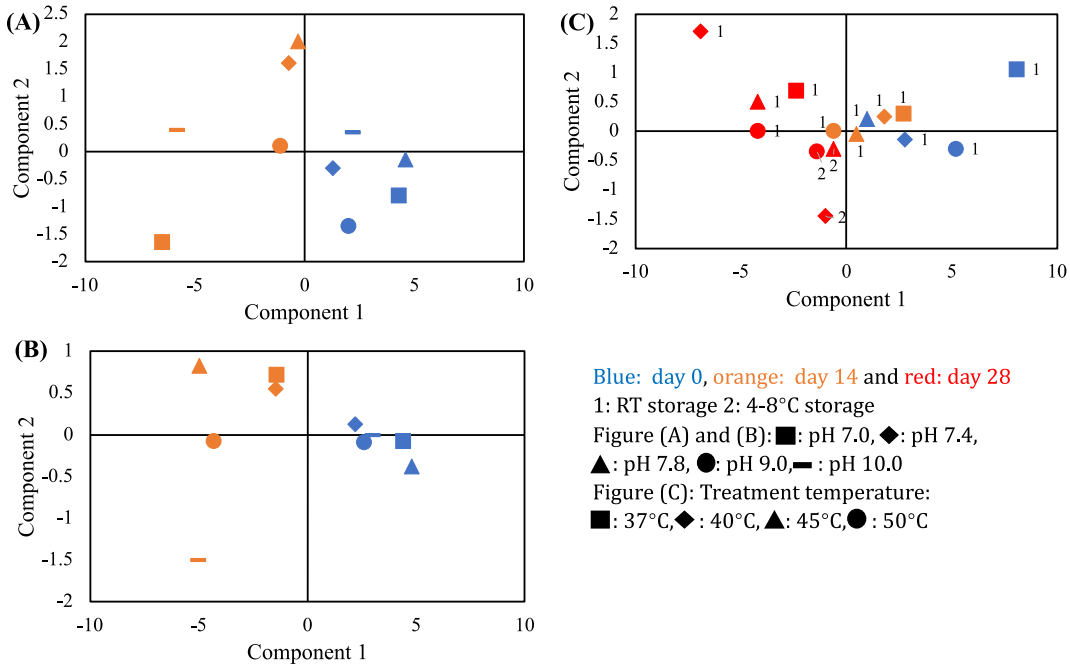

Figure 2.8. Sample similarity analysis based on PCA plot. The first component is proportional to the maximum variance, where 0 is the center of the multi-dimension cloud of data points. The second component is orthogonal to the first and proportional to the second-largest variance. (A)

pH 7.0 (■), pH 7.4 (◆), pH 7.8 (▲), pH 9.0 (●), and pH 10.0 (—); stored at 4-8°C for 14 days. (B) pH 7.0 (■), pH 7.4 (◆), pH 7.8 (▲), pH 9.0 (●), and pH 10.0 (—); stored at RT for 14 days. (C) Treatment at 37°C (■),40°C (◆), 45°C (▲), and 50°C (●); stored at (1) 4-8°C and (2) RT for 0 (blue), 14 (orange) and 28 (red) days.

Table 2.2 uses PCC to characterize AA interactions. When stored at 4-8°C (In dataset 1), most AAs were sensitive to changes to the final preparation pH (correlation coefficients ≥ 0.9). In contrast, MET and TRP acted independent of the other AAs, showing low correlation coefficients (0.85 and 0.86), indicating reduced responsivity to changes to the final preparation pH. All AAs degraded consistently during RT storage (dataset 2). With the exception of ASP (correlation coefficient = 0.87), all AAs exhibited correlation coefficients >0.9 in dataset 3, indicating that AA stability increased as the storage temperature was reduced from RT to 4-8°C.

Table 2.2. AA interaction characterization by Pearson Correlation Coefficient (N=12, Prob>|r| under H0: Rho=0, p value <0.05). Low correlation coefficient indicates that an AA acted independently of others at different final preparation pH, storage temperatures, or preparation temperatures.

Amino acid	Dataset 1	Dataset 2	Dataset 3
ARG	0.92	0.96	0.98
ASN	0.99	0.98	0.98
ASP	0.90	0.96	0.87
GLU	0.97	0.98	0.95
HIS	0.96	0.91	0.96
ILE	0.98	0.99	0.99
LEU	0.95	1.00	0.93
LYS	0.95	0.97	0.97
MET	0.85	0.96	0.98
PHE	0.94	0.99	0.98
PRO	0.99	0.97	0.91
SER	0.95	0.98	0.94
THR	1.00	0.99	0.99
TRP	0.86	0.97	0.98
TYR	0.90	0.97	0.99
VAL	0.95	1.00	0.98

2.4 Discussion

Successful process intensification depends on the development of a stable, highly concentrated feed medium. However, such highly concentrated feeds often exhibit precipitation and degradation of essential feed components such as AAs, resulting in variability that can compromise the development of a robust cell culture process. Here, we examined how different

preparation methods and storage conditions can improve the stability of AAs within concentrated feed media.

Storage conditions impact the stability and solubility of AA's. Degradation of AA's can negatively impact cell culture performance and product quality due to ammonium accumulation[19] or increased protein aggregation.[10, 20, 21] We observed accelerated AA degradation during storage at RT compared to media stored at 4-8°C (**Fig. 2.1**). Moreover, storage at RT resulted in changes to the color of the medium, likely indicating oxidation.[2, 14, 22] Nonenzymatic reaction with reducing sugars such as Maillard reaction could also cause significant AA decrease. Maillard reaction may happen at RT [23] with the increasing intensity at higher temperature and pH,[24] which is consistent with the observations in this study (**Fig. 2.2 and Fig. 2.4**). Media stored at 4-8°C did not exhibit any such color change (**Fig. 2.4**). However, precipitation was apparent after 28 days of storage at 4-8°C, but not in the RT condition, resulting in depletion of AA's from the feed media (**Fig. 2.1**).

We examined if adjusting the preparation pH or temperature could resolve the issues with media precipitation. The AA precipitation seems to be affected by a combination of AA net charge and solubility, which are determined by pH and storage temperature, and the concentration in the medium. For example, ARG was not detected in day 14 precipitation (**Fig. 2.5**). ARG has the highest pI (10.76) among the common AAs. Compared to neutral and high pH conditions, it is highly charged at low pH and therefore experiences significant repulsion, preventing precipitation. Final pH also affected the precipitation speed by day 14, although the day 28 final precipitation amount was comparable among pH 7.0, 7.4, and 7.8. We found that preparation pH values of pH 9-10 improved AA stability and prevented precipitation for both storage conditions (**Fig. 2.2-4**). However, we also observed degradation of some AAs at a pH of 10, likely attributable to an excess of hydroxide and reduced levels of free hydrogen ions (**Fig. 2.2**).[25] Overall changes to AA profiles

over time were evaluated by PCA, revealing that samples prepared at a pH of 9.0 exhibited the most similar profile after 14 days of storage at either 4-8°C or RT [**Fig. 2.8(A) and (B)**].

We also examined if an elevated preparation pH could maintain solubility when basal powder and AA concentrations were further increased. Specifically, we increased the concentration of the basal media in the feed by 1.3x and supplemented varying concentrations of tyrosine, which was chosen as an additive due to its impact on multiple metabolic pathways in cell culture and its comparatively poor solubility.[26, 27] Standard preparation pH values could only support an additional 2.4 g/L tyrosine, while media prepared at a pH of 9.8 remained soluble with a 1.3x higher concentration of basal powder or up to 6 g/L tyrosine (**Fig. 2.3**). It is probably because most AAs carry a net charge with increased solubility at high pH. An elevated preparation pH may enable a further increase in the concentration of AAs and basal powders in feed media. The impact of high pH feed should also be evaluated on cell culture performance and product quality.

Cell culture medium is routinely prepared at 37°C for the sake of consistency with standard cell culture temperatures. We found that preparing media at 40-50°C prevented precipitation during storage at 4-8°C (**Fig. 2.6**). PCA supported our conclusion that an elevated preparation temperature can improve media stability during storage: AA profiles from media prepared at 40-45°C after 14 days of storage remained comparable to the day 0 samples [**Fig. 2.8(C)**]. We speculate that the standard preparation temperature of 37°C may not be sufficient to dissolve the media powder completely, and that undissolved particles small enough to bypass the 0.2 μm filter could trigger precipitation during extended storage. Elevated preparation temperatures may promote the complete dissolution of media powder, including small particles.

However, others have raised concerns about elevated preparation temperature leading to vitamin degradation.[28] Indeed, we did observe mild degradation of AA's at preparation

temperatures from 40-50°C. These tradeoffs may be controlled within an acceptable range. The degradation of vitamins B1, B2, and B6 is not of concern as at a preparation temperature less than 50°C, medium showed a negligible mass reduction (<5%).[29] Krattenmacher et al. observed that precipitation amount differed after 28 days among preparation temperatures of 25°C, 35°C, and 40°C. They used PCA to demonstrate that these preparation temperatures did not significantly impact the chemical composition of the media at the beginning.[30] The optimal preparation temperature can be further evaluated with other process analytical technology (PAT) tools, and the impacts of these preparation temperatures should ultimately be tested in cell culture processes.

Due to the complexity of chemically defined medium, advanced technologies have become essential to comprehensively understand and further develop media. Liquid chromatography tandem mass spectrometry (LC-MS/MS) represents one such technology, and is commonly used to quantify multiple AAs simultaneously.[31] Emerging technologies have also been recently utilized to identify and assess the quality of complex cell culture medium components, including Raman spectroscopy, fluorescence excitation-emission matrix spectroscopy (EEM), nuclear magnetic resonance spectroscopy (NMR), near-infrared fluorescence spectroscopy (NIR), and thermogravimetric analysis (TGA).[32-36] As these technologies become readily available for manufacturing, they could be implemented in medium preparation to improve the process's robustness.

Statistical models have also been developed to address the challenges associated with large datasets and data complexity, such as multivariate curve resolution, principal component analysis (PCA), partial least squares, and parallel factor analysis[33, 37-39]. PCA is the most widely used technique in data processing[40] because it can easily identify the sources of variation in multivariable datasets [41]. In this study, PCA identified degradation and precipitation as the sources

of variation (**Table 2.1**) and revealed conditions that retained similar AA profiles over time (**Fig. 2.8**). This statistical analysis lends further support to our conclusion: AA degradation and precipitation during storage of cell culture media can be minimized by storage at 4-8°C and elevated preparation pH and preparation temperatures. Advanced statistical and technical methods will be essential for the development and characterization of chemically defined cell culture media.

2.5 Conclusion

We systematically evaluated the stability of 16 amino acids under different preparation pH, storage temperatures and durations, and preparation temperatures. Lowering storage temperature to 4-8°C significantly increased AA stability but resulted in precipitation. The precipitation issue of concentrated feed medium was mitigated by increasing the preparation pH or the preparation temperature with minimal impact on AA stability. After evaluating the impact on cell culture and product quality, optimal medium preparation parameters will contribute to a robust production process.

2.6 References

1. Xu, J.; Rehmann, M. S.; Xu, M.; Zheng, S.; Hill, C.; He, Q.; Borys, M. C.; Li, Z. J., Development of an intensified fed-batch production platform with doubled titers using N-1 perfusion seed for cell culture manufacturing. *Bioresources and Bioprocessing* **2020,** *7* (1), 1-16.
2. McCoy, R. E.; Costa, N. A.; Morris, A. E., Factors that determine stability of highly concentrated chemically defined production media. *Biotechnology progress* **2015,** *31* (2), 493-502.
3. Hossler, P.; McDermott, S.; Racicot, C.; Fann, J. C., Improvement of mammalian cell culture performance through surfactant enabled concentrated feed media. *Biotechnology progress* **2013,** *29* (4), 1023-1033.
4. Kuwae, S.; Miyakawa, I.; Doi, T., Development of a chemically defined platform fed-batch culture media for monoclonal antibody-producing CHO cell lines with optimized choline content. *Cytotechnology* **2018,** *70* (3), 939-948.

5. Lin, H.; Leighty, R. W.; Godfrey, S.; Wang, S. B., Principles and approach to developing mammalian cell culture media for high cell density perfusion process leveraging established fed-batch media. *Biotechnology progress* **2017,** *33* (4), 891-901.
6. Mayrhofer, P.; Reinhart, D.; Castan, A.; Kunert, R., Rapid development of clone-specific, high-performing perfusion media from established feed supplements. *Biotechnology progress* **2020,** *36* (2), e2933.
7. Esplugas, S.; Gimenez, J.; Contreras, S.; Pascual, E.; Rodríguez, M., Comparison of different advanced oxidation processes for phenol degradation. *Water research* **2002,** *36* (4), 1034-1042.
8. Arora, M., Cell culture media: a review. *Mater methods* **2013,** *3* (175), 24.
9. Mizdrak, J.; Hains, P. G.; Kalinowski, D.; Truscott, R. J.; Davies, M. J.; Jamie, J. F., Novel human lens metabolites from normal and cataractous human lenses. *Tetrahedron* **2007,** *63* (23), 4990-4999.
10. Calvet, A.; Li, B.; Ryder, A. G., A rapid fluorescence based method for the quantitative analysis of cell culture media photo-degradation. *Analytica chimica acta* **2014,** *807*, 111-119.
11. Lane, M.; Gardner, D., Increase in postimplantation development of cultured mouse embryos by amino acids and induction of fetal retardation and exencephaly by ammonium ions. *Reproduction* **1994,** *102* (2), 305-312.
12. Chen, P.; Harcum, S. W., Effects of elevated ammonium on glycosylation gene expression in CHO cells. *Metabolic Engineering* **2006,** *8* (2), 123-132.
13. Purwaha, P.; Silva, L. P.; Hawke, D. H.; Weinstein, J. N.; Lorenzi, P. L., An artifact in LC-MS/MS measurement of glutamine and glutamic acid: in-source cyclization to pyroglutamic acid. *Analytical chemistry* **2014,** *86* (12), 5633-5637.
14. Kleijkers, S. H.; van Montfoort, A. P.; Bekers, O.; Coonen, E.; Derhaag, J. G.; Evers, J. L.; Dumoulin, J. C., Ammonium accumulation in commercially available embryo culture media and protein supplements during storage at 2–8 C and during incubation at 37 C. *Human Reproduction* **2016,** *31* (6), 1192-1199.
15. Brunner, M.; Brosig, P.; Losing, M.; Kunzelmann, M.; Calvet, A.; Stiefel, F.; Bechmann, J.; Unsoeld, A.; Schaub, J., Towards robust cell culture processes—Unraveling the impact of media preparation by spectroscopic online monitoring. *Engineering in life sciences* **2019,** *19* (10), 666-680.
16. Sanguansat, P., *Principal component analysis*. BoD–Books on Demand: 2012.
17. Xu, J.; Jin, M.; Song, H.; Huang, C.; Xu, X.; Tian, J.; Qian, N.-X.; Steger, K.; Lewen, N. S.; Tao, L., Brown drug substance color investigation in cell culture manufacturing using chemically defined media: A case study. *Process Biochemistry* **2014,** *49* (1), 130-139.
18. Naik, G. R., *Advances in Principal Component Analysis: Research and Development*. Springer: 2017.
19. Ritacco, F. V.; Wu, Y.; Khetan, A., Cell culture media for recombinant protein expression in Chinese hamster ovary (CHO) cells: history, key components, and optimization strategies. *Biotechnology progress* **2018,** *34* (6), 1407-1426.
20. Calvet, A.; Ryder, A. G., Monitoring cell culture media degradation using surface enhanced Raman scattering (SERS) spectroscopy. *Analytica chimica acta* **2014,** *840*, 58-67.
21. Jing, Y.; Borys, M.; Nayak, S.; Egan, S.; Qian, Y.; Pan, S.-H.; Li, Z. J., Identification of cell culture conditions to control protein aggregation of IgG fusion proteins expressed in Chinese hamster ovary cells. *Process Biochemistry* **2012,** *47* (1), 69-75.

22. Schnellbaecher, A.; Lindig, A.; Le Mignon, M.; Hofmann, T.; Pardon, B.; Bellmaine, S.; Zimmer, A., Degradation Products of Tryptophan in Cell Culture Media: Contribution to Color and Toxicity. *International Journal of Molecular Sciences* **2021,** *22* (12), 6221.
23. Mastrocola, D.; Munari, M., Progress of the Maillard reaction and antioxidant action of Maillard reaction products in preheated model systems during storage. *Journal of Agricultural and Food Chemistry* **2000,** *48* (8), 3555-3559.
24. Wei, C.-K.; Ni, Z.-J.; Thakur, K.; Liao, A.-M.; Huang, J.-H.; Wei, Z.-J., Color and flavor of flaxseed protein hydrolysates Maillard reaction products: effect of cysteine, initial pH, and thermal treatment. *International Journal of Food Properties* **2019,** *22* (1), 84-99.
25. Yang, W. C.; Lu, J.; Kwiatkowski, C.; Yuan, H.; Kshirsagar, R.; Ryll, T.; Huang, Y. M., Perfusion seed cultures improve biopharmaceutical fed-batch production capacity and product quality. *Biotechnology progress* **2014,** *30* (3), 616-625.
26. Kang, C.; Wu, H.-L.; Xiang, S.-X.; Xie, L.-X.; Liu, Y.-J.; Yu, Y.-J.; Sun, J.-J.; Yu, R.-Q., Simultaneous determination of aromatic amino acids in different systems using three-way calibration based on the PARAFAC-ALS algorithm coupled with EEM fluorescence: exploration of second-order advantages. *Analytical Methods* **2014,** *6* (16), 6358-6368.
27. Kang, S.; Mullen, J.; Miranda, L. P.; Deshpande, R., Utilization of tyrosine-and histidine-containing dipeptides to enhance productivity and culture viability. *Biotechnology and bioengineering* **2012,** *109* (9), 2286-2294.
28. Schnellbaecher, A.; Binder, D.; Bellmaine, S.; Zimmer, A., Vitamins in cell culture media: Stability and stabilization strategies. *Biotechnology and bioengineering* **2019,** *116* (6), 1537-1555.
29. Fuliaş, A.; Vlase, G.; Vlase, T.; Oneţiu, D.; Doca, N.; Ledeţi, I., Thermal degradation of B-group vitamins: B 1, B 2 and B 6. *Journal of Thermal Analysis and Calorimetry* **2014,** *118* (2), 1033-1038.
30. Krattenmacher, F.; Heermann, T.; Calvet, A.; Krawczyk, B.; Noll, T., Effect of manufacturing temperature and storage duration on stability of chemically defined media measured with LC-MS/MS. *Journal of Chemical Technology & Biotechnology* **2019,** *94* (4), 1144-1155.
31. Qiu, J.; Chan, P. K.; Bondarenko, P. V., Monitoring utilizations of amino acids and vitamins in culture media and Chinese hamster ovary cells by liquid chromatography tandem mass spectrometry. *Journal of pharmaceutical and biomedical analysis* **2016,** *117*, 163-172.
32. Li, B.; Ryan, P. W.; Shanahan, M.; Leister, K. J.; Ryder, A. G., Fluorescence Excitation–Emission Matrix (EEM) Spectroscopy for Rapid Identification and Quality Evaluation of Cell Culture Media Components. *Applied spectroscopy* **2011,** *65* (11), 1240-1249.
33. Li, B.; Ray, B. H.; Leister, K. J.; Ryder, A. G., Performance monitoring of a mammalian cell based bioprocess using Raman spectroscopy. *Analytica chimica acta* **2013,** *796*, 84-91.
34. Hakemeyer, C.; Strauss, U.; Werz, S.; Folque, F.; Menezes, J. C., Near-infrared and two-dimensional fluorescence spectroscopy monitoring of monoclonal antibody fermentation media quality: aged media decreases cell growth. *Biotechnology journal* **2013,** *8* (7), 835-846.
35. Galbraith, S. C.; Bhatia, H.; Liu, H.; Yoon, S., Media formulation optimization: current and future opportunities. *Current opinion in chemical engineering* **2018,** *22*, 42-47.
36. Hoang, D.; Galbraith, S.; Kuang, B.; Johnson, A.; Yoon, S., Characterization of Chinese hamster ovary cell culture feed media precipitate. *Biotechnology Progress* **2021**.
37. Bro, R., PARAFAC. Tutorial and applications. *Chemometrics and intelligent laboratory systems* **1997,** *38* (2), 149-171.

38. De Juan, A.; Tauler, R., Multivariate curve resolution (MCR) from 2000: progress in concepts and applications. *Critical Reviews in Analytical Chemistry* **2006,** *36* (3-4), 163-176.
39. Abdi, H.; Williams, L. J., Principal component analysis. *Wiley interdisciplinary reviews: computational statistics* **2010,** *2* (4), 433-459.
40. Geladi, P., Chemometrics in spectroscopy. Part 1. Classical chemometrics. *Spectrochimica Acta Part B: Atomic Spectroscopy* **2003,** *58* (5), 767-782.
41. Li, B.; Ryan, P. W.; Ray, B. H.; Leister, K. J.; Sirimuthu, N. M.; Ryder, A. G., Rapid characterization and quality control of complex cell culture media solutions using raman spectroscopy and chemometrics. *Biotechnology and bioengineering* **2010,** *107* (2), 290-301.

Chapter 3: Raman spectroscopy monitoring cell culture media quality under different treatment conditions and different storage conditions

3.1. Introduction

Cell culture medium is considered as one of the key contributors to sustain cell growth and increase productivity. In biopharmaceutical industry, it has become a trend to replace serum and hydrolysate media with chemically defined media.[1] Researchers have been interested in chemically defined mammalian cell culture media since the 1960s. Ham reported the growth of Chinese Hamster Ovary cells in chemically defined medium firstly.[2] After that, chemically defined basal and feed media were widely considered in Chinese Hamster Ovary cells culture. In general, basal medium contains more than 50 chemical components, including inorganic salts, sugars, amino acids, vitamins, metals and other nutrients. Feed medium usually contains higher concentration and less content than basal medium. In a biopharmaceutical production process, a basal medium supports initial growth and production, and a feed medium prevents depletion of nutrients and sustains the production phase. Due to the complexity of chemically defined media, it is still a huge challenge to fully understand the interactions between each component and the storage conditions effect during media storage on cell performance and product quality.

Chinese Hamster Ovary cell culture media storage is affected by, for example, exposure to light, treated at high or low pH and exposure at high or low temperatures. At higher temperature, mineral salts and other components will not degrade, but vitamins, carbohydrates and proteins will degrade.[3, 4] The main process of degradation is oxidation, and the concentration of active ingredients will decrease over time.[5] Through deamination, amino acids and proteins slowly release ammonium ions, which have been shown to have a negative effect on the embryo.[6] This

process is very slow, so there will be no noticeable changes in a day at a slightly elevated temperature, but over a week will definitely have an important effect.[7] Upon light exposure, riboflavin, methionine, tryptophan and tyrosine were reported to play a special role in phototoxic effects of cell culture media.[8-11] Among them, the degradation product of tyrosine is dityrosine, while the degradation products of tryptophan are kynurenine, hydroxy-kynurenine, N-formyl-kynurenine and 5-fydroxytryptophan.[10]

It is not easy to test the concentrations of all components when evaluating the quality of cell culture medium. Thus, an easier method is needed. Raman spectroscopy is a physical method which is suitable for substances structure and composition identification. It has been increasingly used in the areas of biotechnology and pharmaceuticals.[12-14] Raman spectroscopy showed significant advantages and weaknesses for the use of cell culture medium analysis. It has low maintenance and high analysis frequency, while is desirable in industry.[15] Sample preparation in many cases is not required, which makes situ sample analysis possible. Besides, the signal of water is weak in Raman signal, which is easily for aqueous solution sample collection. At the same time, it is limited by the complex preprocessing steps, which limit their use for use.

Raman data commonly considered alongside with chemometric and statistical data analyses. Principal component analysis (PCA) is one of the widely used matrix factorization techniques, which can convert data in a high-dimensional space into a low-dimensional space. The advantage of retaining most useful information while reducing noise and other undesirable consequences.[16, 17] The main purpose of PCA is to reduce the dimensionality of a data set in which there are a large number of interrelated variables, while retaining the changes in the data set as much as possible.[18]

In this study, we used the Raman spectroscopy on amino acid concentration analysis in

order to compare the effectiveness of Raman measurements. Raman combined with principal component analysis can generate a quality profile to monitor and detect variances of cell culture media components and amounts of chemical components under different cell culture media treatment conditions and storage conditions. Comparative Raman spectroscopy can be easily applied to check cell culture media quality for batch and fed-batch bioprocesses.

3.2. Materials and methods

3.2.1 Materials

All materials were described in Chapter 2 unless otherwise specified.

3.2.2 Medium preparation

All medium preparation steps were described in Chapter 2 unless otherwise specified (**Table 3.1**).

Table 3.1. Brief description of the cell culture media samples conditions

Media	Initial treatment conditions	Storage conditions	Storage days	No. of samples combination
Cell culture feed media	Adjust pH to 7.0, 7.4,7.8, 9.0 and 10.0	RT / 4°C, light / dark	14	20
Cell culture	3h dark treatment at RT,	RT, 15°C and 4°C in		12

feed media	40°C, 45°C and 50°C in the incubator	dark	14 and 21	
Cell culture basal media	3h dark treatment at RT, 40°C, 45°C and 50°C in the incubator	RT, 15°C and 4°C in dark	14	12

3.2.3 Instrumentation and data collection

Raman data were collected with 785 nm excitation using a Raman Station spectrometer. A laser power of ~70mW with an acquisition time of 60 s was generally used and the spectral resolution was approximately 3.18 cm^{-1} from 200 to 1800 cm^{-1}.

3.2.4 Data pre-treatment

Raman spectroscopies were performed using Origin 8.1 Pro software (OriginLab, USA). Raman data were performed using MINITAB 18 (Mathworks Inc., Cambridge, MA, USA) platform version 7.4 and SAS (SAS institute) on a standard desktop computer.

3.3. Results

3.3.1 Spectral Analysis

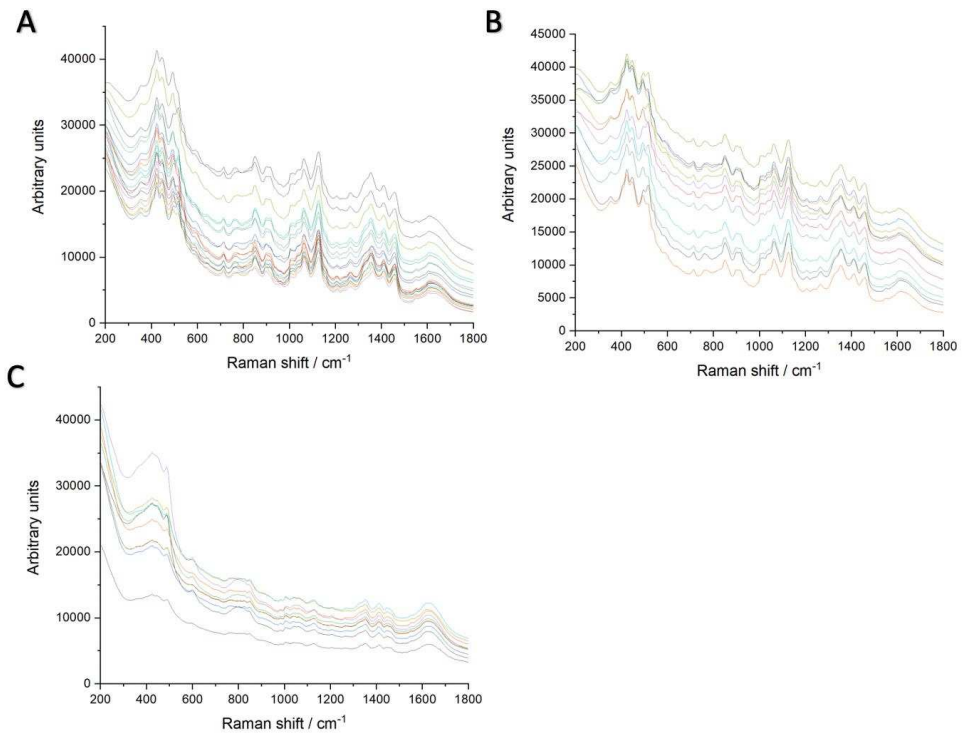

Figure 3.1. The original Raman spectra tested on day 14: (A) cell culture feed media treated under 5 different pH conditions (pH7.0, 7.4, 7.8, 9.0 and 10.0) and 4 storage conditions (dark/light, room temperature and 4°C), (B) cell culture feed media treated under 4 temperature conditions (room temperature, 40°C, 45°C and 50°C) and 3 storage temperature conditions (room temperature, 15°C and 4°C), and (C) cell culture basal media treated under 4 temperature conditions (room temperature, 40°C, 45°C and 50°C) and 3 storage temperature conditions (room temperature, 15°C and 4°C).

Raman spectroscopy can easily separate different media in certain arbitrary units (**Figure 3.1**). It may include clear spectral characteristics and compatibility with aqueous systems.[14, 19] It is obvious that different conditions could be easily distinguished. They have significant differences in spectral information. Samples with different pH, temperature and storage conditions show

highly detailed Raman spectra and relatively strong signals, but the significant baseline fluctuations are evident. One of the important steps in Raman analyzation is baseline correlation. Asymmetric least squares smoothing baseline was tried, but not applicable in this case. The optimal data pre-processing regime of baseline correction for cell culture basal media samples are baseline subtraction, user defined 2nd derivative (zeroes) with adjacent-averaging smoothing in spline, and for cell culture feed media in line. **Figure 3.2** shows the Raman spectrum after baseline correction and it is obvious that the analyte peaks are more visible and comparable, which is easier to interpret the subtle changes under different conditions. Although the differences in Raman spectroscopies were clearly observed, which individual condition cause it and what cell culture media components are responsible for the observed spectral differences should be defined.

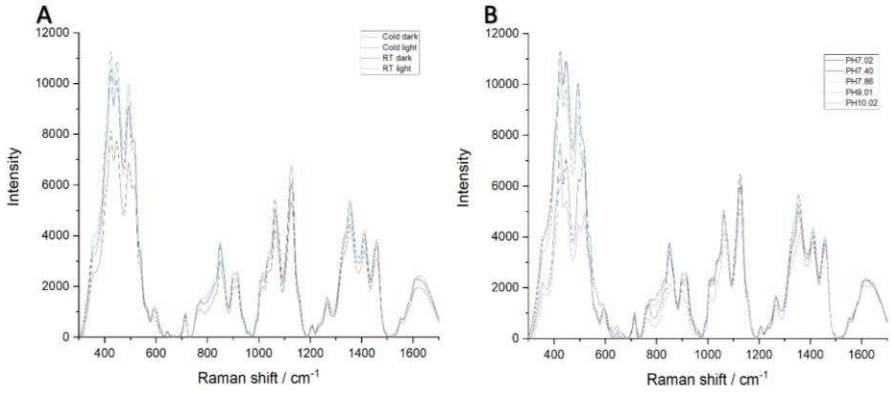

Figure 3.2. Cell culture feed media tested on day 14, (A) pH 7.8 samples under cold and dark/cold and light/room temperature and dark/room temperature and light storage conditions, (B) pH 7.0, 7.4, 7.8, 9.0 and 10.0 samples under room temperature and light conditions.

3.3.2 Raman shifts and compounds

The Raman vibration assignment is still the trickiest step in classic chemometric tools.

There are four main reasons: first due to the different methods to handle original Raman spectra; second, because the overlap peaks in cell culture media Raman spectra; and the last, Raman spectra in the literature are not very similar to each other since all bands are not observed by the whole Raman community. **Tables 3.2 and 3.3** show the Raman shifts and compounds of amino acids.

Table 3.2. Raman shifts and the compounds of their corresponding (or functional) groups. Cell culture feed media at the initial pH of 7.8, then stored under dark and cold conditions. Samples tested on day 14. Notation for modes: ν, stretching frequency, ν_s, symmetric stretching, δ, in-plane deformation, δ_s, symmetric deformation, δ_d, degenerate deformation, γ, out-of-plane bending, γ_p, rocking, γ_w, wagging, γ_t, twisting, τ, torsion, ψ, scissoring modes.

Raman shift (cm^{-1})	**Compound**	**Assignment**	**Reference**
448	Proline	Skeletal	Podstawka et al.[20]
	Cysteine	CCC bending	Brulé et al.[21]
	Threonine	τ (NH_3^+)	Krishnan and Katiyar[22]
	Proline	γ_p (COO^-)	Krishnan and Katiyar[22]
	Cystine	ν (S-S)	Krishnan and Katiyar[22]
495	Threonine	γ_p (COO^-)	Krishnan and Katiyar[22]
513	Leucine	τ (NH_3^+)	Krishnan and Katiyar[22]
852	Glutamic acid	γ_w (CH_2); ψ (COOH)	Numata et al.[23]
	Alanine	ν (C-CH_3)	Suh and Moskovits[24]
	Serine	ν (C-C)	Krishnan and Katiyar[22]
	Leucine	ν (C-C)	Krishnan and Katiyar[22]
	Tyrosine	γ_w (CH) of the ring	Krishnan and Katiyar[22]
	Glutamine	ν (C-C)	Krishnan and Katiyar[22]
899-915	Alanine	ν (C-C)	Numata et al.[23]
	Glycine	ν (C-C)	Numata et al.[23]
	Valine	γ_p (CH_2)	Krishnan and Katiyar[22]
	Cystine	γ_p (CH_2)	Krishnan and Katiyar[22]

	Glutamine	γ_p (CH_2)	Krishnan and Katiyar[22]
1062	Lysine	Cδ-Cε; Cε-Nx; g_w Cδ	Hernandez et al.[25]
1125	Glucose	C-1-O-5	Cerchiaro at al.[26]
	Glycine	γ_τ (NH_2)	Suh and Moskovits[24]
	Isoleucine	γ_p (NH_3^+)	Krishnan and Katiyar[22]
1262	Arginine	γ_t Cδ; γ_w Cγ; γ_t Cβ	Hernandez et al.[25]
	Proline	γ_w (CH_2)	Krishnan and Katiyar[22]
	Tyrosine	γ_t (CH_2)	Krishnan and Katiyar[22]
	Glutamine	γ_w (NH_2)	Krishnan and Katiyar[22]
1354	Tryptophan	Ring bend	Brulé et al.[21]
	Cysteine	γ (CH_2)	Brulé et al.[21]
	Lysine	γ_t Cδ; γ_w Cγ; γ_t Cε	Hernandez et al.[25]
	Arginine	CtOO- sym st; Nt-Cα-Hα; Cβ-Cα-Hα	Hernandez et al.[25]
	Cysteine	γ (C_a*H)	Hernandez et al.[25]
	Valine	γ (C_a*H)	Hernandez et al.[25]
	Valine	δ_s (CH_3)	Krishnan and Katiyar[22]
	Isoleucine	δ_s (CH_3)	Krishnan and Katiyar[22]
	Cystine	ν_s (COO^-)	Krishnan and Katiyar[22]
	Glutamic acid	δ (CCH)	Krishnan and Katiyar[22]
1409	Threonine	ν (CO_2^-)	Gargaro et al.[27]
	Histidine	Nt-Cα-Hα, Cβ-Cα-H, γ_p Cβ	Pflüger et al.[25]
	Glutamic acid	ν (C-O); δ (O-H)	Krishnan and Katiyar[22]
1456	Histidine	Cβ-bend, Nε-Cε, Cδ-Nε-H	Pflüger et al.[25]
	Valine	δ_d (CH_3)	Krishnan and Katiyar[22]
1621	Valine	δ_d (NH_3^+)	Krishnan and Katiyar[22]
	Isoleucine	δ_d (NH_3^+)	Krishnan and Katiyar[22]
	Cystine	δ_d (NH_3^+)	Krishnan and Katiyar[22]
	Glutamine	δ (NH_2)	Krishnan and Katiyar[22]

Table 3.3. Raman shifts and their corresponding compounds. Cell culture basal media at the initial pH of 7.8, then stored under dark and cold conditions. Samples tested on day 14. Notation for

modes: ν, stretching frequency, ν_s, symmetric stretching, δ, in-plane deformation, δ_s, symmetric deformation, δ_d, degenerate deformation, γ, out-of-plane bending, γ_p, rocking, γ_w, wagging, γ_t, twisting, τ, torsion, ψ, scissoring modes.

Raman shift (cm^{-1})	**Compound**	**Assignment**	**Reference**
432	Glycine	Skeletal	Podstawka et al.[20]
	Tyrosine	γ_p (COO^-)	Krishnan and Katiyar[22]
451	Proline	Skeletal	Podstawka et al.[20]
	Threonine	τ (NH_3^+)	Krishnan and Katiyar[22]
829	Isoleucine	ν (C-C)	Krishnan and Katiyar[22]
	Tyrosine	Ring stretch	Krishnan and Katiyar[22]
	Cystine	Skeletal stretch	Krishnan and Katiyar[22]
855	Glutamic acid	γ_w (CH_2); ψ (COOH)	Numata et al.[23]
	Alanine	ν (C-CH_3)	Suh and Moskovits[24]
	Serine	ν (C-C)	Krishnan and Katiyar[22]
	Cystine	Skeletal stretch	Krishnan and Katiyar[22]
1043	Glycine	C-NH_3^+	Podstawka et al.[20]
	Serine	NH_3^+ rock	Krishnan and Katiyar[22]
	Threonine	γ_p (CH_3)	Krishnan and Katiyar[22]
1065	Lysine	Cδ-Cε; Cε-Nx; g_w Cδ	Hernandez et al.[25]
1132	Phenylalanine	NH_3^+	Podstawka et al.[20]
	Serine	γ_p (NH_3^+)	Krishnan and Katiyar[22]
	Glutamic acid	γ_p (NH_3^+)	Krishnan and Katiyar[22]
1354	Proline	C-NH_3^+ or CH_2	Podstawka et al.[20]
	Tryptophan	Ring bend	Li et al.[28]
	Arginine	CtOO- sym st; Nt-CR-HR; Cβ -CR-HR	Hernandez et al.[25]
	Lysine	γ_t Cδ; γ_w Cγ; γ_t Cε	Hernandez et al.[25]
	Cysteine	γ (C_a*H)	Gargaro et al.[27]
	Valine	γ (C_a*H)	Gargaro et al.[27]
	Histidine	Nδ-Cε, γ_t Cβ, Cγ-Nδ	Pflüger et al.[25]
	Valine	δ_s (CH_3)	Krishnan and Katiyar[22]

	Isoleucine	δ_s (CH_3)	Krishnan and Katiyar[22]
	Cystine	δ (CCH)	Krishnan and Katiyar[22]
	Glutamic acid	δ (CCH)	Krishnan and Katiyar[22]
1415	Valine	CH_3	Podstawka et al.[20]
	Aspartic acid	CH_2	Numata et al.[23]
	Serine	ν (CO_2^-)	Hernandez et al.[25]
	Histidine	Nt-Cα-Hα, Cβ-Cα-H, Cβ-rock	Pflüger et al.[25]
	Glycine	ν_s (COO^-)	Suh and Moskovits[24]
	Serine	ν_s (COO^-)	Krishnan and Katiyar[22]
	Leucine	ν_s (COO^-)	Krishnan and Katiyar[22]
1447	Cystine	CH_2	Podstawka et al.[20]
	Arginine	Nη1-Cξ-Nη2 asym st; Cδ-Nε-Hε; Cξ-Nε-Hε	Hernandez et al.[25]
1628	Tryptophan	Ring in plane	Numata et al.[23]
	Valine	δ_d (NH_3^+)	Krishnan and Katiyar[22]
	Leucine	δ_d (NH_3^+)	Krishnan and Katiyar[22]

Raman spectroscopy measures the vibrational energy in chemical bonds, so it has high chemical specificity.[29] Most of the significant spectral information is contained in the range of 300-1700 cm^{-1}, in which specific components of the cell culture media was expected to be found. The Raman spectra of cell culture media samples at pH 7.8 under cold dark, cold light, room temperature dark and room temperature light were shown in **Figure 3.2A**. Different samples all have the same Raman shift of high peaks, while the heights are different. This means dark/light and room temperature/cold storage conditions don't change the compositions in the cell culture media but impact their amounts. Each peak in the Raman spectra is depicted in **Table 3.2** by Raman shifts, compounds, assignments and their references. There are a variety of peaks present in the Raman spectra of cell culture feed media A samples, with the peaks at 425, 448, 495, 514, 852, 899/915, 1062, 1125, 1262, 1354, 1409, 1456 and 1621 cm^{-1} being the most prominent from cold

and dark conditions sample. Some of samples with other conditions have Raman peaks with a small range of deviation of about plus or minus 3 cm^{-1}, which might be because of Raman intensity acquired around the interval of 3.18 cm^{-1}. In the range of 300-600 cm^{-1}, the peak area between the cell culture samples under cold and dark conditions and other three conditions are very different. Room temperature and light conditions showed the biggest peak area, then are the room temperature and dark conditions samples and cold and light conditions samples. The cold and dark conditions sample is the smallest. The peak at 448 cm^{-1} is most likely the characteristic skeletal of proline, the CCC bending of cysteine, the NH_3^+ torsion of threonine, the COO^- rocking of proline and the S-S stretching of cystine. The peak at 495 cm^{-1} is most likely the COO^- rocking of threonine. The peak at 513 cm^{-1} might be the NH_3^+ torsion of leucine. The peak at 852 cm^{-1} is most likely the CH_2 wagging and COOH scissoring of glutamic acid, the C-CH_3 stretching of alanine, the CH wagging of the ring and the C-C stretching of serine, leucine and glutamine. In the range of 900-1700 cm^{-1}, cold and light samples still showed the highest peak, while the cold and dark samples still showed the lowest peak, but the peak area is hard to be estimated. The peak around 899-915 cm^{-1} is mostly like the C-C stretching of alanine and glycine, the CH_2 rocking of valine, cystine and glutamine. The peak at 1062 cm^{-1} is most likely the characteristic of lysine. The peak at 1125 cm^{-1} is seen for glucose, the NH_2 twisting of glycine and the NH_3^+ rocking of isoleucine.

The peak at 1262 cm^{-1} is most likely characteristic of arginine, the CH_2 wagging of proline, the CH_2 twisting of tyrosine and the NH_2 wagging of glutamine. The peak at 1354 cm^{-1} is most likely the ring bending of tryptophan, the CH_2 bending of cysteine, characteristic of lysine and arginine, the C_a*H bending of cysteine and valine, the CH_3 symmetric deformation of valine and isoleucine, the COO^- symmetric stretching of cystine and the CCH of glutamic acid. This peak is more likely to show the CH_2 scissors modes from aliphatic side chain amino acids. The peak at

1409 cm^{-1} is mostly like the CO_2^- stretching of threonine, characteristic of histidine, the C-O stretching and O-H of glutamic acid. The peak at 1456 cm^{-1} might be characteristic of histidine and the CH_3 degenerate deformation of valine. The peak at 1621 cm^{-1} might be the NH_2 of glutamine and the $NH^3{}_+$ degenerate deformation of valine, isoleucine and cystine.

Figure 3.2B showed baseline corrected Raman spectra of cell culture feed media adjusted pH to 7.02, 7.40, 7.86, 9.01 and 10.02 and then stored in dark and cold conditions for 14 days. Cell culture samples with both low and high pH values showed the lowest peak intensity in the scale of 300-600 cm^{-1}, while samples under medium pH values showed higher peak intensity, especially for samples with pH 7.4 and pH 7.8 values. In the scale of 600-1700 cm^{-1}, pH 10.02 samples almost still showed the lowest intensity, while pH 7.0 samples almost showed the highest intensity.

Figure 3.3 showed Raman spectra of cell culture basal media A samples treated at room temperature, 40°C, 45°C and 50°C for 3h and then stored in room temperature and cold conditions for 14 days in the Raman shift 300-1700 cm^{-1}. In the scale of 300-700 cm^{-1} and 1000-1700 cm^{-1}, room temperature and 40°C treated samples are almost overlapped and showed the lowest intensity, while 45°C treated samples and 50°C treated samples showed higher intensity and accumulated higher integrated area. The Raman spectra of each peak are depicted in **Table 3.3** by Raman shifts, compounds, assignments and their references. The peak at 432 cm^{-1} is most likely characteristic for the skeletal of glycine and the COO^- rocking of tyrosine. The peak at 451 cm^{-1} is most likely characteristic for the skeletal of proline and the NH_3^+ torsion of threonine. The peak at 486 cm^{-1} is difficult to directly ensure the assignment, but it might be the acetoacetate and phenylalanine. The peak at 603 cm^{-1} is difficult to directly ensure the assignment, but it might be glycine and glutamate. In the scale of 700-1000 cm^{-1}, 50°C samples showed the lowest intensity. The peak at 829 cm^{-1} might be the C-C stretching of isoleucine, the ring stretching of tyrosine and the skeletal stretching

of cystine. The peak at 855 cm^{-1} is most likely the CH_2 wagging and COOH scissoring of glutamic acid, the C-CH_3 stretching of alanine, the C-C stretching of serine and the skeletal stretching of cystine. It also could be characteristic singlet of tyrosine, and may overlap with alanine, serine or glutamate. The peak at 1043 cm^{-1} can be attributed to the C-NH_3^+ of glycine, the NH_3^+ rock of serine and the CH_3 rocking of threonine. The peak at 1065 cm^{-1} might be characteristic of lysine and arginine. The peak at 1132 cm^{-1} can be attributed to the NH_3^+ of phenylalanine, the NH_3^+ rocking of serine and glutamic acid. The peak at 1354 cm^{-1} can be attributed to the C-NH_3^+ or CH_2 of proline, the ring bending of tryptophan, characteristic of arginine, lysine and histidine, the C_a*H bending of cysteine and valine, the CH_3 symmetric deformation of valine and isoleucine, the CCH bending of cystine and glutamic acid. The peak at 1415 cm^{-1} is seen for the CH_3 of valine, the CH_2 of aspartic acid, the CO_2^- stretching of serine, characteristic of histidine, the COO^- symmetric stretching of glycine, serine and leucine. The peak at 1447 cm^{-1} might be the characteristic of arginine and the CH_2 of cystine. It reported as the CH_2 scissors modes from aliphatic side chain amino acids.[21] The peak at 1628 cm^{-1} might be the ring in plane of tryptophan, the NH_3^+ degenerate deformation of valine and leucine.

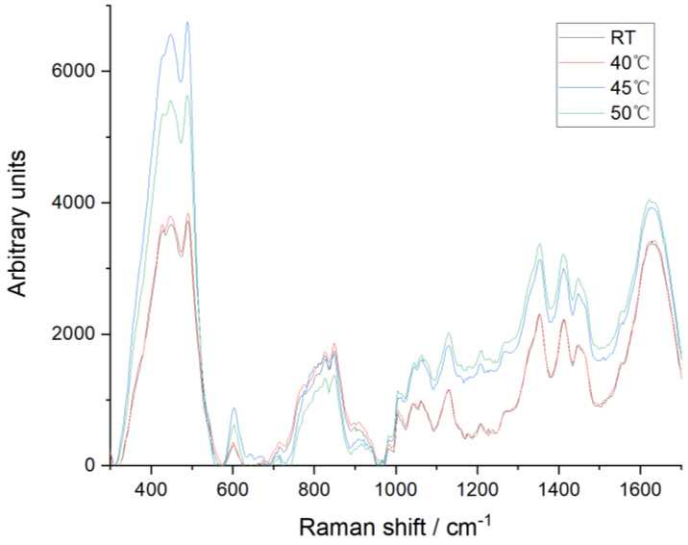

Figure 3.3. Baseline corrected Raman spectra for cell culture basal media A samples treated at room temperature, 40°C, 45°C and 50°C for 3h and then stored at room temperature and dark conditions for 14 days.

Because the Raman signal in this case was obtained every 3.18 cm^{-1}, this makes it difficult to distinguish some very close peaks, especially for the analysis of complex cell culture media. The cell culture feed media sample contains more than 50 substances. The complexity of the substances makes some peaks overlap or connect together, and some of them show weak Raman signals in aqueous solutions, so it is difficult to distinguish. The perception of this cell culture feed media is more inclined to be thought that most of the obvious peaks are overlapping peaks, covering multiple information.

The above provides the band assignment of some important amino acids in the Raman spectrum. Owing to the complexity of the cell culture media, low Raman resolution and the confidential nature of the basal media, it is impossible to provide more accurate band assignment. In any case, the use of Raman spectroscopy with easier analysis rather than accurate diagnostic tools is being explored.

3.3.3 Principal component analysis

The exact formulation of these propriety media are commercial secrets. Due to the complexity of the media, some substances overlap and appear on the same Raman spectral peak. Therefore, it is impossible to discuss in detail the precise origin or particular compounds with their differences between each media, and it is impossible to specify precise specifications for each spectral band. Principal component analysis was used to extract the differences from Raman

spectroscopy and visualize the cell culture media samples under different conditions.

Whether PCA is useful depends on the similarity of the measured signal against the impact factors. **Figure 3.4** shows the planar plats identifying all the samples banded on the first two most significant PC's. PC1 attained over 90% information or changes in the Raman spectra with the impact factors for all the samples tested.

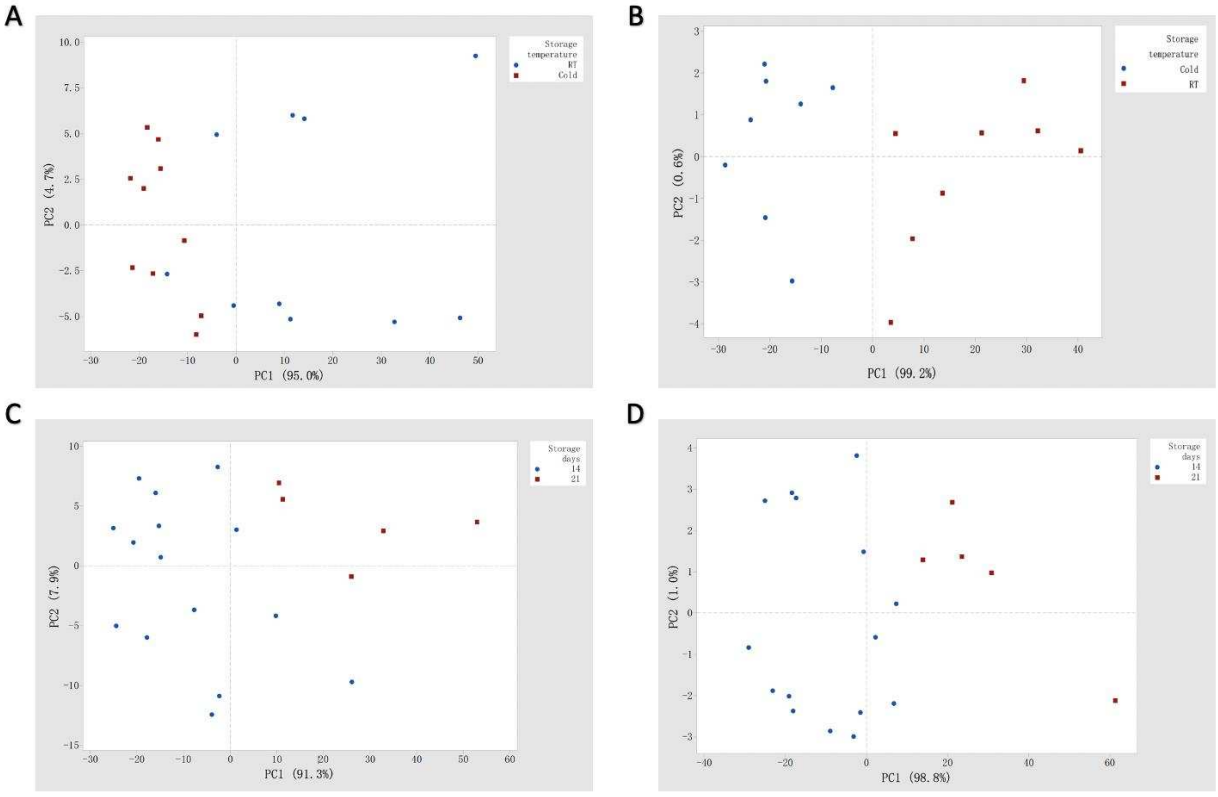

Figure 3.4. Planar identification of samples on the first two most significant principal components based on baseline corrected Raman spectra. (A) Principal component analysis of cell culture feed media treated at different pH, then stored at different conditions for 14 days. Blue: room temperature storage samples Red: 4°C storage samples. (B) Principal component analysis of cell culture feed media treated at different temperatures, then stored at different temperatures for 14 days. Red: room temperature storage samples Blue: 4°C storage samples. (C) Principal component analysis of cell culture feed media treated at different pH, then stored at 4°C and light/dark

conditions and cell culture feed media treated at different temperatures, then stored at 4°C. Blue: samples stored 14 days Red: samples stored 21 days. (D) Principal component analysis of cell culture feed media treated at different pH, then stored at room temperature and light/dark conditions and cell culture feed media treated at different temperatures, then stored at room temperature. Blue: samples stored 14 days Red: samples stored 21 days.

Figures 3.4A and 3.4B show the significant difference between room temperature storage samples and cold storage samples in principal component 1 of cell culture feed media under different treatment conditions and different storage conditions. Principal component 1 in **Figure 3.4A** attained 95% information, while principal component 1 in **Figure 3.4B** attained 99.2% information. Thus, comparing with the different treatment temperature, different treatment pH and different dark/light storage, different storage temperature is the most impact factor in cell culture feed media storage. In order to identify which specific components of the samples are causing differences in principal component 1 for samples with different storage temperatures, room temperature storage samples and 4°C storage samples were separated to be run by principal component analysis.

Figures 3.4C and 3.4D show the significant difference between day 14 and day 21 stored samples in principal component 1 of cell culture feed media under different treatment conditions and different dark/light storage conditions of cold storage samples and room temperature storage samples. Principal component 1 of **Figure 3.4C** attained 91.3% information, while principal component 1 of **Figure 3.4D** attained 98.8% information. Thus, comparing with the different treatment temperature, different treatment pH, different dark/light storage and different storage temperature, storage time is the most important impact factor in cell culture feed media storage. The eigenvalue of principal component 1 of the samples stored under cold condition is lower than

the samples stored under room temperature condition. Even when we consider principal component 2, it is not obvious which specific components of the samples are causing the principal components differences. Therefore, principal component loadings were introduced.

The impact of storage temperature conditions on cell culture media quality showed a strong negative result on Raman spectroscopy. It is easy to separate cell culture media samples with different storage temperature conditions by Raman on visual principal component figure.

In **Figures 3.5A and 3.5B**, there principal component 1 loadings are all around 0.4, which means samples under room temperature storage and cold storage have no clear difference on PC1 loadings and each Raman shift contributes similar in PC1, while principal component 2 loadings show similar trend, which means samples with room temperature storage and cold storage have no clear difference on PC2 loadings. At this level, each Raman shift could be used to separate same samples under different storage temperature conditions. In **Figure 3.5A** of PC3, there is no obvious peak, while in **Figure 3.5B** of PC3, the Raman shift around 1128 cm^{-1} has the biggest absolute loading value peak. Combined with the analysis results in the previous section, it might be glucose, glycine, isoleucine, phenylalanine, serine or glutamic acid. Besides the Raman shift of 1128 cm^{-1}, the Raman shifts around 390 cm^{-1}, 485 cm^{-1}, 520 cm^{-1}, 800 cm^{-1}, 1090 cm^{-1} and 1363 cm^{-1} also showed prominent contributions to PC3. Considering with the different treatment conditions of those cell culture media samples, Raman shift peaks on PCA loadings indicate differences in the specific components level in cell culture media. Comparing PC1 proportions of cell culture media samples under room temperature and cold storage conditions, the PC1 proportion of cell culture media under room temperature storage condition is higher, which illustrated that the variances of cell culture media under room temperature storage condition is more regular and similar.

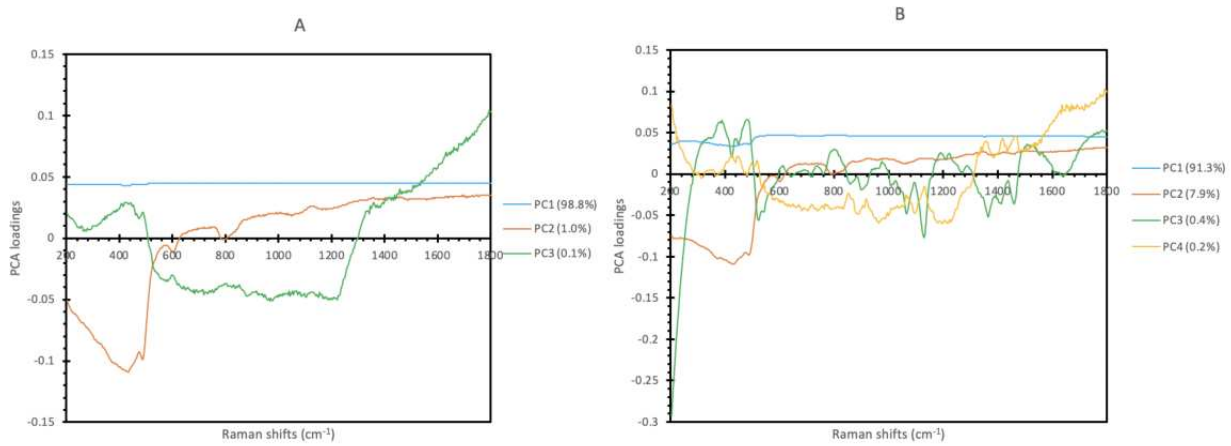

Figure 3.5. Principal vector loading plots of the components generated by the PCA analysis of the data collected on the samples stored under (A) room temperature and (B) cold storage conditions from different pH treatment and temperature treatment conditions.

3.3.4 The variance of PCA scores

Comparing the PC1 scores of cell culture media samples under light and dark conditions, the scores of samples under dark condition are still lower than the scores of samples under light condition at room temperature storage, while the scores of samples under dark and light conditions are similar at cold temperature storage. It indicates that at cold temperature storage, there is no clear difference in dark and light conditions, while at room temperature storage, dark and light conditions showed significant impact on the cell culture media. It might because the cell culture media are unstable at cold temperature storage (**Figure 3.6**).

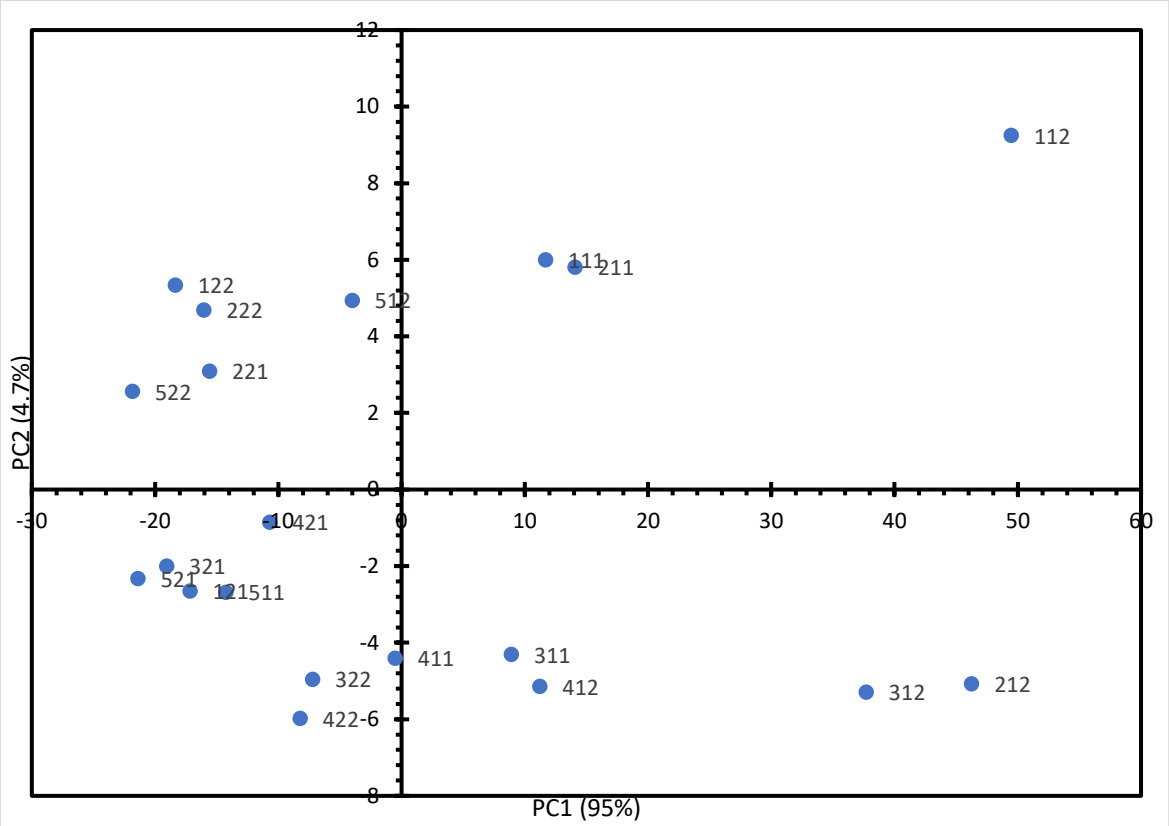

Figure 3.6. Identification of cell culture medium samples on the planar space concerned of the two most important PC's. In the legend, the first number represent initial pH (1: pH 7.0, 2: pH 7.4, 3: pH 7.8, 4: pH 9.0 and 5: pH 10.0), the second number represent temperature storage (1: room temperature and 2: 4°C) and the third number represent storage condition (1: dark and 2: light).

The pH adjustment on cell culture media samples were modelled using two components (99.7% explained spectral variance). In 4 different storage conditions, the variances of PC1 and PC2 scores versus initial media pH follow the rules. PC1 scores almost decreased with pH for the room temperature storage samples, PC1 scores waved with pH for the cold and dark conditions storage samples, while PC1 scores increased then decreased with pH for the room temperature and light storage samples which suggested that these components were associated with OH^- of chemical reaction (**Figure 3.7**). One reason that could explain the wave of PC1 scores of cold

storage samples is the precipitation occurred before test days in cold storage samples. It resulted in the change of the composition of liquid media samples. PC2 scores decreased first to keep stable, then increased with pH for the room temperature storage samples and cold light storage samples, while PC2 scores waved with pH for the cold temperature and light storage samples (**Figure 3.8**). Thus, PC2 explained the variance of pH, while just the pH 7.02 cell culture media sample under dark and cold conditions showed a different score on PC2.

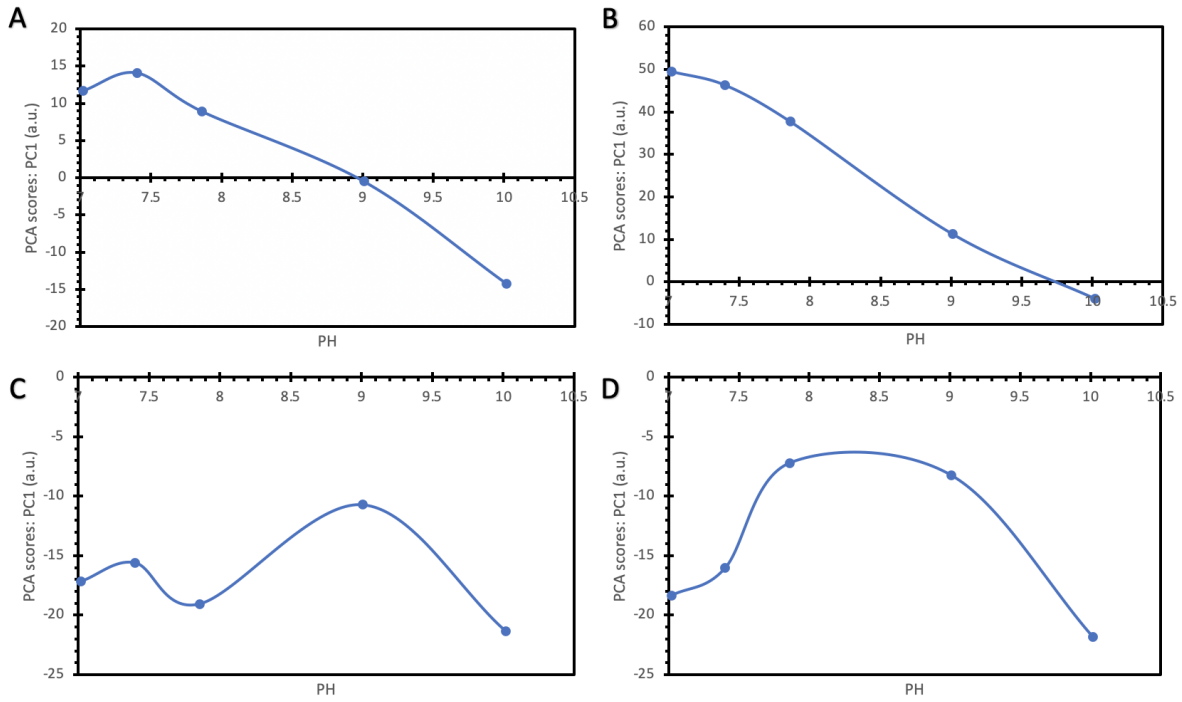

Figure 3.7. Plots of changes in the individual principal component 1 scores with pH generated by various PCA models: (A) at room temperature under dark storage condition samples, (B) at room temperature under light storage condition samples, (C) at 4°C under dark storage condition samples and (D) at 4°C under light storage condition samples.

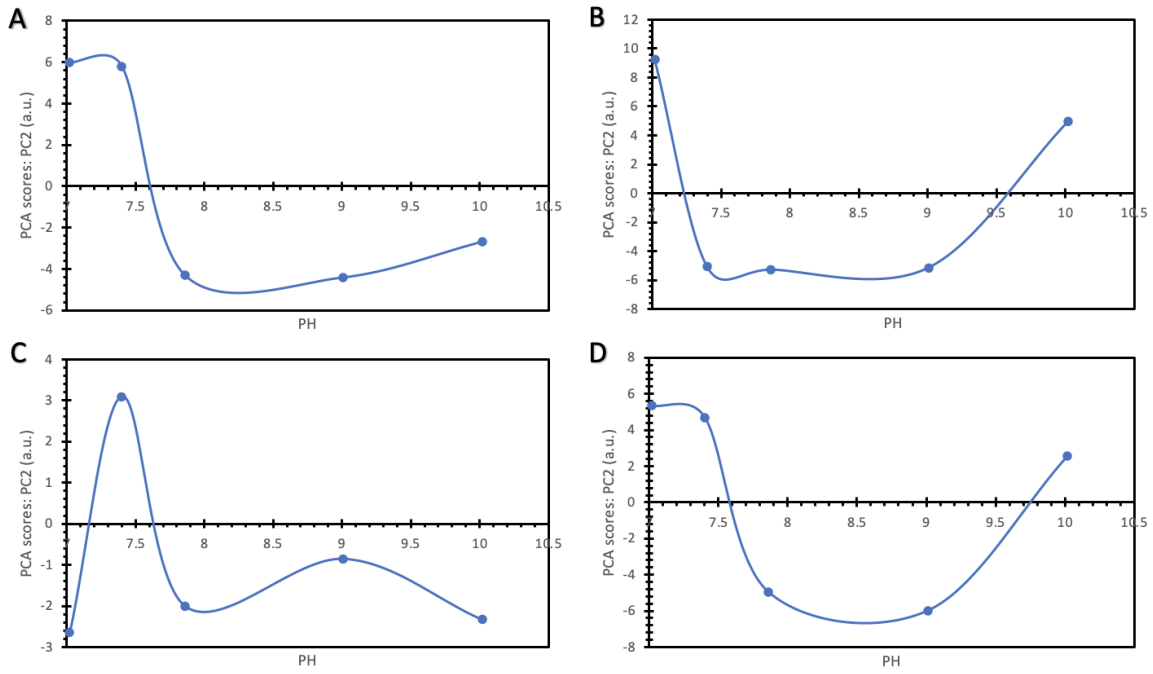

Figure 3.8. Plots of changes in the individual principal component 2 scores with pH generated by various PCA models: (A) at room temperature under dark storage condition samples, (B) at room temperature under light storage condition samples, (C) at 4°C under dark storage condition samples and (D) at 4°C under light storage condition samples.

Combining with PC2 loadings (**Figure 3.9**), the treatment pH impacted a lot on the components which around the Raman shifts of 345-485 cm^{-1}, 1141 cm^{-1}, 1360 cm^{-1} and 1437 cm^{-1}. It might be because of the concentration differences of glutamic acid and aspartic acid under different pH treatment conditions.

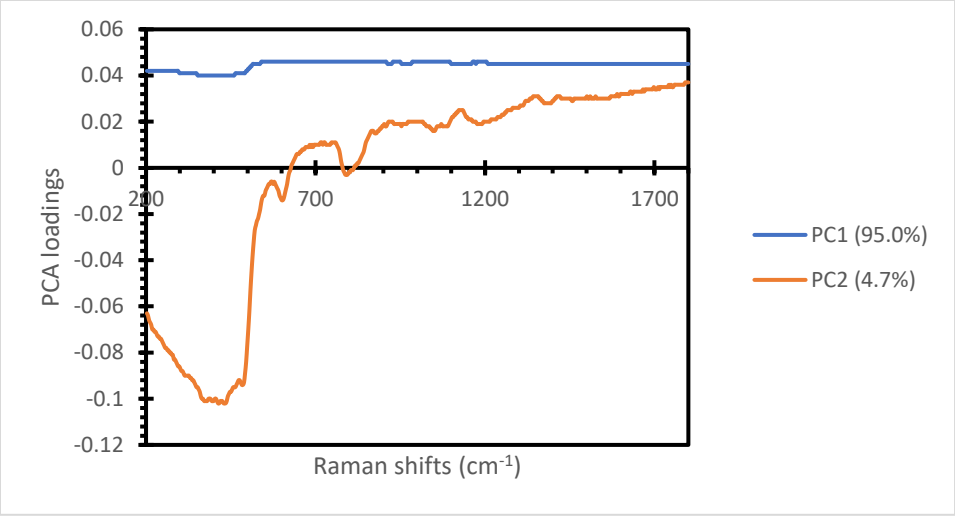

Figure 3.9. Loadings plots of the components generated by the PCA analysis of the data collected from cell culture feed media treated at different pH, then stored at different conditions.

3.3.5 Amino acid concentrations

Amino acid concentrations were measured to ascertain the reliability of Raman spectra analysis of the cell culture media. As shown in **Figure 3.10**, almost all amino acid concentrations are higher at 4°C storage than at room temperature storage, excepting tyrosine concentration, which cell culture media samples treated at room temperature and aspartic acid, which cell culture media samples treated at 40°C for 3h at day 0. This amino acid concentration results can confirm the correctness of the conclusion of Raman spectrum. 90% of differences in all amino acid concentrations at cold and room temperature are attained in principal component 1 of Raman result, while some of the component variances different from principal component 2 are shown in other principal components.

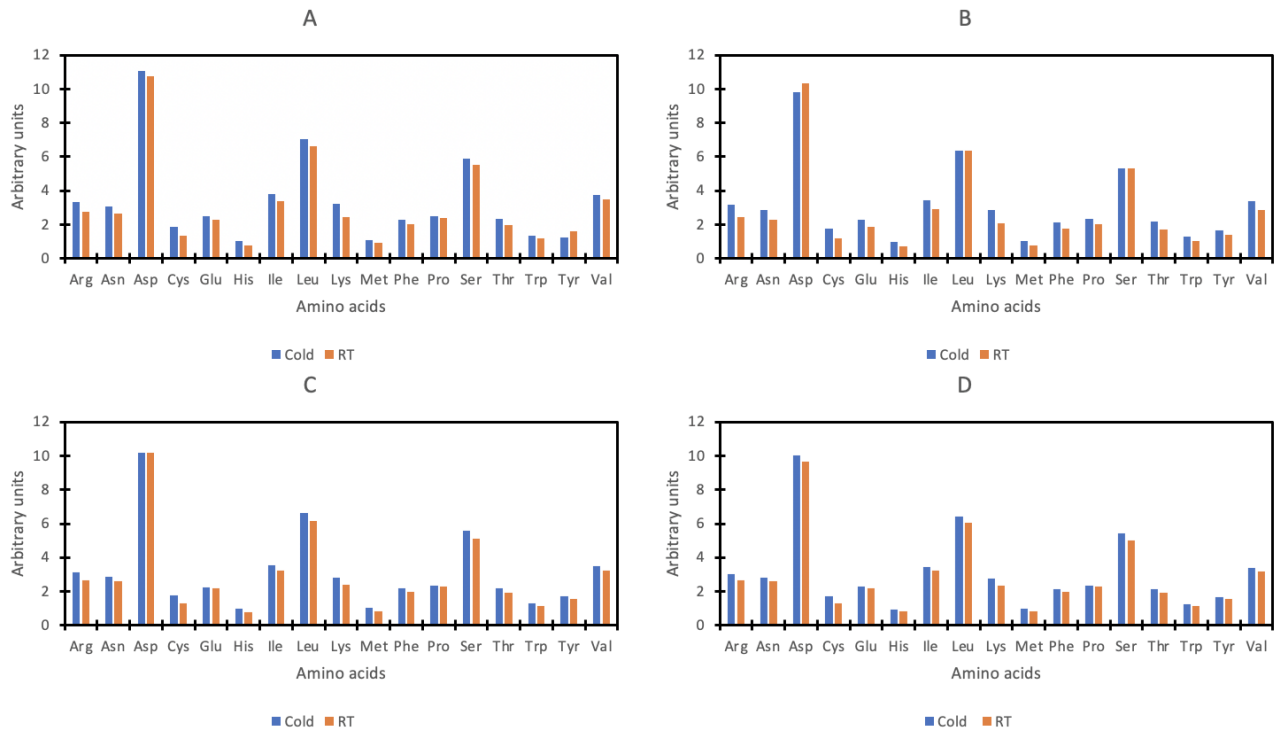

Figure 3.10. The concentrations of 16 amino acids and glucose tested on day 28. Cell culture feed media treated at (A) RT, (B) 40°C, (C) 45°C and (D) 50°C for 3h at day 0, then stored at 4°C (cold) or room temperature under dark conditions. The color of blue represents 4°C storage and the color of orange represents room temperature storage.

Since the concentrations of amino acids in cell culture media samples under cold storage conditions are almost always higher than those under room temperature conditions, it is confirmed that the principal component diagram can separate cell culture media samples by different temperature storage conditions.

3.4. Discussion

Conventional Raman spectroscopy combined with principal component analysis is an effective and inexpensive method to distinguish cell culture media under different treatment and

different storage conditions. We have demonstrated the feasibility of distinguishing different media based on the results of Raman spectroscopy with principal component analysis. Storage temperature has the great of influence on the concentration of substances on cell culture media, which is consistent with the results of amino acid concentrations. These Raman spectra data can be applied to distinguish the cell culture media, judging treatment conditions and storage conditions sustained, and to assist in understanding cell culture media quality. Raman spectroscopy can be applied to rapid diagnosis of the quality of the cell culture medium to determine whether the concentrations of the substances and the variances of substances meets the intended standard by comparing with the standard cell culture medium.

3.5. References

1. Xu, J.; Rehmann, M. S.; Xu, X.; Huang, C.; Tian, J.; Qian, N.-X.; Li, Z. J. In *Improving titer while maintaining quality of final formulated drug substance via optimization of CHO cell culture conditions in low-iron chemically defined media*, MAbs, Taylor & Francis: 2018; pp 488-499.
2. Ham, R. G., Clonal growth of mammalian cells in a chemically defined, synthetic medium. *Proceedings of the National Academy of Sciences* **1965,** *53* (2), 288-293.
3. Russell, J. B.; Sniffen, C.; Van Soest, P., Effect of carbohydrate limitation on degradation and utilization of casein by mixed rumen bacteria. *Journal of Dairy Science* **1983,** *66* (4), 763-775.
4. Zang, L.; Frenkel, R.; Simeone, J.; Lanan, M.; Byers, M.; Lyubarskaya, Y., Metabolomics profiling of cell culture media leading to the identification of riboflavin photosensitized degradation of tryptophan causing slow growth in cell culture. *Analytical chemistry* **2011,** *83* (13), 5422-5430.
5. Esplugas, S.; Gimenez, J.; Contreras, S.; Pascual, E.; Rodríguez, M., Comparison of different advanced oxidation processes for phenol degradation. *Water research* **2002,** *36* (4), 1034-1042.
6. Lane, M.; Gardner, D., Increase in postimplantation development of cultured mouse embryos by amino acids and induction of fetal retardation and exencephaly by ammonium ions. *Reproduction* **1994,** *102* (2), 305-312.
7. Kleijkers, S. H.; van Montfoort, A. P.; Bekers, O.; Coonen, E.; Derhaag, J. G.; Evers, J. L.; Dumoulin, J. C., Ammonium accumulation in commercially available embryo culture media and protein supplements during storage at 2–8 C and during incubation at 37 C. *Human Reproduction* **2016,** *31* (6), 1192-1199.

8. Edwards, A.; Silva, E.; Jofré, B.; Becker, M.; De Ioannes, A., Visible light effects on tumoral cells in a culture medium enriched with tryptophan and riboflavin. *Journal of Photochemistry and Photobiology B: Biology* **1994,** *24* (3), 179-186.
9. Mayrhofer, P.; Reinhart, D.; Castan, A.; Kunert, R., Monitoring of heat-and light exposure of cell culture media by RAMAN spectroscopy: Towards an analytical tool for cell culture media quality control. *Biochemical Engineering Journal* **2021,** *166*, 107845.
10. Calvet, A.; Li, B.; Ryder, A. G., A rapid fluorescence based method for the quantitative analysis of cell culture media photo-degradation. *Analytica chimica acta* **2014,** *807*, 111-119.
11. Stoien, J. D.; Wang, R. J., Effect of near-ultraviolet and visible light on mammalian cells in culture II. Formation of toxic photoproducts in tissue culture medium by blacklight. *Proceedings of the National Academy of Sciences* **1974,** *71* (10), 3961-3965.
12. Enejder, A. M.; Scecina, T. G.; Oh, J.; Hunter, M.; Shih, W.-C.; Sasic, S.; Horowitz, G. L.; Feld, M. S., Raman spectroscopy for noninvasive glucose measurements. *Journal of biomedical optics* **2005,** *10* (3), 031114-031114-9.
13. Li, M. Y.; Ebel, B.; Paris, C.; Chauchard, F.; Guedon, E.; Marc, A., Real-time monitoring of antibody glycosylation site occupancy by in situ Raman spectroscopy during bioreactor CHO cell cultures. *Biotechnology progress* **2018,** *34* (2), 486-493.
14. Bhatia, H.; Mehdizadeh, H.; Drapeau, D.; Yoon, S., In-line monitoring of amino acids in mammalian cell cultures using raman spectroscopy and multivariate chemometrics models. *Engineering in Life Sciences* **2018,** *18* (1), 55-61.
15. Buckley, K.; Ryder, A. G., Applications of Raman spectroscopy in biopharmaceutical manufacturing: a short review. *Applied spectroscopy* **2017,** *71* (6), 1085-1116.
16. Sanguansat, P., *Principal component analysis*. BoD–Books on Demand: 2012.
17. Abdi, H.; Williams, L. J., Principal component analysis. *Wiley interdisciplinary reviews: computational statistics* **2010,** *2* (4), 433-459.
18. Naik, G. R., *Advances in Principal Component Analysis: Research and Development*. Springer: 2017.
19. Kiefer, W., Recent advances in linear and nonlinear Raman spectroscopy I. *Journal of Raman Spectroscopy: An International Journal for Original Work in all Aspects of Raman Spectroscopy, Including Higher Order Processes, and also Brillouin and Rayleigh Scattering* **2007,** *38* (12), 1538-1553.
20. Podstawka, E.; Ozaki, Y.; Proniewicz, L. M., Part III: Surface-enhanced Raman scattering of amino acids and their homodipeptide monolayers deposited onto colloidal gold surface. *Applied spectroscopy* **2005,** *59* (12), 1516-1526.
21. Brulé, T.; Yockell-Lelièvre, H. l. n.; Bouhélier, A.; Margueritat, J. r. m.; Markey, L.; Leray, A.; Dereux, A.; Finot, E., Sorting of enhanced reference Raman spectra of a single amino acid molecule. *The Journal of Physical Chemistry C* **2014,** *118* (31), 17975-17982.
22. Krishnan, R.; Katiyar, R., Raman and infrared spectra of β-alanine. *Bulletin of the Chemical Society of Japan* **1969,** *42* (8), 2098-2101.
23. Numata, Y.; Otsuka, M.; Yamagishi, K.; Tanaka, H., Quantitative determination of glycine, alanine, aspartic acid, glutamic acid, phenylalanine, and tryptophan by Raman spectroscopy. *Analytical Letters* **2017,** *50* (4), 651-662.
24. Suh, J.; Moskovits, M., Surface-enhanced Raman spectroscopy of amino acids and nucleotide bases adsorbed on silver. *Journal of the American Chemical Society* **1986,** *108* (16), 4711-4718.

25. Hernández, B.; Pflüger, F.; Derbel, N.; De Coninck, J.; Ghomi, M., Vibrational analysis of amino acids and short peptides in hydrated media. VI. amino acids with positively charged side chains: L-Lysine and L-Arginine. *The Journal of Physical Chemistry B* **2010,** *114* (2), 1077-1088.
26. Cerchiaro, G.; Sant'Ana, A. C.; Temperini, M. L. A.; da Costa Ferreira, A. M., Investigations of different carbohydrate anomers in copper (II) complexes with D-glucose, D-fructose, and D-galactose by Raman and EPR spectroscopy. *Carbohydrate research* **2005,** *340* (15), 2352-2359.
27. Gargaro, A.; Barron, L.; Hecht, L., Vibrational Raman optical activity of simple amino acids. *Journal of Raman spectroscopy* **1993,** *24* (2), 91-96.
28. Li, B.; Ryan, P. W.; Ray, B. H.; Leister, K. J.; Sirimuthu, N. M.; Ryder, A. G., Rapid characterization and quality control of complex cell culture media solutions using raman spectroscopy and chemometrics. *Biotechnology and bioengineering* **2010,** *107* (2), 290-301.
29. Singh, G. P.; Goh, S.; Canzoneri, M.; Ram, R. J., Raman spectroscopy of complex defined media: biopharmaceutical applications. *Journal of Raman Spectroscopy* **2015,** *46* (6), 545-550.

Chapter 4: Characterization of cell culture medium under different treatment conditions by excitation-emission matrix fluorescence spectroscopy

4.1 Introduction

The information available in the cell culture medium sample depends on the analytical method used. Excitation-emission matrix spectroscopy is an effective and beneficial method of expressing fluorescence data. Excitation/emission matrix (EEM) spectroscopy could rapidly assess qualitative and quantitative cell culture media changes.[1, 2] However, due to Rayleigh scattering, Raman scattering, signal overlap, signal interference, and other reasons, the fluorescence signals' analysis is very complicated.[3] It is usually necessary to assemble a data set before developing a preliminary model, correct bias, remove scatter, and remove outliers.[4] Besides, the trilinearity of the EEM data usually impacted by the inner filter, which caused by high concentrations, scattering, and quenching.[5] Therefore, it is necessary to process the excitation-emission matrix data before application.

More recent methods for the analysis of cell culture medium EEMs include Principal Component Analysis (PCA), Partial Least Squares regression (PLS), multi-way data analysis using parallel factor analysis (PARAFAC), N-way partial least squares (N-PLS), and Tucker.[5, 6] They are used to estimate underlying chemical compositions and concentrations.

PARAFAC is a multiway data analysis method, which has been shown to decompose the suite of complex EEM landscapes into chemically significant spectral components.[5, 7, 8] The assumptions used based on the PARAFAC model can be summarized into three points: variability, trilinearity, and additivity. Variability means that no two chemical components can have completely co-variable fluorescence intensity or the same spectrum. Trilinearity means that in each

mode of the data set, the same number of components are the basis of chemical changes. Additivity means that the total signal can be regarded as a linear superposition of a fixed number of components.[5] The establishment of a PARAFAC model can realize the judgment of the fluorescent chemical composition in the cell culture medium.[9]

PCA is a widely used matrix factorization technique that can convert data in a high-dimensional space into a low-dimensional space. The advantage of retaining the most useful information while reducing noise and other undesirable consequences.[10, 11] The main purpose of PCA is to reduce the dimensionality of datasets where there are a large number of interrelated variables, while preserving as much variation in the dataset as possible.[12] By establishing a PCA model, the quality of the cell culture medium can be monitored.[13]

4.2 Materials and Methods

4.2.1 Materials

All materials were described in Chapter 2 unless otherwise specified.

4.2.2 Medium preparation

All medium preparation steps were described in Chapter 2 unless otherwise specified (**Table 4.1**).

Table 4.1. Brief description of the cell culture media samples conditions

Media	Initial treatment conditions	Storage conditions	Storage	No. of samples combination

			days	
Cell culture feed media	Adjust pH to 7.0, 7.4,7.8, 9.0 and 10.0	RT / 4°C, light / dark	0, 14 and 28	45
Cell culture feed media	3h dark treatment at RT, 40°C, 45°C and 50°C in the incubator	RT, 15°C and 4°C, light /dark	0, 14, 21 and 28	35
Cell culture basal media	3h dark treatment at RT, 40°C, 45°C and 50°C in the incubator	RT, 15°C and 4°C, light / dark	0, 14, 21 and 28	35

4.2.3 Instrumentation and data collection

Excitation-emission matrix (Horiba, Horiba Aqualog, USA) data were collected at room temperature with spectral ranges of 240 to 600 nm excitation and 240 to 800 nm emission, a data interval of 5 nm, and measurement typically took around 5 min. Samples diluted with PBS buffer before being pipetted into cuvettes and sealed. For basal medium, 20μL sample in 10 mL PBS buffer. For feed medium, 100μL sample in 10 mL PBS buffer. A DI water and a PBS buffer background spectrum were measured every day before testing.

4.2.4 Data preprocessing and analysis

Parallel factor analysis modelling was performed using the drEEM toolbox

of MATLAB R2020b. In order to avoid the influence of the internal filter as much as possible and work above the cut-off value to obtain high interference components, the EEM wavelength range studied in this study is limited to the range of Em. 250-800nm and Ex. 240-600nm.

4.3 Results

4.3.1 Spectral Analysis

Figures 4.1A and 4.1C show the EEM spectrum of the mixture, recorded in the emission domain from 250 to 800 nm and in the excitation domain from 243 to 603 nm. Obvious peaks can be observed in both figures, but the difference is not significant. Color outlines (**Figures 4.1B and 4.1D**) were used to display the same information through the same color bar. A smaller light-colored center circle in the pH7.0 sample and a more extensive and darker central circle color in the pH10.0 sample.

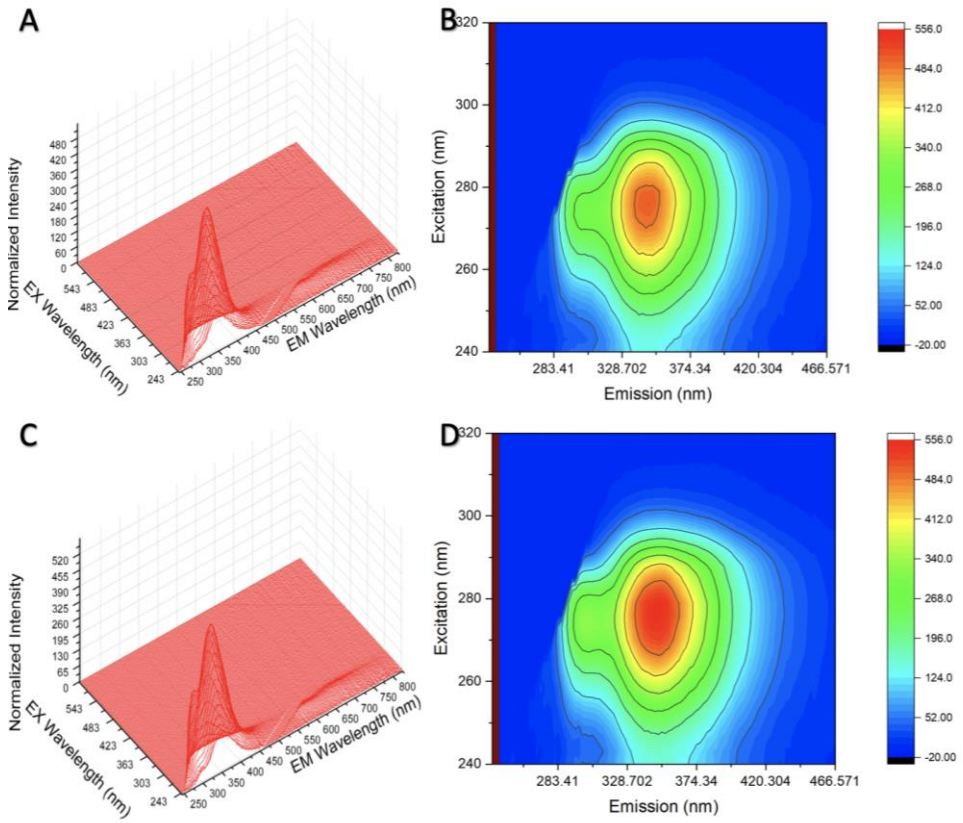

Figure 4.1. The samples were stored under dark and cold conditions and tested on day 28. (A) Three-dimensional diagram of pH7.0 feed medium. (B) Fluorescence excitation/emission matrix spectrum of pH7.0 feed medium. (C) Three-dimensional diagram of pH10.0 feed medium. (D) Fluorescence excitation/emission matrix spectrum of pH10.0 feed medium.

4.3.2 EEM peaks and peak ratio

In this study, three-dimensional EEM spectroscopy was applied to characterize the complex cell culture media. As shown in **Tables 4.2, 4.3, and 4.4,** feed media A treated with five different pH conditions (pH 7.0, 7.4, 7.8, 9.0, and 10.0) and four storage conditions (dark/light, room temperature, and 4°C). Feed media treated with four temperature conditions (room temperature, 40°C, 45°C, and 50°C) and five storage conditions (dark/light, room temperature,

15°C, and 4°C), and basal media treated with four temperature conditions (room temperature, 40°C, 45°C, and 50°C) and five storage conditions (dark/light, room temperature, 15°C, and 4°C).

Table 4.2. EEM of feed media for pH treatment on day14.

			Peak A		**Peak B**		
PH	**Storage temp**	**Dark/Light**	**Ex/Em**	**Intensity**	**Ex/Em**	**Intensity**	**A/B**
7.0	Cold	Dark	276/345	668	273/304	432	1.55
7.4	Cold	Dark	276/349	659	273/304	403	1.64
7.8	Cold	Dark	276/347	696	273/301	437	1.59
9.0	Cold	Dark	276/347	501	273/301	321	1.56
10.0	Cold	Dark	276/347	588	273/301	369	1.59
7.0	RT	Dark	276/345	631	273/301	387	1.63
7.4	RT	Dark	276/345	622	273/301	393	1.58
7.8	RT	Dark	276/345	622	273/304	386	1.61
9.0	RT	Dark	276/349	576	273/301	358	1.61
10.0	RT	Dark	276/345	656	273/301	407	1.61
7.0	Cold	Light	276/347	1260	273/301	440	2.86
7.4	Cold	Light	276/345	1388	273/301	553	2.51
7.8	Cold	Light	276/349	1204	273/301	531	2.27
9.0	Cold	Light	276/347	1491	273/301	952	1.57
10.0	Cold	Light	276/347	1715	273/301	1082	1.59
7.0	RT	Light	276/345	605	276/304	379	1.60

7.4	RT	Light	276/342	637	276/301	404	1.58
7.8	RT	Light	276/345	651	276/304	405	1.61
9.0	RT	Light	276/349	391	276/304	241	1.62
10.0	RT	Light	276/347	753	276/304	466	1.62

Table 4.3. EEM of feed media for temperature treatment on day14.

			Peak A		**Peak B**		
Treatment temp	**Storage temp**	**Dark/Light**	**Ex/Em**	**Intensity**	**Ex/Em**	**Intensity**	**A/B**
RT	4°C	Dark	276/345	622	273/301	392	1.59
RT	15°C	Dark	276/347	547	273/301	347	1.58
RT	RT	Dark	276/342	558	273/304	356	1.57
RT	4°C	Light	276/345	556	273/308	339	1.64
RT	15°C	Light	276/345	531	273/301	335	1.59
RT	RT	Light	276/345	548	273/304	346	1.58
40	4°C	Dark	276/347	579	273/301	370	1.56

40	15°C	Dark	276/345	585	273/301	367	1.59
40	RT	Dark	276/347	546	273/308	342	1.60
45	4°C	Dark	276/345	569	273/301	364	1.56
45	15°C	Dark	276/345	566	273/301	360	1.57
45	RT	Dark	276/345	531	273/301	338	1.57
50	4°C	Dark	276/345	523	273/301	340	1.54
50	15°C	Dark	276/345	529	273/301	340	1.56
50	RT	Dark	276/345	541	273/304	345	1.57

Table 4.4. EEM of basal media for pH treatment on day14.

			Peak A		**Peak B**		
Treatment temp	**Storage temp**	**Dark/Light**	**Ex/Em**	**Intensity**	**Ex/Em**	**Intensity**	**A/B**
RT	4°C	Dark	276/347	788	273/301	697	1.13

RT	15°C	Dark	276/345	885	273/301	792	1.12
RT	RT	Dark	276/345	895	273/301	795	1.13
RT	4°C	Light	276/345	971	273/301	845	1.15
RT	15°C	Light	276/345	926	273/301	826	1.12
RT	RT	Light	276/345	903	273/301	820	1.10
40	4°C	Dark	276/345	947	273/301	843	1.12
40	RT	Dark	276/342	1752	273/301	1486	1.18
45	4°C	Dark	276/345	927	273/301	822	1.13
45	15°C	Dark	276/345	946	273/301	823	1.15
45	RT	Dark	276/347	942	273/298	817	1.15
50	4°C	Dark	276/347	937	273/298	819	1.14
50	15°C	Dark	276/34	958	273/30	822	1.17

50	RT	Dark	5 276/345 944		1 273/301 818		1.15

Figures 4.2, 4.3, and 4.4 show EEM fluorescence spectra under each condition. The results showed that the spectral shapes and the profile of the cell culture media contours in different treatment conditions and different storage conditions were quite similar. The EEM fluorescence spectra of the feed media and basal media were all showed two peaks. The central peak was identified at excitation/emission wavelengths of 276/342–349nm (Peak A), while the second central peak was identified at excitation/emission of 273/298-308nm (Peak B). Peak B was attributed to the tyrosine-like fluorophores, and peak A to the specific molecule-like fluorophores.[14]

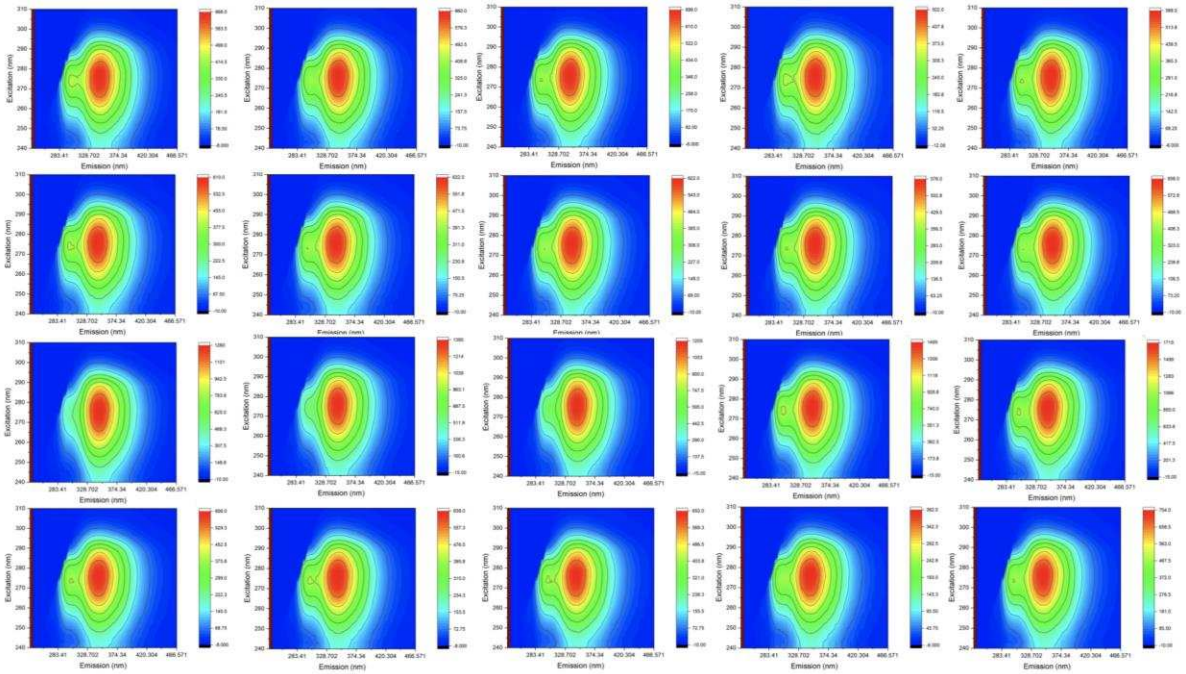

Figure 4.2. EEM fluorescence spectra of feed media at various pH values stored in different conditions.

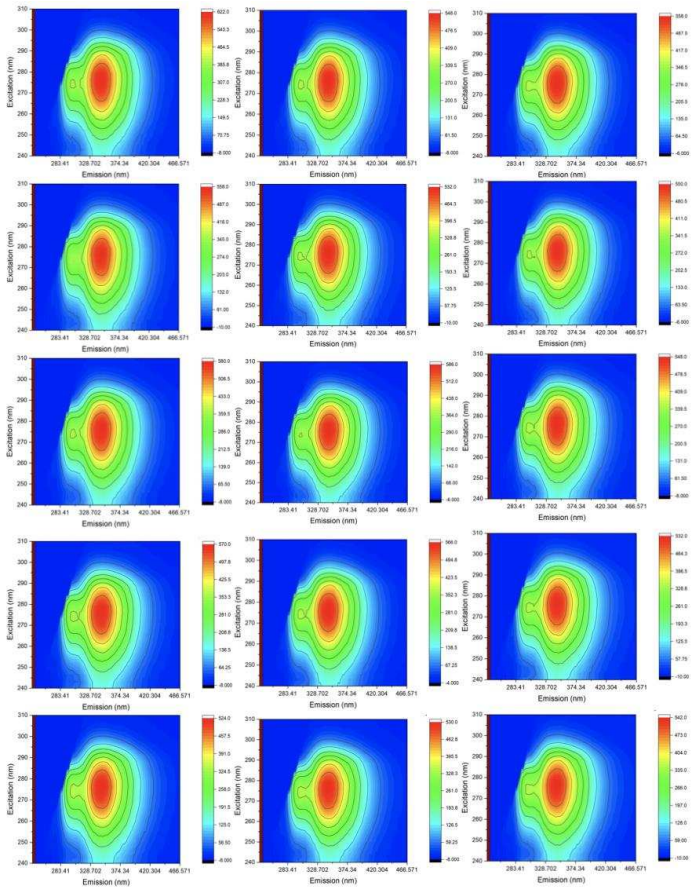

Figure 4.3. EEM fluorescence spectra of feed media treated with different temperature and stored in different conditions.

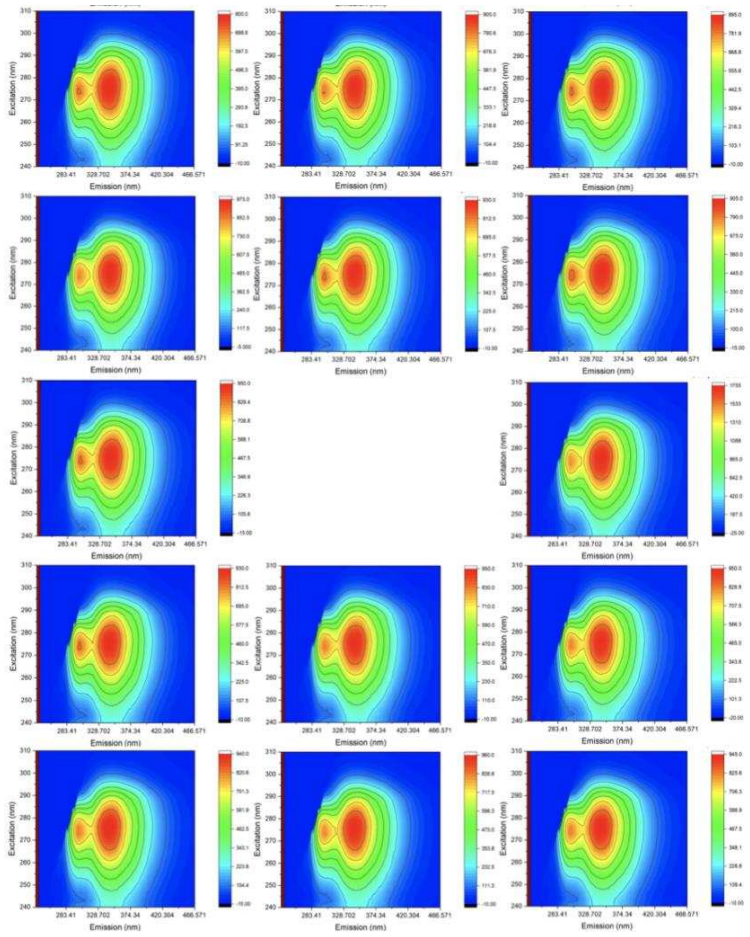

Figure 4.4. EEM fluorescence spectra of basal media treated with different temperatures and stored in different conditions.

EEM spectra of the cell culture feed media at pH 7.0-10.0 are illustrated in **Figure 4.2**. In **Table 4.2**, peak A's site is at 273/342-349nm, while Peak B is at 276/301-304nm. Dark and cold storage conditions give rise to a more stable peak location than light and room temperature conditions. The intensity ratio of A/B is around 1.57-1.64 except for three cold, and light storage conditions feed media near-neutral pH (7.0, 7.4, and 7.8).

EEM spectra of the cell culture feed media and basal media treated with different temperatures were illustrated in **Figures 4.3 and 4.4**, whereas their spectral characteristics are

listed in **Tables 4.3 and 4.4**. Under the same conditions, Peak A/ Peak B's intensity ratios for feed media remained around 1.6, and basal media remained 1.13. Different peak ratios at equal treatment and storage conditions are likely to suggest that Peaks A and B's fluorophores in the cell culture media samples have a different composition. Besides, the different values of the two cell culture media's peak intensity ratio imply that the composition differences and amount differences in the compounds are responsible for the fluorescence characteristics of the feed media and basal media. EEM spectra show two peaks which means at least two components were tested in the cell culture media.

4.3.3 Conditions variance analysis

According to the excitation-emission matrix contour, the center of peak A and peak B are around the excitation of 273nm. The emission from 283.4nm to 825.5nm is shown in **Figure 4.5.** In **Figures 4.5A and 4.5B**, the highest sample intensity was shown around the emission of 345nm, while another small peak was shown around the emission of 301nm. The intensities were identified as the accumulation of the substances in the samples. In **Figure 4.5A**, the sample stored at 4°C showed the highest intensity and the biggest integrate area, while the samples stored at 15°C and room temperature showed lower intensity. The temperature of 4°C is better to maintain the substances in the cell culture media samples. In **Figure 4.6B**, the intensity increases with the decrease of temperature. The relationship between treatment temperature and intensity was shown in **Figure 4.6**. In the treatment temperature scale from room temperature to 45°C, the intensity decreases slowly, while from 45°C to 50°C, the intensity decreases sharply. It seems because of the deterioration of certain amino acids in the cell culture medium at high temperatures.

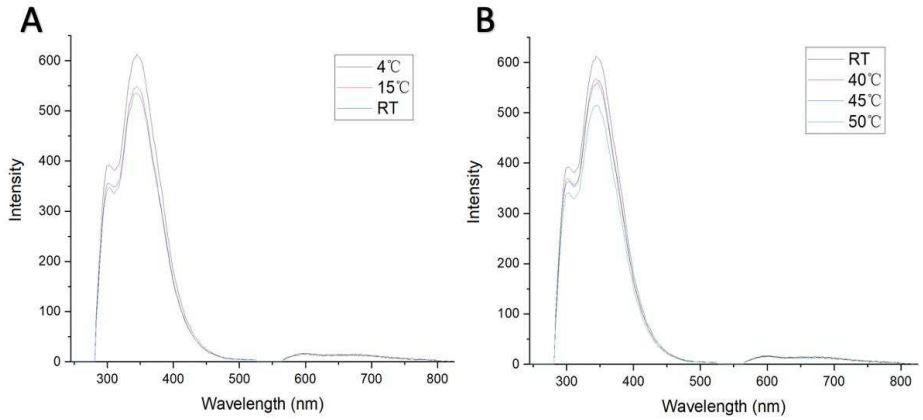

Figure 4.5. Cell culture feed media samples at the excitation of 273 nm, (A) treated with room temperature for three hours and then stored at 4°C, 15°C and room temperature for 14 days, (B) treated with room temperature, 40°C, 45°C, and 50°C for three hours and then stored at 4°C for 14 days.

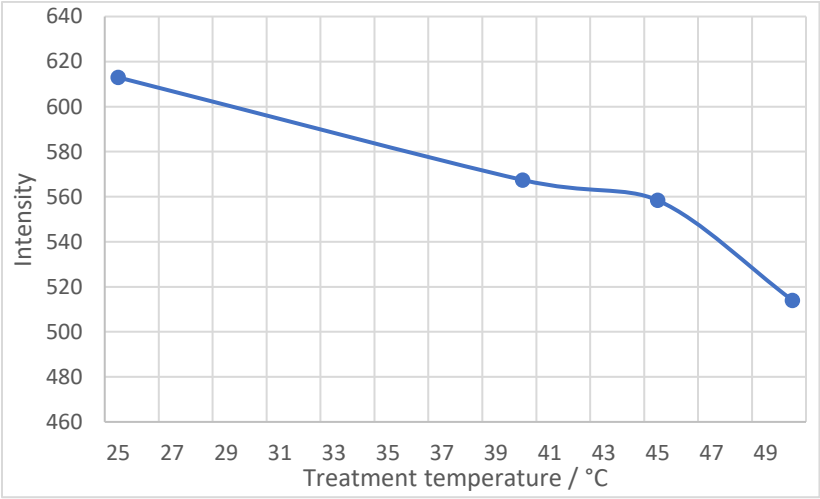

Figure 4.6. Cell culture feed media under different temperature treatment conditions with the variance of intensity at the excitation of 273nm and the emission of 345nm.

4.3.4 PARAFAC model

4.3.4.1 Building the PARAFAC cell culture medium model

The schematic of the steps involved in building the PARAFAC cell culture medium model by fluorescence EEMs (**Figure 4.7**).

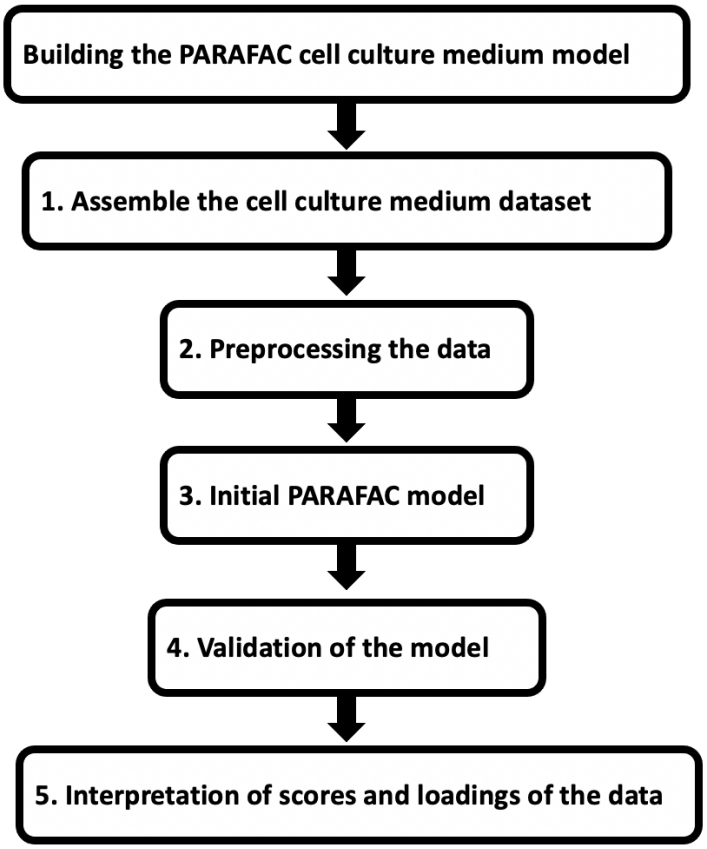

Figure 4.7. The overall approach to building a PARAFAC cell culture medium model. The basic steps are (1) assemble the cell culture medium dataset; (2) preprocessing the data to correct biases, remove scatter and outliers, eliminate non-trilinear data and normalize datasets having significant intensity differences between samples; (3) initial PARAFAC model (4) validation of the model, and (5) interpretation of scores and loadings of the data.

4.3.4.2 Evaluation of PARAFAC model

The main methods for determining the correct number of components and verifying the PARAFAC model can be summarized as the following three: split-half experiments, core consistency diagnostic, and compare with external knowledge of the data being modeled.[5] The number of components was selected based on the core consistency and percentage of explanation of the data.

The explained variance indicates that with the increase of the number of components, the explained variance increased (**Figure 4.8**). To evaluate which number of components can explain the variance, one is to consider the trend of the explained variance is increased or decreased; the other is to consider which explained variance is sufficient. Two components were selected for the data studied (**Table 4.5**). It is because the fluorescent landscape contains two visually identifiable peaks (**Figure 4.1**). However, due to the dominant response of other fluorophores that may be present in the cell culture medium due to differences in light / dark storage conditions, pH treatment, and temperature, some peaks with low concentration of fluorophores. Therefore, more than two fluorophores may contribute to the fluorescence spectrum obtained here.

From another perspective, even the explained variance of the six components is only 95%, which may partly reflect that there may be many low-level fluorophores in the cell culture medium. In this case, there may not be an exact amount of PARAFAC components to capture them.

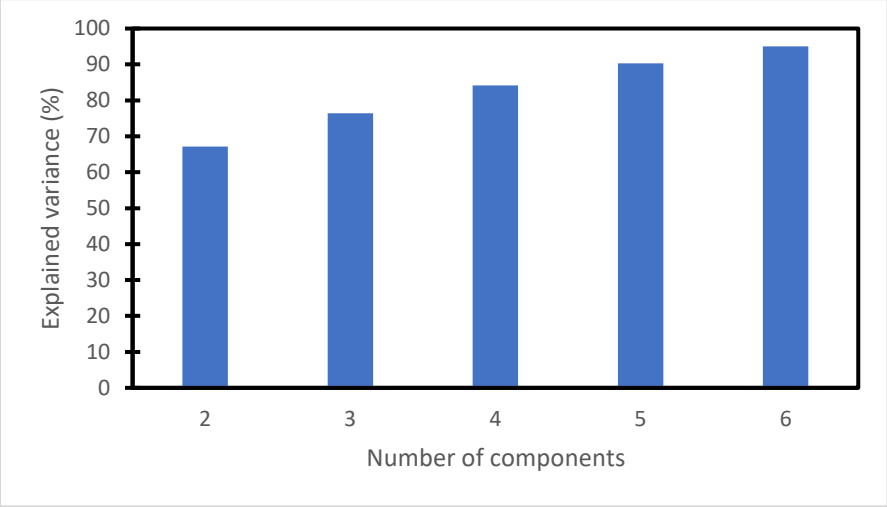

Figure 4.8. Explained variance vs 2-6 components in PARAFAC model

Table 4.5. Core consistency and explained variance for PARAFAC models with 2–6 components.

Components#	Core consistency (%)	Explained variance (%)
6	2	95
5	38.1	90.3
4	77.3	84.2
3	87.1	76.4
2	96.7	67.1

Core Consistency Diagnostics is a recommended method for finding the number of components to use in PARAFAC. Core consistency and explained variance for PARAFAC models with 2–6 components were shown in **Table 4.5.** The core consistency decreases as the number of components increases (**Figure 4.9**). The decrease of the core consistency can attain an appropriate number of components. For a one-component model, the core consistency is always 100%. A two-

component model gives a core consistency of 96.7%. The six-component model's core agreement is only 2%, which is far below the ideal value of 100%, indicating that they may be over-fitting. The six-component model is not stable, so the core consistency suggests that the two components are optimal.

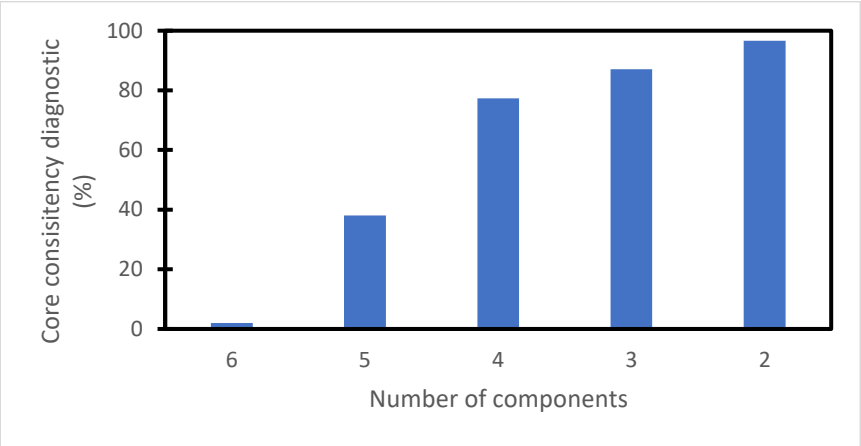

Figure 4.9. Core consistency diagnostic vs 2-6 components in PARAFAC model

In conclusion, the two components are sufficient to explain the variation in the data. Whether it is the two peaks shown in the EEM spectrum or the results given by the diagnosis can provide enough evidence to prove the correctness of the two components.

4.3.4.3 Visual appearance of the loadings

Figure 4.10 shows the loadings for the two-component and three-component models. The emission spectra in both models have features that are not consistent with expectations. The two sharp peaks smaller than 300 nm and 350 nm indicate that the model cannot correctly identify the spectrum of pure chemical components. Since it is known that this spectrum contains tryptophan based on the position of excitation and emission, it is speculated that the peaks less than 300 nm may be a mixture of other low-concentration fluorophores. According to experience, the

photochemical fluorescence products of tryptophan and tyrosine mainly include kynurenine (λ_{ex} 355 nm, λ_{em} 485 nm), hydroxykynurenine (λ_{ex} 370 nm, λ_{em} 460 nm), N-formylkynurenine (λ_{ex} 265-330 nm, λ_{em} 440 nm), 5-hydroxytryptophan (λ_{ex} 280 nm, λ_{em} 340 nm) and dityrosine (λ_{ex} 300 nm, λ_{em} 400 nm).[15-18] The speculation of these photochemical products can also make preliminary judgments from the changes in the cell culture medium's appearance, which also explains the slight increase in excitation wavelength compared to pure tryptophan in the PARAFAC model. Besides, the double peaks in the loadings also indicate that the true spectrum may not limit non-negativity.

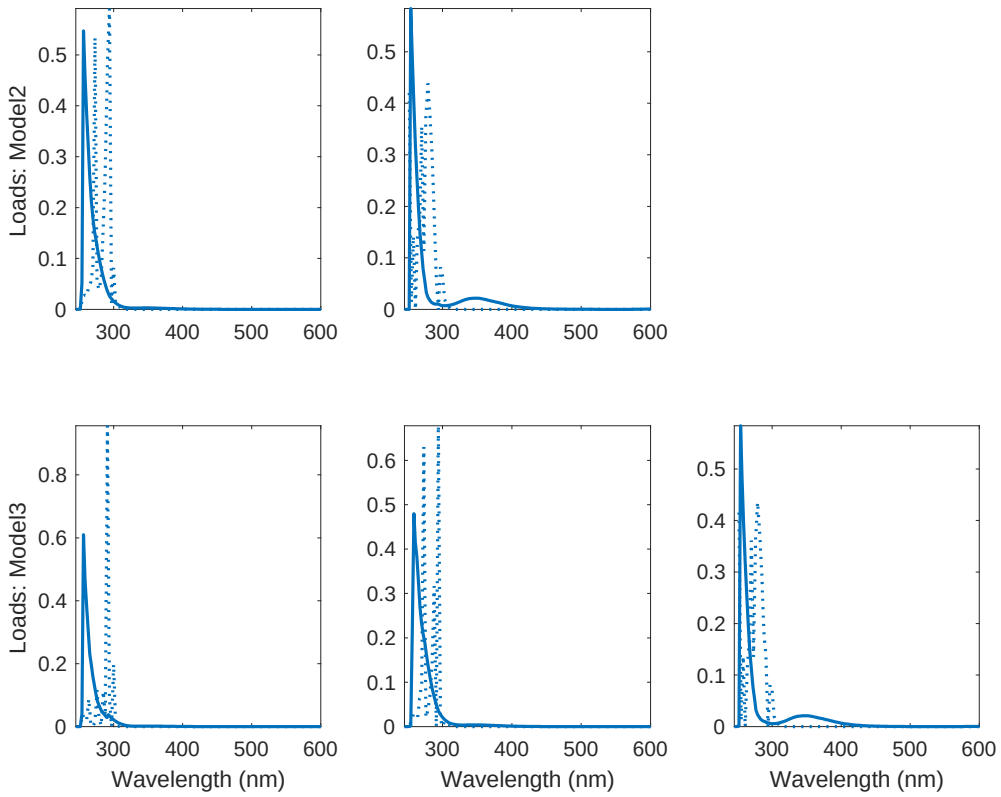

Figure 4.10. Emission and excitation loadings of two- and three-component PARAFAC models. The lines indicate excitation (solid) and emission (dotted).

Considering that there is no significant difference between the two-component model and

the three-component model, and it is known that the tryptophan, tyrosine, and phenylalanine we have added into the cell culture medium is fluorescent within the range of the excitation-emission spectrum (Although phenylalanine only shows a small part in theory), the three-component model would be the first choice.

4.3.4.4 Applying constraints

The results of with non-negativity and the results without non-negativity did not show a big difference between the three components to the six components within 1% (**Table 4.6**). However, as the number of components increases from three to six, the explained variance increases from 84.3% to 96.8%. By definition, the fit of the constrained model will be lower than that of the unconstrained model. The similarity results show that the constrained model mainly filters out little noise rather than system changes. Therefore, from this point of view, the constraints also seem to be effective.

Table 4.6. With non-negativity constraint and without non-negativity constraint of 3-6 components.

Number of components	**With non-negativity constraint**	**Without non-negativity constraint**
3	84.3	83.9
4	90.2	90.3
5	94.6	95.1
6	96.8	97.3

4.3.4.5 Evaluation of score values

Figure 4.11 shows a scatter plot of the three-component PARAFAC model scores (loads are shown in **Figure 4.10**). The distribution of these scores is relatively neat and does not indicate extreme outliers based on the score value. After marking the scattered points, it is found that the cell culture medium samples under the same storage conditions have similar scores in the model. These scores point to the consistency or similarity of the fluorescent chemical composition in the cell culture medium under the same storage conditions and the fluorescent chemical composition in the culture medium under different storage conditions. Through the analysis of the composition score in the PCA model, more details are found. The meaning of the score will be further elaborated in the subsequent PCA model.

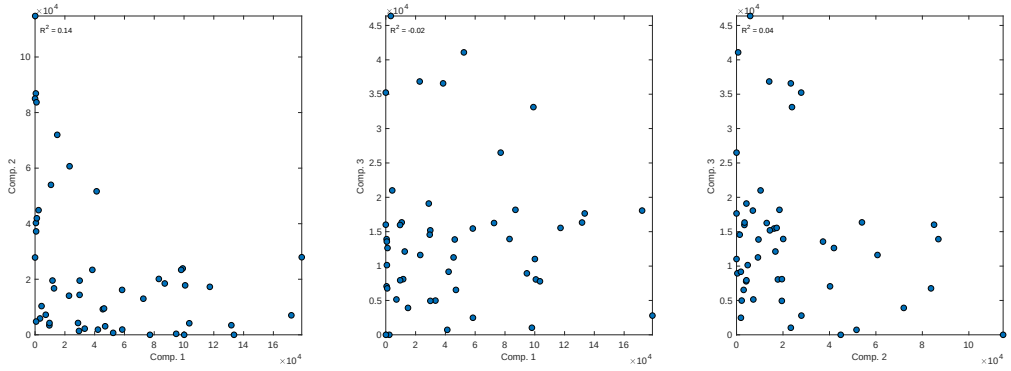

Figure 4.11. Scatter plot of the score values for the three-component PARAFAC model.

4.3.5 PCA model

Principal component 1 of **Figure 4.12** attained 71.885% information, while principal component 2 attained 27.323% information (**Table 4.7**). The cell culture medium sample's stored at 15°C show positive values in principal component 1 and principal component 2. In comparison, the cell culture medium sample's stored at 4°C show positive values in principal component 1 and

negative values in principal component 2. The cell culture medium sample's stored at room temperature are almost shown negative values in principal component 1 and positive values in principal component 2. Thus, comparing with the different treatment temperatures, different dark/light storage, and different storage temperature, storage temperature is the most important impact factor in storage conditions.

Table 4.7. The eigenvalues and proportions of PC1 and PC2.

	PC1	**PC2**
Eigenvalue	71.885	27.323
Proportion	0.719	0.273

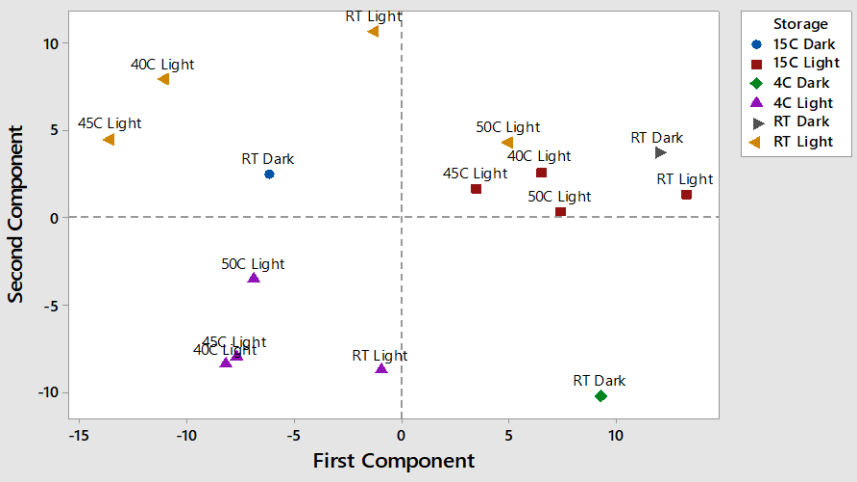

Figure 4.12. Principal component analysis for cell culture feed media samples treated at room temperature / 40°C / 45°C / 50°C for 3h and then stored at room temperature / 15°C / 4°C and light / dark conditions for 28 days.

This result implies that the storage temperature has a relatively significant effect on the fluorescent chemicals in the cell culture medium, consistent with the analysis results of changes in

the amino acid concentration.

Principal component 1 of **Figure 4.13** attained 82.3% information, while principal component 1 attained 11.7% information (**Table 4.7**). The effect of different treatment pH, different dark/light storage, and different storage temperature on the cell culture medium does not seem to have a significant impact on the excitation-emission spectroscopy analysis of the cell culture medium, and the difference is not significant. This result suggests that the changes in the fluorescent chemical composition of the cell culture medium are similar.

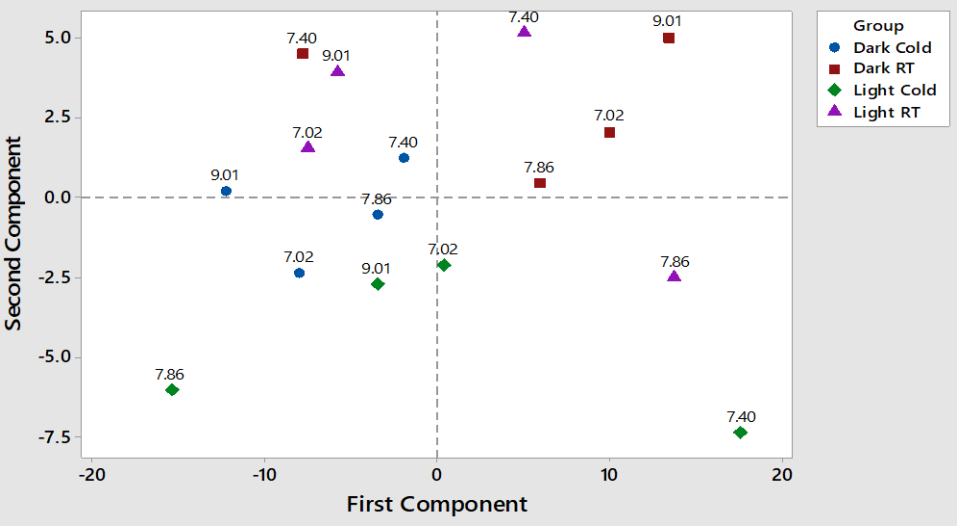

Figure 4.13. Principal component analysis of cell culture feed media samples treated to pH7.0 / pH7.4 / pH7.8 / pH 9.0. Then stored at room temperature / 4°C and light / dark conditions for 28 days.

Table 4.7. The eigenvalues and proportions of PC1 and PC2.

	PC1	**PC2**
Eigenvalue	98.819	14.048
Proportion	0.823	0.117

By comparison, it is found that the scores of the two cell culture media with an initial pH of 7.8 and stored under dark conditions are both around zero. The cell culture medium that has been acid-base adjusted or not stored under dark conditions will be too high or too low in the first two primary principal component analyses compared to the cell culture medium without initial acid-base adjustment or stored under dark conditions. The cell culture medium's quality can be quickly judged based on the distance between these two scores and zero. Therefore, this PCA model can be applied to the quality monitoring of cell culture media.

4.4 Conclusion

This chapter has discussed the best PARAFAC model of known cell culture medium data and obtained the PCA model. Excitation emission matrix spectroscopy has high sensitivity and throughput and can qualitatively quantify the fluorescent chemical molecules in the cell culture medium. This function makes it very suitable for detecting and monitoring changes in medium composition and comparing differences. We analyzed the fluorescent chemical composition of cell culture media under different treatment temperatures, different treatment pH, different dark/light storage, and different storage temperature to monitor the cell culture medium's quality.

The excitation-emission matrix spectroscopy application method combined with PARAFAC and PCA models can be easily transferred to conventional quality control applications in industrial biotechnology production. Rapid monitoring of the quality of the cell culture medium has been achieved.

4.5 References

1. Li, B.; Ryan, P. W.; Shanahan, M.; Leister, K. J.; Ryder, A. G., Fluorescence Excitation–Emission Matrix (EEM) Spectroscopy for Rapid Identification and Quality Evaluation of Cell

Culture Media Components. *Applied spectroscopy* **2011,** *65* (11), 1240-1249.

2. Brunner, M.; Brosig, P.; Losing, M.; Kunzelmann, M.; Calvet, A.; Stiefel, F.; Bechmann, J.; Unsoeld, A.; Schaub, J., Towards robust cell culture processes—Unraveling the impact of media preparation by spectroscopic online monitoring. *Engineering in life sciences* **2019,** *19* (10), 666-680.
3. Suciu, R.-C.; Zarbo, L.; Guyon, F.; Magdas, D. A., Application of fluorescence spectroscopy using classical right angle technique in white wines classification. *Scientific reports* **2019,** *9* (1), 18250.
4. Murphy, K. R.; Hambly, A.; Singh, S.; Henderson, R. K.; Baker, A.; Stuetz, R.; Khan, S. J., Organic matter fluorescence in municipal water recycling schemes: toward a unified PARAFAC model. *Environmental science & technology* **2011,** *45* (7), 2909-2916.
5. Murphy, K. R.; Stedmon, C. A.; Graeber, D.; Bro, R., Fluorescence spectroscopy and multi-way techniques. PARAFAC. *Analytical methods* **2013,** *5* (23), 6557-6566.
6. Stedmon, C. A.; Bro, R., Characterizing dissolved organic matter fluorescence with parallel factor analysis: a tutorial. *Limnology and Oceanography: Methods* **2008,** *6* (11), 572-579.
7. Ohno, T.; Bro, R., Dissolved organic matter characterization using multiway spectral decomposition of fluorescence landscapes. *Soil Science Society of America Journal* **2006,** *70* (6), 2028-2037.
8. Wheeler, K.; Levia, D.; Hudson, J., Tracking senescence-induced patterns in leaf litter leachate using parallel factor analysis (PARAFAC) modeling and self-organizing maps. *Journal of Geophysical Research: Biogeosciences* **2017,** *122* (9), 2233-2250.
9. Andersen, C. M.; Bro, R., Practical aspects of PARAFAC modeling of fluorescence excitation-emission data. *Journal of Chemometrics: A Journal of the Chemometrics Society* **2003,** *17* (4), 200-215.
10. Sanguansat, P., *Principal component analysis*. BoD–Books on Demand: 2012.
11. Abdi, H.; Williams, L. J., Principal component analysis. *Wiley interdisciplinary reviews: computational statistics* **2010,** *2* (4), 433-459.
12. Naik, G. R., *Advances in Principal Component Analysis: Research and Development*. Springer: 2017.
13. Ryan, P. W.; Li, B.; Shanahan, M.; Leister, K. J.; Ryder, A. G., Prediction of cell culture media performance using fluorescence spectroscopy. *Analytical Chemistry* **2010,** *82* (4), 1311-1317.
14. Jordan, M.; Mac Kinnon, N.; Monchois, V.; Stettler, M.; Broly, H., Intensification of large-scale cell culture processes. *Curr. Opin. Chem. Eng.* **2018,** *22*, 253-257.
15. Zhang, L.; Henson, M. J., A practical algorithm to remove cosmic spikes in Raman imaging data for pharmaceutical applications. *Applied spectroscopy* **2007,** *61* (9), 1015-1020.
16. Pirie, A., Fluorescence of N'-formylkynurenine and of protein exposed to sunlight. *Biochemical Journal* **1972,** *128* (5), 1365.
17. Calvet, A.; Li, B.; Ryder, A. G., A rapid fluorescence based method for the quantitative analysis of cell culture media photo-degradation. *Analytica chimica acta* **2014,** *807*, 111-119.
18. Neutsch, L.; Kroll, P.; Brunner, M.; Pansy, A.; Kovar, M.; Herwig, C.; Klein, T., Media photo-degradation in pharmaceutical biotechnology–impact of ambient light on media quality, cell physiology, and IgG production in CHO cultures. *Journal of Chemical Technology & Biotechnology* **2018,** *93* (8), 2141-2151.

Chapter 5: The application of Process Analytical Technology on cell culture medium quality and subsequent CHO cell culture performance

5. 1 Introduction

In the biopharmaceutical industry, cell culture performance and biologics are affected by medium preparation conditions. The previous chapter examined if adjusting the preparation pH or temperature could resolve the issues resulted from media precipitation. It also examined if an elevated preparation pH could maintain solubility when basal powder and AA concentrations were further increased. The previous chapter described the medium preparation parameters to improve AA stability and mitigate precipitation issues. The result suggested that increasing pH and preparation temperature could prevent feed media precipitation during storage.[1]

PCA is a widely used statistical analysis method that can decrease the dimension of a large data set and retain the variance of data while reducing noise and other undesirable consequences.[2, 3] PCA is a useful tool for the evaluation and characterization of cell culture media quality and cell culture metabolomics.[4-6]

EEM spectroscopy is effective in showing fluorescence data and could be used to detect the qualitative and quantitative changes of components in the liquid sample by statistical analysis.[7] Raman spectroscopy has low maintenance and high analysis frequency, which is desirable in industry.[8, 9] It is used as an analytical tool for cell culture media control in the biopharmaceutical industry.[10] FTIR spectroscopy is easy to process and analyze, which is also desirable.[11] In this chapter, three PAT tools – EEM, Raman and FTIR were used to evaluate the cell culture medium quality under different preparation temperatures and pH by PCA and subsequent CHO cell culture performance to validate the result.

5.2 Materials and methods

5.2.1 Materials

All materials were described in Chapter 2 unless otherwise specified.

5.2.2 Medium preparation

As shown in **Figure 5.1**, medium preparation starts with adding water into the container and then heating the water to the designed temperature. For the temperature study, control, conditions 1, 2, and 3 are 40°C, 50°C, 60°C, and 80°C. The basal powder was then added to the water. For the pH study, adjusted conditions 1 and 2 to pH 9 and 10 and recorded the control pH. The next step was mixing all powders until they were fully dissolved. For the temperature study, cool down the temperature to 30°C for all conditions. The heat-sensitive components were added after cooling down. After that, the other components were added to the water, and all powders were mixed until fully dissolved. For the pH study, the control pH was adjusted to 7.4 and the pH of conditions 1 and 2 were tested. The final step is to QS the media and filter it.

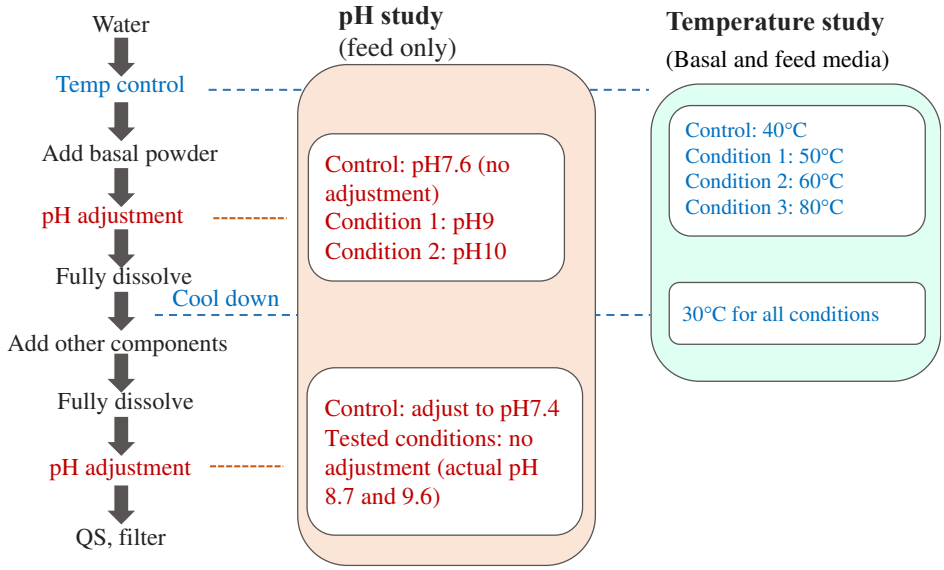

Figure 5.1. Medium preparation workflow and optimization strategy

5.2.3 Instrumentation and data collection

FTIR spectra were recorded using a ReactIR 702L (Mettler Toledo Inc., USA) equipped with an Attenuated Total Reflectance (ATR) probe and Masterflex L/S Easy-load II system at a sample volume speed of 3.6 ml/min. Spectra were collected at 8 cm^{-1} resolution and 512 scans.

Raman spectra acquisition was performed by iCRaman Software 4.1 (Mettler Toledo Autochem, Columbia, MD) operating the Raman RXN2 in this study. An acquisition of 20 s × 35 acquisition was used to acquire intensities for each sample, increasing the signal-to-noise ratio.

EEM measurements were performed using a HORIBA Aqualog model (HORIBA, USA) at room temperature. These measurements involved scanning the emission wavelength at the scale of 244.64-826.67nm (2.33nm increments) with excitation wavelength at the scale of 240-600nm (3 nm increments) of 0.08 seconds integration. A background spectrum of deionized water was measured at the beginning and end of each sample collection run.

5.2.4 Data analysis

Raman data were preprocessed by SIMCA, applying the 1^{st} derivative with 17 points and cubic condition, one distance between each point.

EEM data was preprocessed by Solo (Eigenvector Research Inc., Wenatchee, WA, USA), applied the normalization method for the unit length vector; after that, it was applied the second polynomial order and smoothing, and finally, the data was mean centered.

FTIR, Raman, and EEM data were then performed using MATLAB software Version 7.8 (R2009a) with PLS Toolbox software 7.0.1 (Eigenvector Research Inc., Wenatchee, WA, USA) on a standard desktop computer.

5.2.5 Cell culture performance

Fed-batch production culture was performed in 50 mL TubeSpin bioreactors inoculated at the 4×10^6 cells/mL seeding density. The TubeSpin tubes were incubated in the incubator (Infors, Laurel, MD) at 300 rpm, 5% CO2, 80% humidity, and 37 °C. The feeding strategy started from day 4 with the initial working volume at 18 mL. Viable cell density and viability were tested by Vi-Cell XR automatic cell counter (Beckman Coulter) on days 0, 1, 2, 4, 6, 8, 10, 12, and 14. Glucose, glutamine, glutamate, lactate, and ammonia were quantified using a BioProfile FLEX analyzer (Nova Biomedical). The mAb titer was measured on days 6, 8, 10, 12, and 14 by Cedex BioHT analyzer (Roche). The Tecan handler (Tecan, Männedorf, Switzerland) was used for inoculation, sampling, and feeding operations.

5.3 Result

5.3.1 Mechanism of EEM, Raman and FTIR spectroscopy

As shown in **Figure 5.2**, EEM spectroscopy is based on fluorescence investigation. The cell culture media sample tested by EEM showed excitation wavelength, emission wavelength, and intensity, which is a 3D dataset. EEMs usually have been selected when characterizing the dissolved organic matter or studying the conformational changes. The peak location can provide fluorescence information, while PARAFAC can quantitative the fluorescence amount.[11, 12] Raman spectroscopy is based on Rayleigh scattering.[13] Raman data need preprocessing before the

statistical analysis. Raman is usually selected when investigating carbon bonds in aliphatic and aromatic rings. FTIR spectroscopy is based on IR radiation.[14] Data preprocessing is not necessary. FTIR is usually selected when bonds with significant changes or the reactions in which reagents and reactants are low concentration (**Table 5.1**).

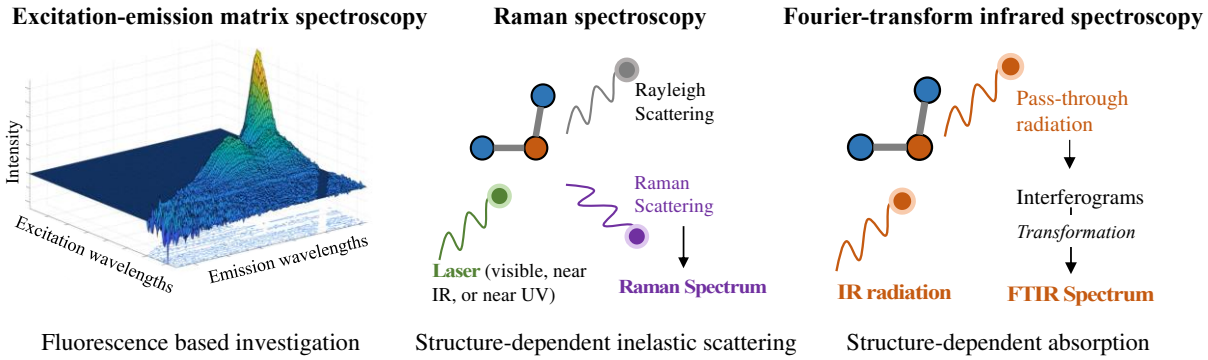

Figure 5.2. Mechanism of three spectroscopy for media characterization.

Table 5.1. Comparison on different PAT tools.

Method	Original spectrum information	Complication of data analysis	When choose:
FTIR	Peak location; peak shape; peak area	Data preprocessing is not necessary	□ Bonds with strong dipole changes, e.g., C=O, O-H, N=O □ Reactions in which reagents and reactants are at low concentration □ Samples under different pH condition
Raman	Peak location; peak area	Need data preprocessing	□ Investigating carbon bonds in aliphatic and aromatic rings are of primary interest □ Bonds that are difficult to see in FTIR, e.g., 0-0, S-H, C=S, N=N, C=C
EEM	Peak location; amount of fluorescence item	Need data preprocessing	□ Characterize dissolved organic matter □ Protein conformational changes

5.3.2 Data pre-processing

The raw FTIR data spectrum showed multiple signals at different wavelengths, which does not need any preprocessing. At 1600 cm^{-1}, control, pH9 and pH10 samples showed different shapes and a sequence peak integration trend. 1600 cm^{-1} wavenumber is contributed to the amide group.[11, 15] Different pHs impact the state of ions in cell culture media [**Figure 5.3(A)**].

Raw Raman data spectrum showed less information, which needs to be preprocessed. Pre-processed data distinguished the pH variance of cell culture media at multiple wavelengths [**Figure 5.3(B)**]. Raw EEM data spectrum showed a center amino acid fluorescence, which must also be pre-processed.

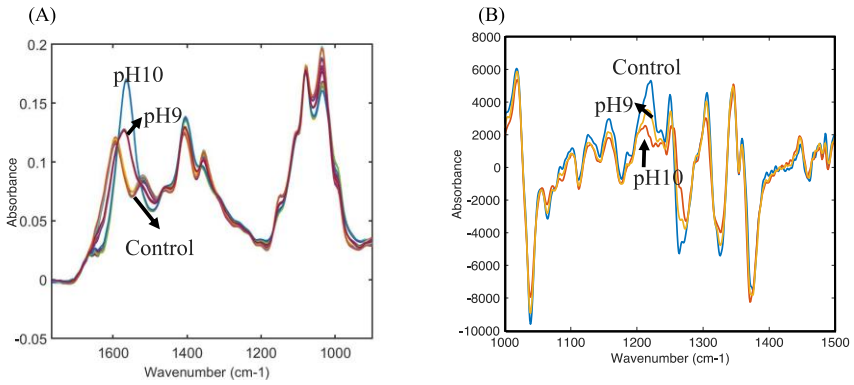

Figure 5.3. Data preprocessing strategies for spectrum data, A) non processing FTIR data, and B) pre-processing Raman data.

5.3.3 Resolution of each method on different temperature

The PCA result of feed media and basal media are shown in the first line and second line in **Figure 5.4**. For the feed media samples on PC1, 80°C treatment conditions are separated by FTIR and Raman, while they are conducted together by EEM. Control, 50°C, and 60°C feed media samples have no significant difference. FTIR collected 45.08% information with all negative scores of 80°C treatment condition samples and almost all positive scores of the other condition

samples on PC1. Raman collected 51.46% of information with the same number of conditions. This result indicates that 80 °C treatment condition samples showed different compositions than the others. High temperature denatures some components of the feed medium. Besides, all 80°C treatment condition samples, including the day 0 sample, are grouped in the negative section. The composition of feed media changed at 80°C treatment condition. This impaction is even higher than the storage days. PC2 by FTIR collected 18.11% of the information, while PC2 by Raman collected 24.40%. PC2 might include the storage time impaction and data process impaction. FTIR and Raman can clearly identify the high-temperature and low-temperature treatment media by PCA.

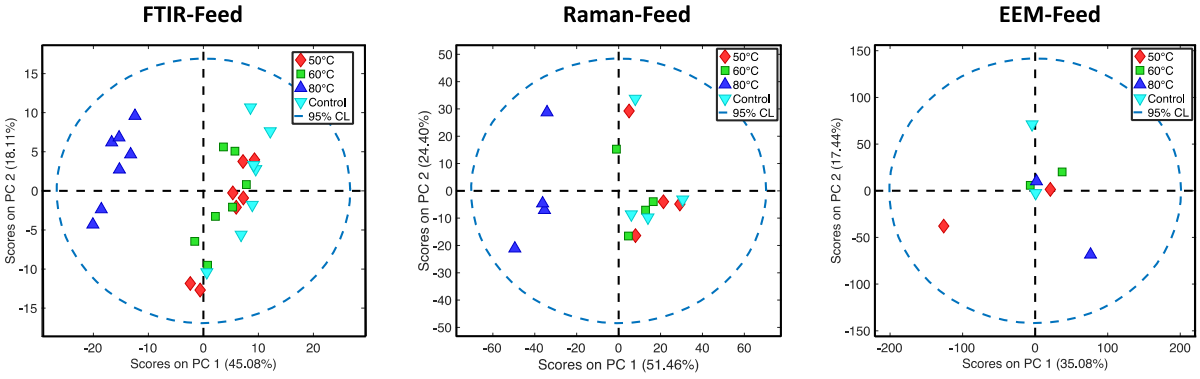

Figure 5.4. Resolution of each PAT method on temperature. The confidence level is 95%. Raman data and EEM data were pre-treatment, as described before.

5.3.4 Cell culture performance on different temperature

The basal and feed media were prepared at escalated temperatures to improve powder solubility and cold room stability. As shown in **Figure 5.5**, at the control condition, viable cell density increased from 4×10^6 cells/mL on day 0 to around 20×10^6 cells/mL on day 10, then decreased to around 15×10^6 cells/mL on day 14. Cell viability decreased from around 95% to 50% after 14 days of culture. The titer amount increased to around 4 g/l after 14 days. The brown line

showed the feed and basal at 80°C temperature condition result. It obviously showed the lowest cell density around day 4 to day 14 and a low titer amount after 14 days of culture. Feed and basal were prepared at 80°C used together to have a negative impact on cell culture performance and titer. Based on ANOVA, it showed a significant impact on viable cell density and titer amount after 14-day fed-batch culture (p-value > 0.05).

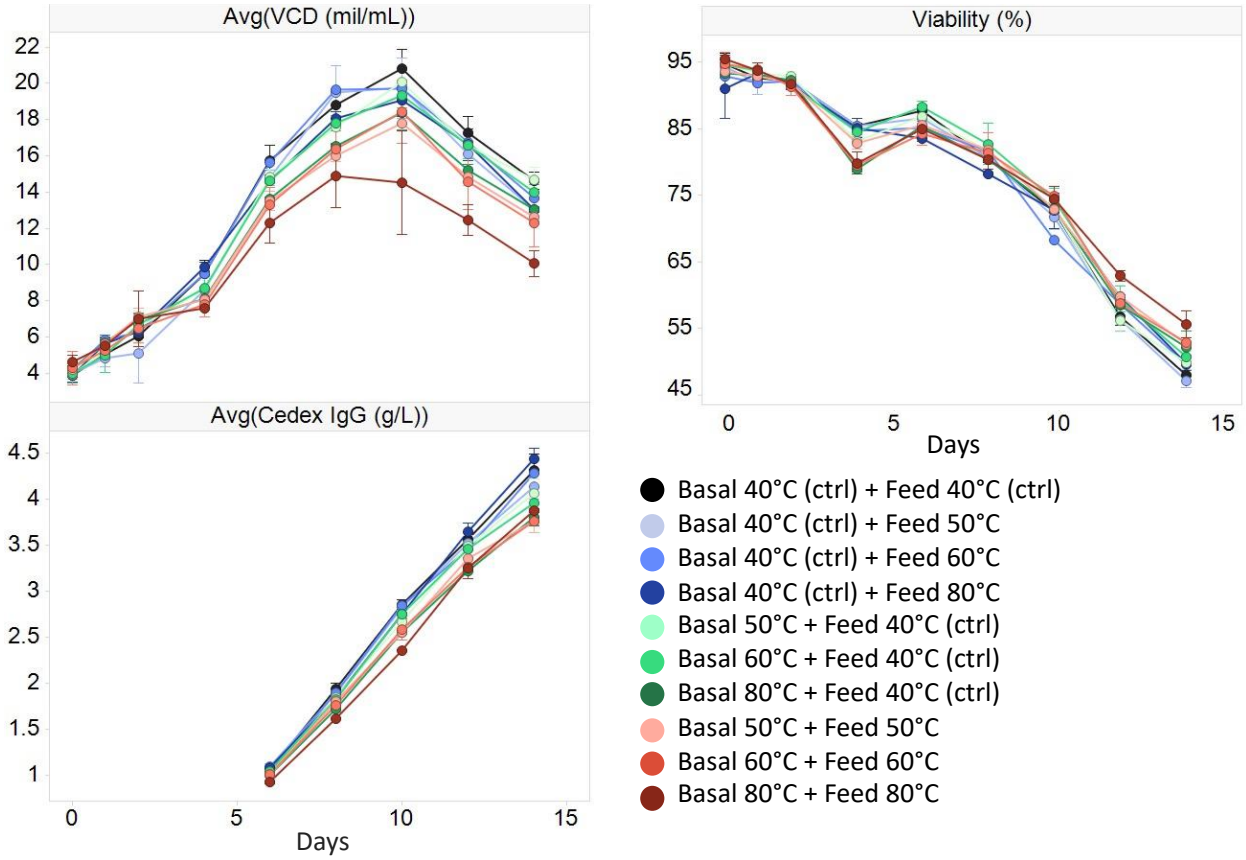

Figure 5.5. Impact of preparation temperature on cell culture performance.

5.3.5 Resolution of each method on different pH

In **Figure 5.5**, the control, pH9, and pH10 conditions are separated by FTIR and Raman,

while they are conducted together by EEM for the feed media samples on PC1. FTIR collected 77.74% of information with negative scores of control condition samples, around zero scores of pH9 samples, and positive scores of pH10 samples on PC1. Raman collected 52.97% of information with negative scores of pH10 samples, around zero scores of pH9 samples, and positive scores of control condition samples on PC1. This result indicates FTIR, and Raman are sensitive to media pH difference, while EEM is not sensitive to media pH difference. FTIR and Raman can identify different pH treatment feed media by PCA. Compared with Raman, FTIR is more sensitive to the pH variance.

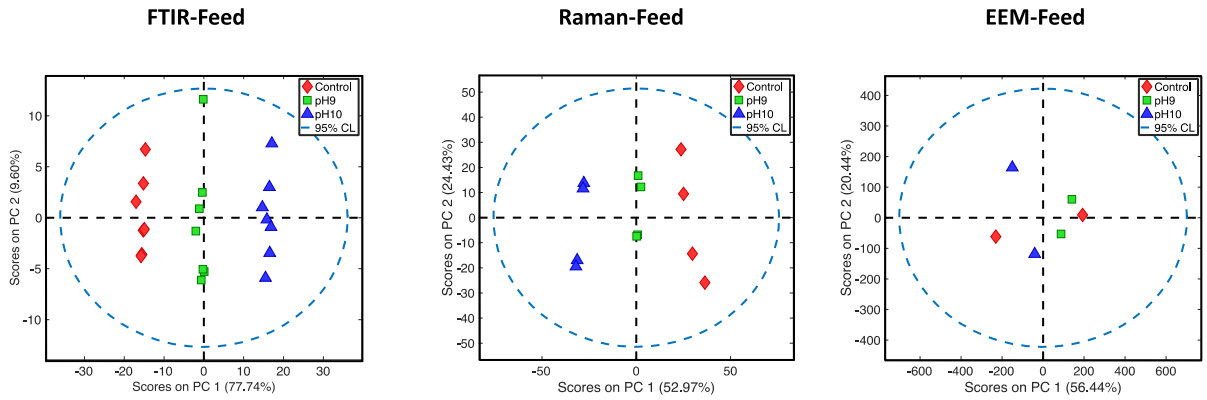

Figure 5.6. Resolution of each method on pH. PCA of feed media under pH9, pH10 and control treatment, tested by A) FTIR, B) Raman and C) EEM. The confidence level is 95%. Raman data and EEM data were pre-treatment, as described before.

5.3.6 Cell culture performance on different pH

The basal and feed media were prepared at pH9 and pH10 to improve powder solubility. As shown in **Figure 5.7**, at the control condition, viable cell density increased from 4×10^6 cells/mL on day 0 to around 20×10^6 cells/mL on day 10, then decreased to around 15×10^6 cells/mL on day 14. Cell viability decreased from around 95% to 50% after 14 days of culture. The

titer amount increased to around 4 g/l after 14 days. Feed and basal were prepared at high pH use individually had no signification impact on cell culture performance and titer. The light green and dark green lines showed the feed and basal at pH9 and pH10 condition results. It obviously showed low cell density around day 4 to day 14 and a low titer amount after 14 days of culture for the pH9 condition, while almost no cell was alive, and no titer was produced for the pH10 condition. Feed and basal were prepared at high pH that was used together to impact cell culture performance and titer negatively. Based on ANOVA, it showed a significant impact on viable cell density and titer amount after 14-day fed-batch culture (p-value > 0.05).

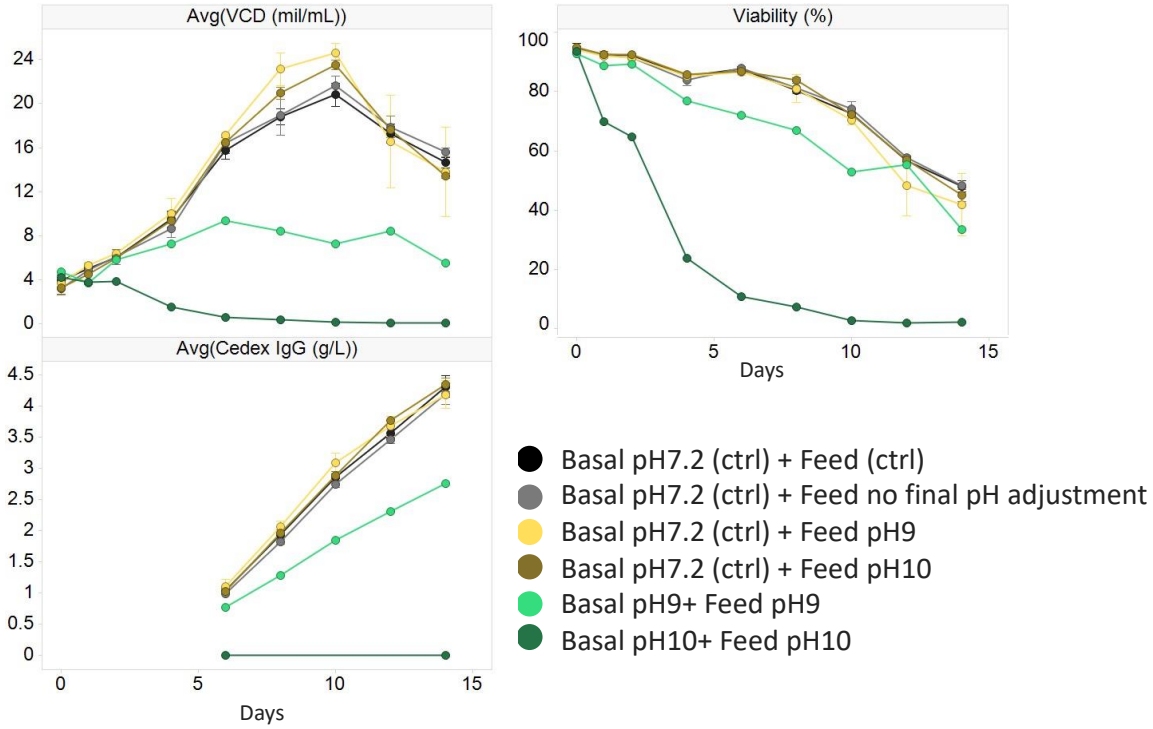

Figure 5.7. Impact of preparation pH on cell culture performance.

5.3.7 Resolution of each method by storage conditions

In **Figure 5.8 (A), (B), and (C)**, day 0, cold storage and RT storage conditions are separated

by FTIR and Raman for the feed media samples on PC2. The RT storage samples' scores all showed negative numbers, day 0 samples were close to zero, and cold storage samples almost showed positive numbers on PC2 by FTIR. The RT storage samples' scores all showed negative numbers, and day 0 and cold storage samples all showed positive numbers on PC2 by Raman. This result explains the variance of different pH treatment feeds media samples during storage time. PC2 collected 9.60% of information by FTIR while collected 24.43% of information by Raman. Feed media samples under different storage days tested by EEM on PCA are separated clearly by PC1 and PC2. PC1 collected 43.11% of the information, while PC2 collected 16.76%. This result illustrates EEM can identify the storage days of feed media samples. Still, when reducing the 3D EEM data to 2D formatting and then converting to PC format, some information may be lost, like the pH impaction of those feed media samples.

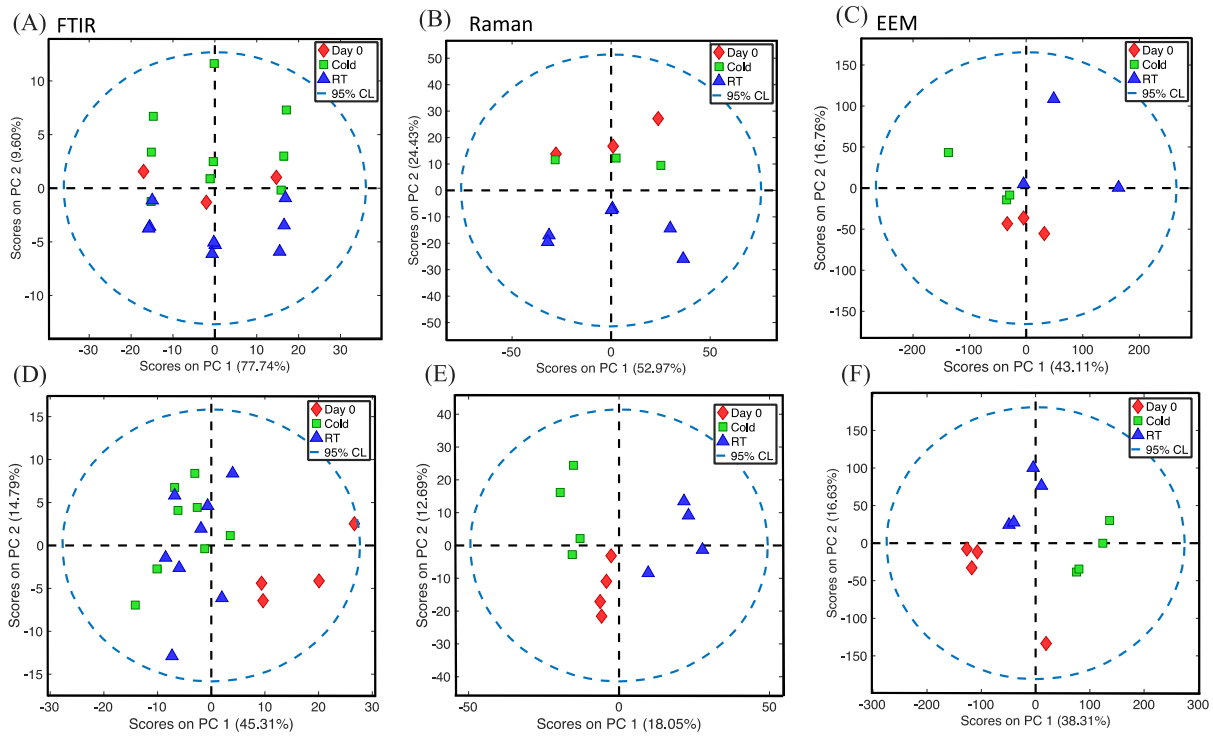

Figure 5.8. PAT application on the storage temperature of cell culture media. Feed media by A)

FTIR, B) Raman, C) EEM; basal media by D) FTIR, E) Raman, F) EEM. The confidence level is 95%. Raman data and EEM data were pre-treatment, as described before.

In **Figure 5.8 (D), (E), and (F)**, The feed media samples under day 0, cold storage, and RT storage conditions are separated clearly by Raman on PC1 with 18.05% of the information. Cold storage samples all showed negative scores, day 0 samples are almost close to zero scores, while RT storage samples all showed positive scores. This result illustrates PCA can identify the basal sample under different storage times. The impact of temperature treatment conditions is less than the storage duration in basal media. In comparison, the impact of temperature treatment conditions is higher than the storage duration in feed media. The basal media samples under day 0 are separated clearly by FTIR on PC1 with 45.31% of the information. Day 0 samples all showed positive scores. Cold and RT storage samples are conducted with zero and less than zero scores. There is no significant difference between the cold storage and the RT storage samples, but they differ from the day 0 sample. The basal media samples under different storage days tested by EEM on PCA are separated clearly by PC1 and PC2. PC1 collected 38.31% of the information, while PC2 collected 16.63%. This result illustrates EEM can identify the storage days of basal media samples.

5.3.8 Application of FTIR and Raman on media characterization

PCA can be used to identify the storage time of the feed media sample. To identify the unknown feed media samples (three months storage samples used here), day 0 and day 30 RT storage samples are used to build the PCA model (**Figure 5.9**). PC1 and PC2 identified the unknown samples, with 52.95% information on PC1 and 25.01% information on PC2 by FTIR.

Day 0 samples and day 30 RT storage samples all showed negative scores, while the unknown samples showed positive scores on PC1, which means the unknown samples were stored longer than one month. Day 0 samples all showed positive scores, while the day 30 RT storage samples and the unknown samples all showed negative scores on PC2, meaning the unknown samples were stored under RT conditions. In conclusion, the unknown feed media samples were stored longer than one month. The unknown samples are not suggested to use in the future.

In **Figure 5.9 (B)**, PC1 and PC2 identified the unknown samples, with 48.56% of information on PC1 and 36.75% information on PC2 by Raman. Day 0 samples, day 30 RT storage samples, and the unknown samples showed a trend sequence from the bottom right to the top left, which means the unknown feed media samples were stored under RT conditions longer than one month.

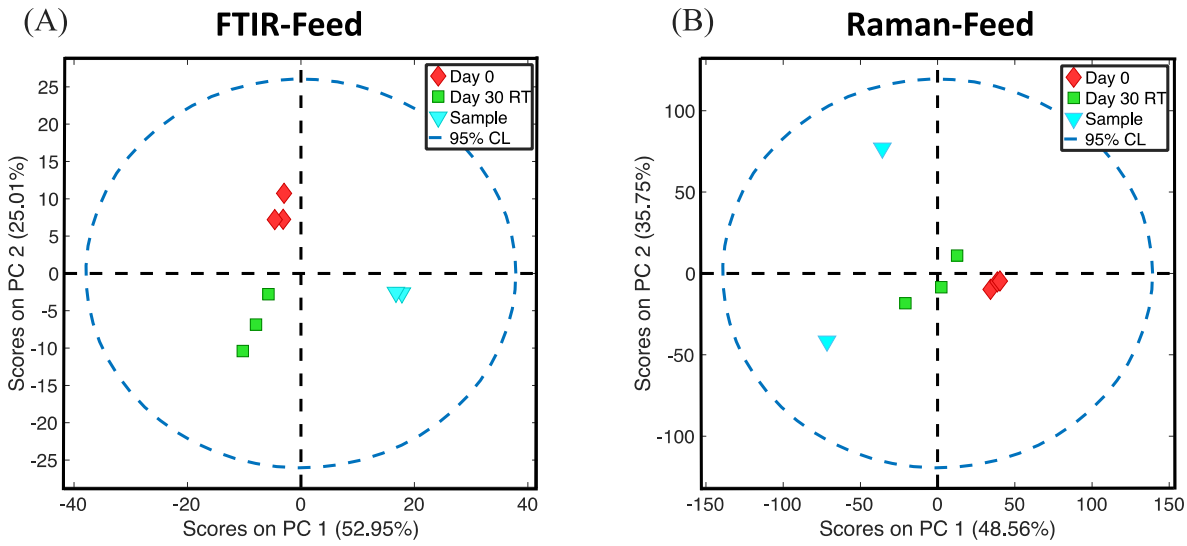

Figure 5.9. Application of FTIR and Raman on media characterization. A) FTIR-Feed media and B) Raman-Feed media. The confidence level is 95%. Raman data and EEM data were pre-treatment, as described before.

Comparing the FTIR and Raman using the media quality evaluation model, Raman provided a clear sample storage trend on PC1, from day 0 storage to one-month storage to three-month storage from higher to lower scores. In contrast, the storage duration variance on the PCA of FTIR is shown on PC1 and PC2. When analyzing the FTIR PC1 and PC2, it needs to combine with more information. Raman is more desired than FTIR for the quick media quality evaluation due to its visualization on PC1. FTIR is more desired than Raman for the deep study on media component concentration variance due to its information detailing.

5.4 Conclusion

This chapter compared three PAT tools – EEM, Raman, and FTIR to evaluate the cell culture medium quality by PCA. The result showed FTIR and Raman could split the high pH (pH9 and pH10) and high-temperature treatment media (80°C), different storage temperature media (cold and RT), and extended storage media (one month and three months) from the control media, which are useful for media characterization. The CHO cell culture performance result also validated the use of FTIR and Raman for media quality evaluation. The cell used high pH (pH9 and pH10) and high-temperature treatment media (80°C) showed lower live cell density and lower titer amount. Using this method to test the media quality requires less than ten minutes for quick evaluation. In contrast, using the original method to test the vital component's concentration may cost more than five hours. EEM showed unsatisfied results by PCA because, as mentioned in the previous chapter, EEM spectroscopy is a 3D data set. At the same time, PCA is a 2D data set analysis method, which means some data will lose when using PCA to handle EEM data. Multiway PCA and PARAFAC are the more desirable for EEM data analysis in recent years. However, PCA is fair for the three PAT tools for comparison. Based on this research, FTIR and Raman can further

apply to the in-situ metabolic monitor by PLS and offline media evaluation by PCA.

5.5 References

1. Cui, W.; Ou, J.; Xu, J.; Anderson, N.; Borys, M.; Li, Z.; Khetan, A.; Liu, S., Impact of preparation pH and temperature on amino acid stability of highly concentrated cell culture feed media. *Journal of Chemical Technology & Biotechnology* **2022,** *97* (8), 2078-2086.
2. Abdi, H.; Williams, L. J., Principal component analysis. *Wiley interdisciplinary reviews: computational statistics* **2010,** *2* (4), 433-459.
3. Sanguansat, P., *Principal component analysis*. BoD–Books on Demand: 2012.
4. Kim, J. Y.; Rhim, W.-K.; Seo, H. J.; Lee, J. Y.; Park, C. G.; Han, D. K., Comparative analysis of msc-derived exosomes depending on cell culture media for regenerative bioactivity. *Tissue Engineering and Regenerative Medicine* **2021,** *18* (3), 355-367.
5. Li, B.; Ryan, P. W.; Ray, B. H.; Leister, K. J.; Sirimuthu, N. M.; Ryder, A. G., Rapid characterization and quality control of complex cell culture media solutions using raman spectroscopy and chemometrics. *Biotechnology and bioengineering* **2010,** *107* (2), 290-301.
6. Čuperlović-Culf, M.; Barnett, D. A.; Culf, A. S.; Chute, I., Cell culture metabolomics: applications and future directions. *Drug discovery today* **2010,** *15* (15-16), 610-621.
7. Li, B.; Ryan, P. W.; Shanahan, M.; Leister, K. J.; Ryder, A. G., Fluorescence Excitation–Emission Matrix (EEM) Spectroscopy for Rapid Identification and Quality Evaluation of Cell Culture Media Components. *Applied spectroscopy* **2011,** *65* (11), 1240-1249.
8. Graf, A.; Lemke, J.; Schulze, M.; Söldner, R.; Rebner, K.; Hoehse, M.; Matuszczyk, J., A novel approach for non-invasive continuous in-line control of perfusion cell cultivations by Raman spectroscopy. *Frontiers in Bioengineering and Biotechnology* **2022**, 642.
9. Veronique Chotteau, Hubert Schwarz, Liang Zhang, Ye Zhang, Caijuan Zhan, Matthew Cheeks, Richard Turner, Andreas Castan, and Francisco Vilaplana, "Strategy for targeted delivery of key nutrients in high cell density perfusion" in "Integrated Continuous Biomanufacturing IV", Veena Warikoo, Roche, USA Alois Jungbauer, BOKU, Austria Jon Coffman, Boehringer Ingelheim, USA Jason Walther, Sanofi, USA Eds, ECI Symposium Series, (2019).
10. Mayrhofer, P.; Reinhart, D.; Castan, A.; Kunert, R., Monitoring of heat-and light exposure of cell culture media by RAMAN spectroscopy: Towards an analytical tool for cell culture media quality control. *Biochemical Engineering Journal* **2021,** *166*, 107845.
11. Amir, R. M.; Anjum, F. M.; Khan, M. I.; Khan, M. R.; Pasha, I.; Nadeem, M., Application of Fourier transform infrared (FTIR) spectroscopy for the identification of wheat varieties. *Journal of food science and technology* **2013,** *50*, 1018-1023.
12. Murphy, K. R.; Stedmon, C. A.; Graeber, D.; Bro, R., Fluorescence spectroscopy and multi-way techniques. PARAFAC. *Analytical methods* **2013,** *5* (23), 6557-6566.
13. Ball, D. W., Theory of Raman spectroscopy. *Spectroscopy* **2001,** *16* (11), 32-34.
14. Simonescu, C. M., Application of FTIR spectroscopy in environmental studies. *Advanced aspects of spectroscopy* **2012,** *29* (1), 77-86.
15. Gallagher, W., FTIR analysis of protein structure. *Course manual Chem* **2009,** *455*.

Chapter 6: Optimization of adaptation parameters from adhesion cell culture in serum-containing media to suspension in chemically defined media by superlative box design

6.1 Introduction

Mammalian cell cultures are widely used to produce biopharmaceuticals[1, 2]. The adherent cell lines, such as Chinese hamster ovary (CHO) cells, are cultivated in a medium supplemented with serum[3-5]. However, besides the difficulty in scaling up for high throughput process operations, there are many concerns about the use of serum in mammalian culture media. On the one hand, the serum is an undefined mixture of components that raises ethical and animal issues[6, 7]. On the other hand, the serum has a variable composition that impacts product quality[1, 7, 8]. Therefore, it is essential to adapt the cells in a serum-free medium[9, 10]. However, transferring adherent cells to serum-free suspension culture is still a major challenge in process development[3, 7].

In bioprocess engineering, the design of experiment (DoE) is used in processes to optimize multiple factors[11, 12]. Factorial design is uniform, but it is time-consuming and laborious with high costiveness to perform more significant experimental variables[13, 14]. Doehlert design is attractive because of the uniformity of experimental points[12, 15, 16]. However, the levels in each factor may lead to the non-representativeness of the real experimental values[12]. In this paper, we used an experimental design – superlative box design, a seven-level quadratic response experimental design that includes the uniformity of experimental points while lowering the number of experiments required[12]. The uniformity of this DoE contains: that the level of each factor is the same; the number of occurrences of the given level is the same; the distance between adjacent points is the same.

Response surface methodology (RSM) is a multivariate statistical technique widely used to optimize multiple factors, which can observe the interactions between the variables[17-19]. This paper uses RSM to couple with SBD to build fitted polynomial models of cell adaptation process variables.

ATCC® CRL-10762, which is CTLA-4-Ig-24 CHO cells. CTLA-4 is an abbreviation of cytotoxic T lymphocyte-associated protein 4, which is a negative costimulatory molecule expressed on the surface of activated and regulatory T cells[20-22]. This work describes a CHO cell line that produces the fusion protein (CTLA-4-Ig) was adapted for growth and CTLA4Ig production in serum-free conditions. The results showed that the CHO cells were successfully adapted to suspension growth and CTLA-4-Ig production in the serum-free conditions remained unchanged. This work reports the first application of the SBD to optimize cell adaptation conditions and predict cell density. The quadratic response was evaluated by RSM. The optimized cell adaptation process is robust, efficient, and cost-effective for reaching the optimum cell density.

6.2 Materials and Methods

6.2.1 Cell line and culture conditions

Adherent CTLA-4-Ig-24 CHO cells (ATCC® CRL-10762) (ATCC, USA) with the initial concentration of 5×10^4 cells/mL were seeded in 75 cm^2 T-flasks (Thermo Scientific, USA) in 90% Dulbecco's modification of Eagle's medium (DMEM) (Corning, Manassas, VA, USA) with 0.2 mM proline (MP, Solon, OH, USA), 0.001 mM methotrexate (Tocris Bioscience, Bristol, UK) and 10% fetal bovine serum (FBS) (Corning, Manassas, VA, USA). Cells were cultured at 37 °C in a humidified atmosphere of 5% CO_2.

6.2.2 Gradual adaptation to serum-free suspension growth

The adaptation of adherent CTLA-4-Ig-24 CHO cells to serum-free conditions was performed from T-flasks (Thermo Scientific, USA) to Erlenmeyer bottles (Thermo Scientific, Rochester, NY, USA) in DMEM with 10% FBS to adapt in a serum-free HyCell CHO medium (HyClone Laboratories, Utah, USA). The cells were maintained at 37 °C in a humidified atmosphere of 5% CO_2.

The adaptation approach for suspension growth of CTLA-4 CHO cells was designed based on the pre-experiment (See results). As shown in **Fig. 6.1**, CHO cells were cultured in one T-flask No.1, then subcultured into three T-flasks No.2, and then subcultured into nine T-flasks No.3. Trypsin-EDTA (Corning, Manassas, VA, USA) was used to disperse the adherent cell layer. All cells were cultured in a 75 cm^2 T-flask with a working volume of 20 ml. All CHO cells from T-flasks No.3 were collected and transferred to one shake flask No.1 while a fixed rotation mixing was provided to the culture. The cells were then transferred to another shake flask No.2 while rotation mixing was provided to the culture. Finally, all CHO cells were transferred to shake flask No.3 on a rotary shaker at 120 rpm. Shake flasks No.1 and No.2 were cultured in a 125 ml Erlenmeyer flask with a working volume of 50 ml, while shake flasks No.3 were cultured in a 500 ml Erlenmeyer flask with a working volume of 200 ml. Cells were cultured in each flask for three days. Cells were centrifuged at 125 g for 5 min at room temperature before inoculating to the next flask. At the end of the optimized run adaptation process, the CTLA-4 CHO cells were successfully adapted to suspension growth in the HyCell CHO medium in a 500 ml Erlenmeyer flask on a rotary shaker at 120 rpm.

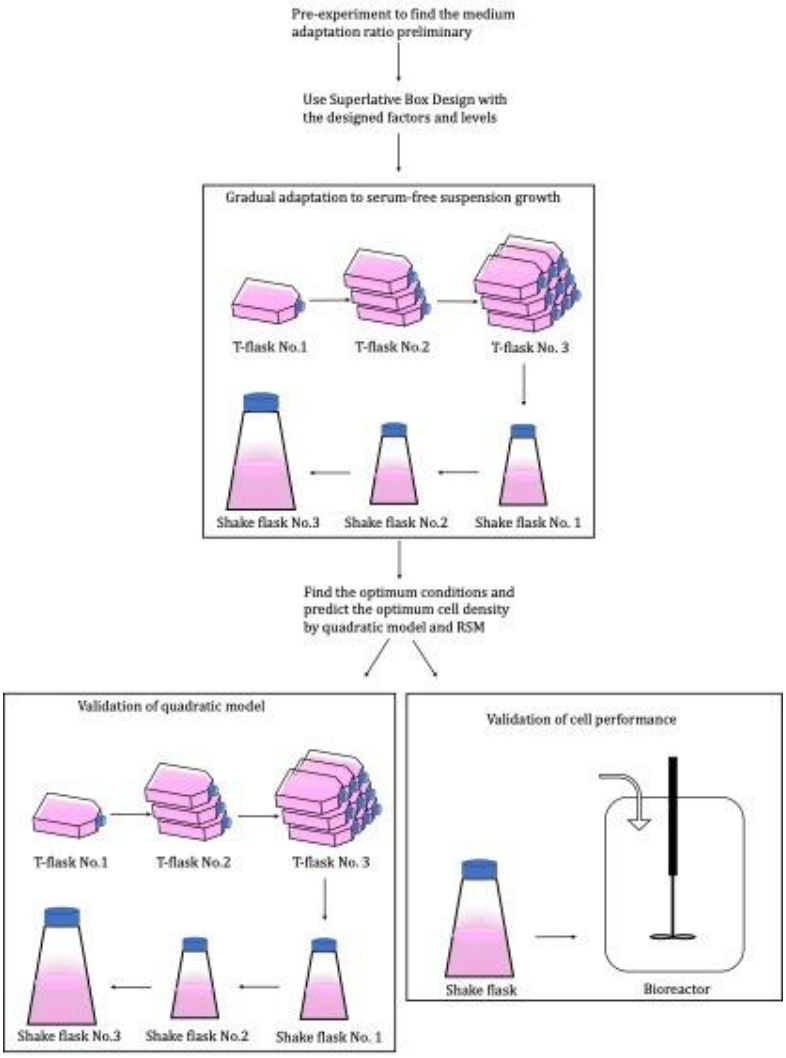

Figure 6.1. Schematic image summarizing the cell adaption strategy

Note: T-flask No.1, No.2 and No.3 are the 75 cm^2 T-flask with a working volume of 20 ml. Shake flasks No.1 and No.2 are the 125 ml Erlenmeyer flask with a working volume of 50 ml, while shake flasks No.3 is a 500 ml Erlenmeyer flask with a working volume of 200 ml.

6.2.3 Suspension culture

A batch suspension culture was conducted in 500 ml Erlenmeyer flasks on a rotary shaker at 120 rpm after the cell was fully adapted to the HyCell medium. Cells were cultured at 37 °C in

a humidified atmosphere of 5% CO_2. Cells were sub-cultured every 3 days in the exponential growth phase for at least five passages. After a stable specific growth rate for three consecutive passages, cells are ready for fed-batch culture.

The fed-batch culture was carried out in a 500 mL glass bioreactor (Applikon, USA) with a starting volume of 350 ml for 14 days. Cells were cultured at 37 °C, pH 7.2, agitation rate of 130 rpm and DO 40% with the initial concentration of 0.4-0.5 × 10^6 cells/mL. The pH was controlled by CO_2 sparging and adding either 7.5% sodium bicarbonate or 0.5M sodium carbonate. Feed medium was added daily from the second day through the end of the cultivation period to maintain the proprietary glucose concentration.

6.2.4 Cell growth assessment

During cultivation and adaptation of CTLA-4 CHO cells to serum-free suspension growth, samples were taken from shake flask No. 3 under serum-free medium at 120 rpm after three-day cultivation. Samples were taken daily during fed-batch suspension culture. Live cell density, cell viability, and cell diameter were determined by counting chamber (Fisher scientific, USA) using 0.4% Trypan-blue dye (Gibco, Grand Island, NY, USA). All samples were measured in triplicates. Light microscopy (Fisher scientific, USA) was used to determine the morphological changes of the cells from adherence to suspension.

6.2.5 Sandwich ELISA Assay

Secretions of CTLA-4 CHO cells were quantified by a sandwich enzyme-linked immunosorbent assay (ELISA). CTLA-4-Ig fusion protein concentration in the culture medium after centrifugation was determined using Mouse CTLA-4 ELISA Kit (Thermo scientific,

Frederick, MD, USA). Color development was measured at 450 nm in a 96-well plate reader by Microplate Photometer (Multiskan FC, Thermo Scientific).

6.2.6 NMR Analysis

The glucose concentrations were determined by 1H nuclear magnetic resonance (NMR) spectroscopy (AVANCE 600, Bruker BioSpin co.) operated at 600 MHz. A modified NMR sample composition was provided by Wang et.al [23], with 0.1 ml internal standard, 0.4 ml D_2O, and 0.5 ml sample. The internal standard solution was prepared by dissolving 4.208% (w/w) glucosamine, 0.223% (w/w) trimethylamine hydrochloride (TMA), and 0.052% (w/w) 3-(trimethylsilyl) propionic-2,2,3,3-D4 acid (TSP). The internal was stored at −20 °C after preparation. TSP was used as a chemical shift reference to set zero. The peak area of glucosamine was used to calibrate the peak area of glucose.

6.2.7 Superlative box design

Fig. 6.2 shows the SBD examples of two-factor and three-factor. All experimental runs are in the factor space. The number of independent experiments (N) is determined by:

$$N = I^2 + I + 1 \tag{1}$$

Where I is the number of factors (or independent variables).

The coefficient of seven SBD levels (α_{SBD}) is determined by:

$$\alpha_{SBD} = \frac{1+\sqrt{I+1}}{I} \tag{2}$$

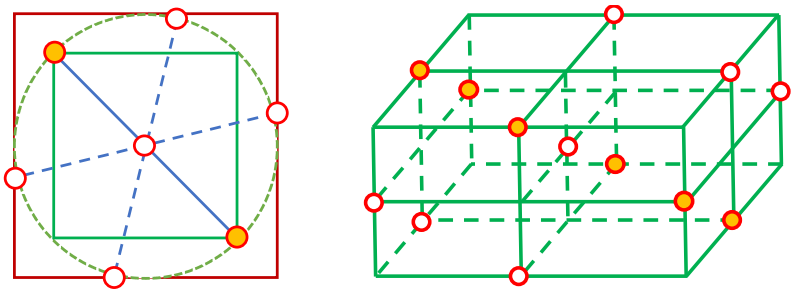

Two-factor SBD Three-factor SBD

Figure 6.2. A simple example of Superlative Box Design with two factors and three factors. In two-factor SBD, all experimental points except the center point are on the circle, and the distance between all adjacent two points is equal. In three-factor SBD, all experimental points except the center point are on the cuboid, and the distance between all adjacent two points is equa

Seven levels and six factors are applied in this experimental design with 43 runs plus three more repeating center runs, as shown in **Tables 6.1, 6.2, and 6.3.** All runs of cell culture were repeated in triplicate at each condition. Compared to the six-factor factorial design needs 729 experimental runs, the central composite design needs 77 experimental runs, and the Box-Behnken design needs 61 experimental runs, SBD needs a lower number of designed experimental runs for quadratic response systems. The repeating center runs are used to ensure the accuracy of the SBD quadratic model.

Level number	**1**	**2**	**3**	**4**	**5**	**6**	**7**
Level coefficient	1	α_{SBD}	1-α_{SBD}	0	α_{SBD}-1	-α_{SBD}	-1

Level constant	1	0.608	0.392	0	-0.392	-0.608	-1

Table 6.1. SBD level constants

Note: The coefficient of seven SBD levels (α_{SBD}) is determined by Equation 2.

Table 6.2. SBD factors

Level number	**X_1** T-flask No.2 FBS (%)	**X_2** T-flask No.3 FBS (%)	**X_3** Shake flask No.1 FBS (%)	**X_4** Shake flask No.1 Rotation speed (rpm)	**X_5** Shake flask No.2 FBS (%)	**X_6** Shake flask No.2 Rotation speed (rpm)
1	9	6	5	150	2.5	150
2	8.4	5.4	4.2	138	1.9	139
3	8.1	5.1	3.8	132	1.6	132
4	7.5	4.5	3	120	1	120
5	6.9	3.9	2.2	104	0.6	104
6	6.6	3.6	1.8	96	0.4	96
7	6	3	1	80	0	80

Note: Seven levels and six factors are chosen in this study to adapt adhesion cells in serum media to suspension in chemically defined media. X_1, X_2, X_3, and X_5 represent the proportion of FBS in the whole medium in T-flask No.2, T-flask No.3, shake flask No.1, and shake flask No.2. X_4 and X_6 represent rotation speed in shake flask No.1 and No.2.

Table 6.3. Analysis of Variance (ANOVA) based on the SBD method in experiments for cell density

Source	Sum Sq.	d.f.	Mean Sq.	F	Prob> F
X_1	13.12	1	13.12	16.86	0.0005
X_2	14.36	1	14.35	18.44	0.0003
X_3	11.57	1	11.57	14.86	0.0009
X_4	0	1	0.0001	0	0.99
X_5	8.00	1	7.99	10.27	0.004
X_6	0.27	1	0.27	0.35	0.56
Error	17.12	22	0.78		
Total	112.09	45			

Note: X_1, X_2, X_3, and X_5 represent the proportion of FBS in the whole medium in T-flask No.2, T-flask No.3, shake flask No.1, and shake flask No.2. X_4 and X_6 represent rotation speed in shake flask No.1 and No.2.

6.2.8 Analysis of Variance

Statistical analysis using analysis of variance (ANOVA) was performed in MATLAB (version R2018a) for determination of significant variables. The significance of each factor was calculated by the P-value. All p-values below 0.05 were considered significant.

6.2.9 Quadratic response calculation

The experimental design adopted the SBD for six variables at seven levels each. The six independent variables were X_1-X_6. X_1, X_2, X_3, and X_5 are the FBS proportion in the total medium in T-flask No.2, T-flask No.3, shake flask No.1 and shake flask No.2, respectively (**Fig.6.1**). Each medium proportion during cell adaptation can be calculated by:

$$V_{DMEM} = 9X \times V_{Total} \tag{3}$$

$$V_{FBS} = X \times V_{Total} \tag{4}$$

$$V_{\text{Serum-free medium}} = (1 - 10X)V_{Total} \tag{5}$$

Where X stands for X_1, X_2, X_3, and X_5. V_{Total}, V_{DMEM}, V_{FBS}, and $V_{Serum\text{-}free\ medium}$ are total working volume, DMEM volume, FBS volume, and serum-free medium volume. X_4 and X_6 are the rotation speed for the shake flask No.1 and No.2, respectively. The independent variable coded regions were −1 (lowest level), α_{SBD}, 1-α_{SBD}, 0 (middle level), $\alpha_{SBD} - 1$, $-\alpha_{SBD}$ and 1 (highest level). The experimental conditions of each experimental run from the pre-experiment studies and the values of the six independent variables are given in **Table 6.1 and 6.2**. There are totally 46 experimental runs, including four center point replications. The 46 experimental runs were performed in random order. The response $\hat{y}$ was assumed to be affected by the six independent variables X_1-X_6. Based on data from this design, we fit a second-order polynomial regression model to optimize cell adaptation steps.

The response function is expressed as

$$\hat{y} = a_0 + \sum_{i=1}^{I} a_i x_i + \sum_{i=1}^{I} \sum_{j=i}^{I} a_{j+I+\frac{2I-i}{2}(i+1)} x_i x_j \tag{6}$$

where $\hat{y}$ stands for the responses to be predicted; i and j represent linear and quadratic coefficients, correspondingly; x_i and x_j correspond to six independent variables; a_0 (intercept), a_i (linear effects), and $a_{j+I+\frac{2I-i}{2}(i+1)}$ (interaction terms) were for regression coefficients. Excel was

performed to calculate the function and predict the optimized factors. The predicted optimum levels of X_1, X_2, X_3, X_4, X_5, and X_6 were obtained by applying regression analysis to Equations (3), (4), and (5) using Excel. The optimum conditions were found through Excel virtual basic programming.

6.2.10 Response surface methodology

The interactive effects of each two factors were analyzed using RSM. Response surface analysis of data was displayed by 3D surface and contour plots performed by MATLAB (version R2018a). Quadratic model keeps four variable constants at the center point (constant) and varies the other two variables within the experimental range to show the cell density. RSM was used to determine the influence of cell adaptation factors on the response of viable cell density.

6.3 Results and Discussion

6.3.1 Design of cell adaptation factors

When the ratio of serum-containing medium (90% DMEM with 0.2 mM proline, 0.001 mM methotrexate and 10% FBS) in the overall medium was reduced, and the ratio of HyCell CHO medium was increased, cells were unable to be adapted well when FBS was decreased by 4% (54% DMEM with proline, methotrexate, 6% FBS and 40% HyCell CHO medium). Moreover, reducing the ratio of the initial medium too slowly will also increase the time cost. Rotation speed is another consideration after cell transfer to the shake flask. Increased rotation speed improves the oxygen transfer rate in the growth medium but also increases the shear stress on cells, which may extend the lag phase. Based on these considerations, a medium adaptation level was designed (**Tables 6.1 and 6.2**). Besides the media gradual adaptation strategy, considering the initial cell density was

also necessary due to the shear stress[24]. The inoculation cell densities in the first T-flask and the first shake flask need to reach a minimum level to promote cell growth and consequently reach the maximum growth phase in the designed days.

6.3.2 ANOVA results

To examine the statistical significance of the factors, an ANOVA was conducted, as shown in **Table 6.3**. P-value Prob> F parameter should be less than 0.05 to be significant. The P-value of 0.0005 of X_1, 0.0003 of X_2, 0.0009 of X_3, and 0.004 of X_5 indicate they are significant in the cell adaptation process. The P-value of X_4 is 0.99, and the P-value of X_6 is 0.56, which indicates they are not significant in the cell adaptation process. Compared with the impact of rotation speed in the shake flask, medium proportion or medium variance during cell adaptation is much more important because cells take time to adapt to changes in culture medium and changes from adherent to suspension type. However, the suspension-type cells in the shake flask are to be rotated on a safety scale (80-150 rpm), which may not impact by the low dissolved oxygen caused by low rotation speed or cell damage caused by fast rotation speed.

6.3.3 Quadratic model

A second-order polynomial model as shown in Equation (6) was used to correlate the experimental data. The quadratic model result for six independents, X_1, X_2, X_3, X_4, X_5 and X_6, outputs are shown in **Table 6.4**, including the regression coefficients of the quadratic polynomial models, and the optimized Y, X_1-X_6. All the response variables shown in Table 4 have the corresponding quadratic response correlation coefficient of determination (R) is 0.93, indicating the regression model was suitable to explain the cell adaptation process. **Fig. 6.3(a)** shows the plot

of predicted versus actual data of the quadratic model, which indicate they are matched well.

Table 6.4. Quadratic model output table

a_{i0}	a_{i1}	a_{i2}	a_{i3}	a_{i4}	a_{i5}	a_{i6}
4.43	-1.21	1.6	1.6	-0.004	-4.85	0.07
Coefficient a_{ij}	a_{1j}	a_{2j}	a_{3j}	a_{4j}	a_{5j}	a_{6j}
a_{i1}	-0.34	0.16	0.29	0.01	0.56	0.01
a_{i2}	0	-0.53	0.31	0.009	0.04	0.006
a_{i3}	0	0	-0.39	-0.01	-0.03	-0.01
a_{i4}	0	0	0	-0.0002	0.002	-0.0006
a_{i5}	0	0	0	0	-0.55	0.01
a_{i6}	0	0	0	0	0	-0.0004
Y_{opt}	X_{1opt}	X_{2opt}	X_{3opt}	X_{4opt}	X_{5opt}	X_{6opt}
7.02	6	4.67	3.37	80	0	100

Note: a_0-a_6 and a-output are the parameters in Equation 6. R is the correlation coefficient. X_{1opt}, X_{2opt}, X_{3opt}, and X_{5opt} represent the optimized condition of the proportion of FBS in the whole medium in T-flask No.2, T-flask No.3, shake flask No.1, and shake flask No.2. X_{4opt} and X_{6opt} represent the optimized conditions of rotation speed in shake flask No.1 and No.2. Y_{opt} represent the optimized condition of cell density.

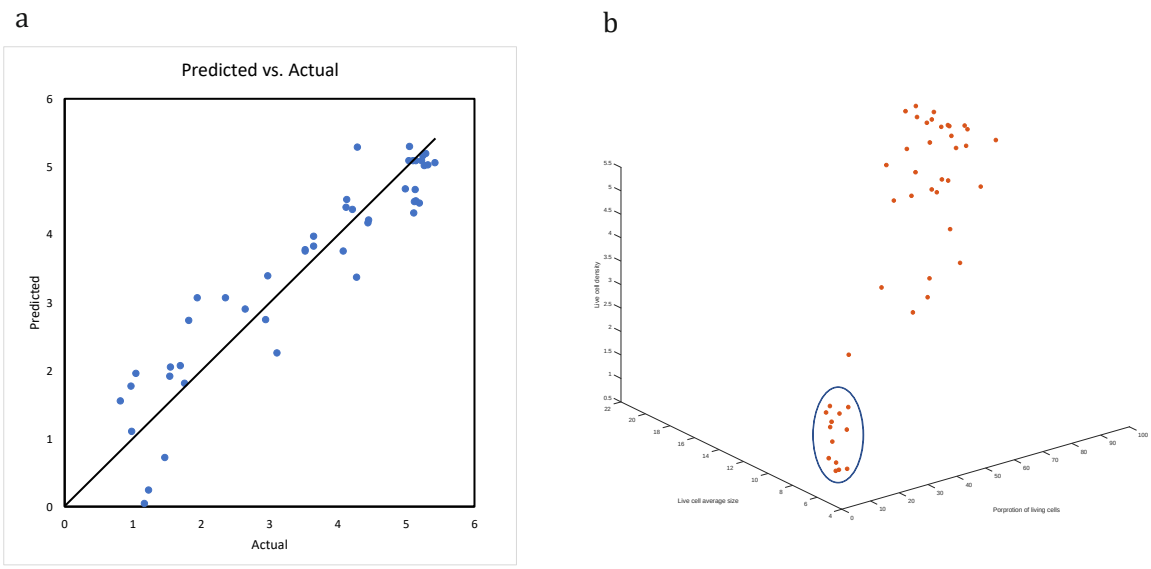

Figure 6.3. (a) The plot of predicted versus actual data of the quadratic model. (b) 3D plot of X: proportion of living cells (%), Y: live cell average size (μm) and Z: live cell density (× 10^5 cells/mL).

In the a-output in **Table 6.4**, $a_{1\times1}$ is -0.34, $a_{2\times2}$ is -0.53, $a_{3\times3}$ is -0.39, $a_{4\times4}$ is -0.0002, $a_{5\times5}$ is -0.55 and $a_{6\times6}$ is -0.0004, they are all less than 0, which indicate X_1-X_6 all has ("local") maximum levels. While a_0 is 4.43, a_1 is -1.21, a_2 is 1.60, a_3 is 1.60, a_4 is -0.004, a_5 is -4.85 and a_6 is 0.07. The absolute value of them multiply by the corresponding X value indicates the importance of each term in the equation to calculate the cell density. Therefore, it can be seen that the terms X_1, X_2, X_3 and X_5 contributed more to the cell density equation. However, X_4 and X_6 contributed less to the cell density equation. The lower X_1 and X_5 selected within the limit, the higher cell density could be reached; the higher X_2 and X_3 selected within the limit, the higher cell density can be reached. Y_{opt} is 7.02 when X_{1opt} is 6, X_{2opt} is 4.67, X_{3opt} is 3.37, X_{4opt} is 80, X_{5opt} is 0 and X_{6opt} is 100. This optimized result showed that: (1) the step from T-flask to shake flask showed a minor change in the proportion of medium than other steps; (2) the cells can adapt to the serum-free

medium one step earlier; (3) the rotational speed of the shake flask can be gradually increased from 80 rpm to 100 rpm to 120 rpm.

6.3.4 RSM results

Optimized transferring CHO cells from adhesion to suspension culture process parameters and their interaction effects on cell density were visualized using RSM. The cell density contour of the quadratic model was visualized by the response surface plots shown in **Fig. 6.4.** Moreover, quadratic response surface plots illustrate the media sequential adaptation strategy in optimizing two media adaptation parameters by keeping other variables at the control (center) point. All the predicted levels of the cell density variables were in the range of the experimental design (**Table 6.1 and 6.2**).

a

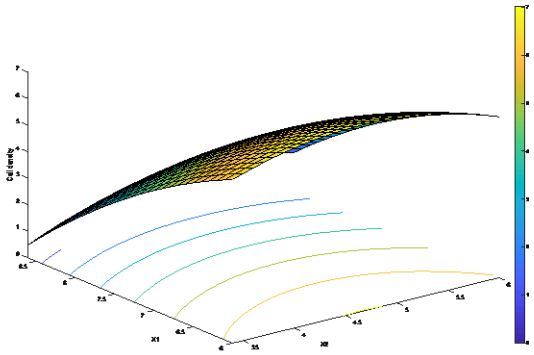

b

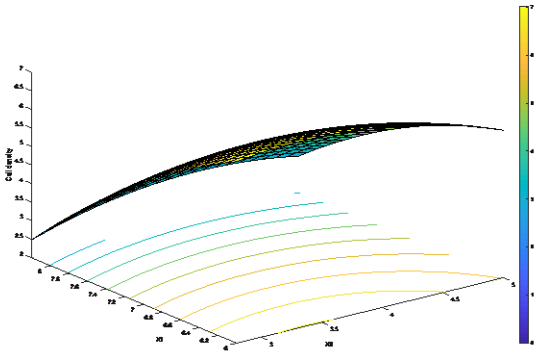

c

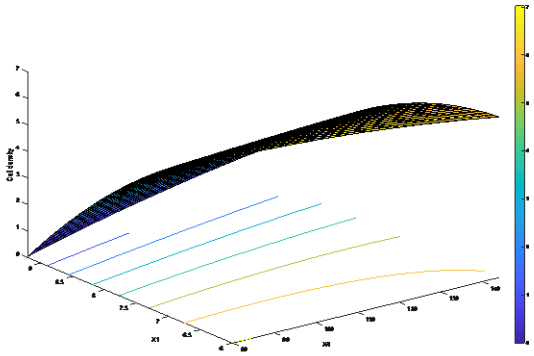

d

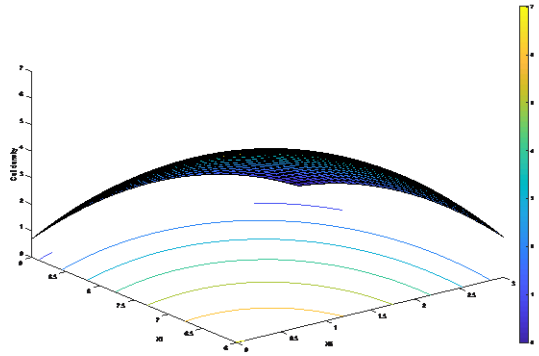

e

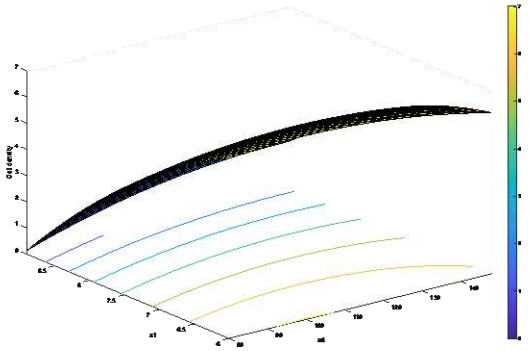

f

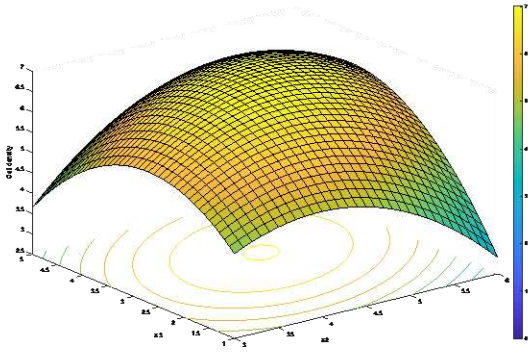

g

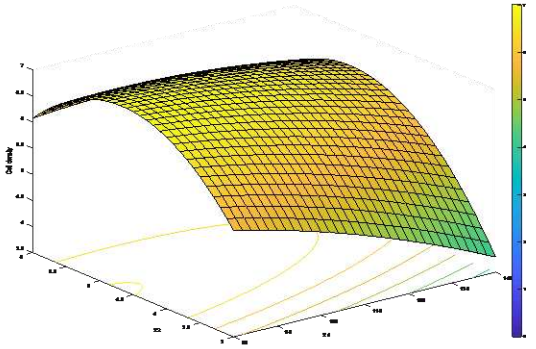

h

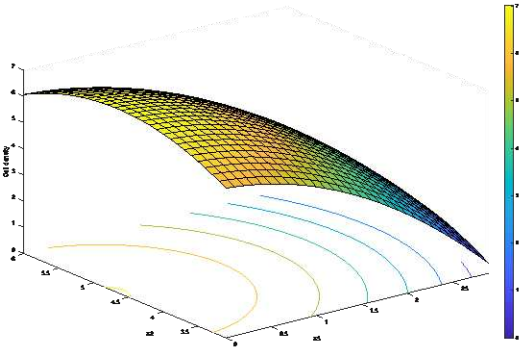

i

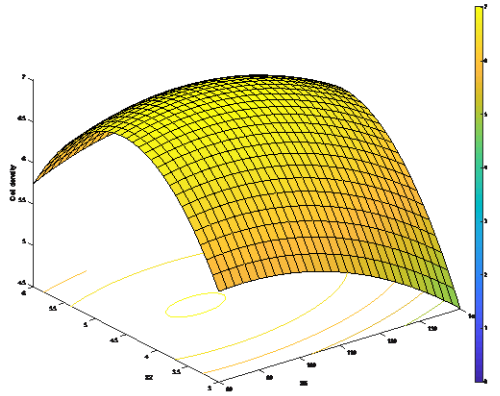

j

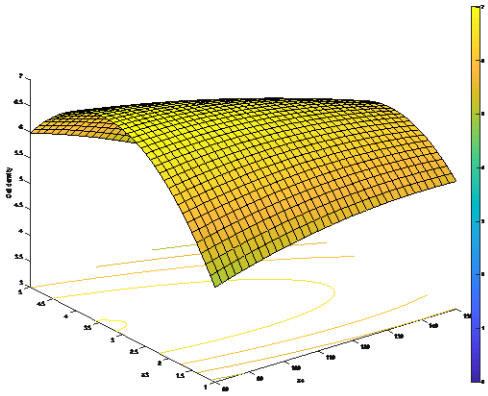

k

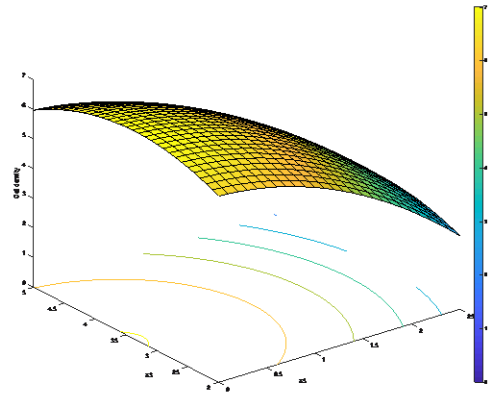

l

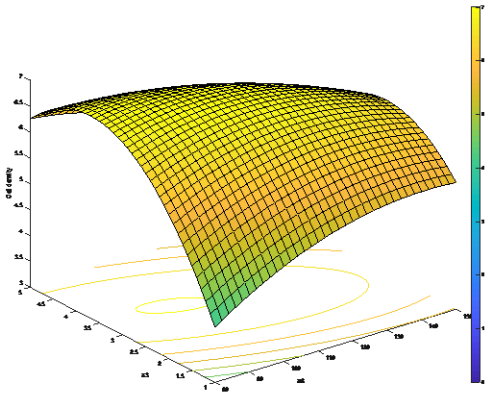

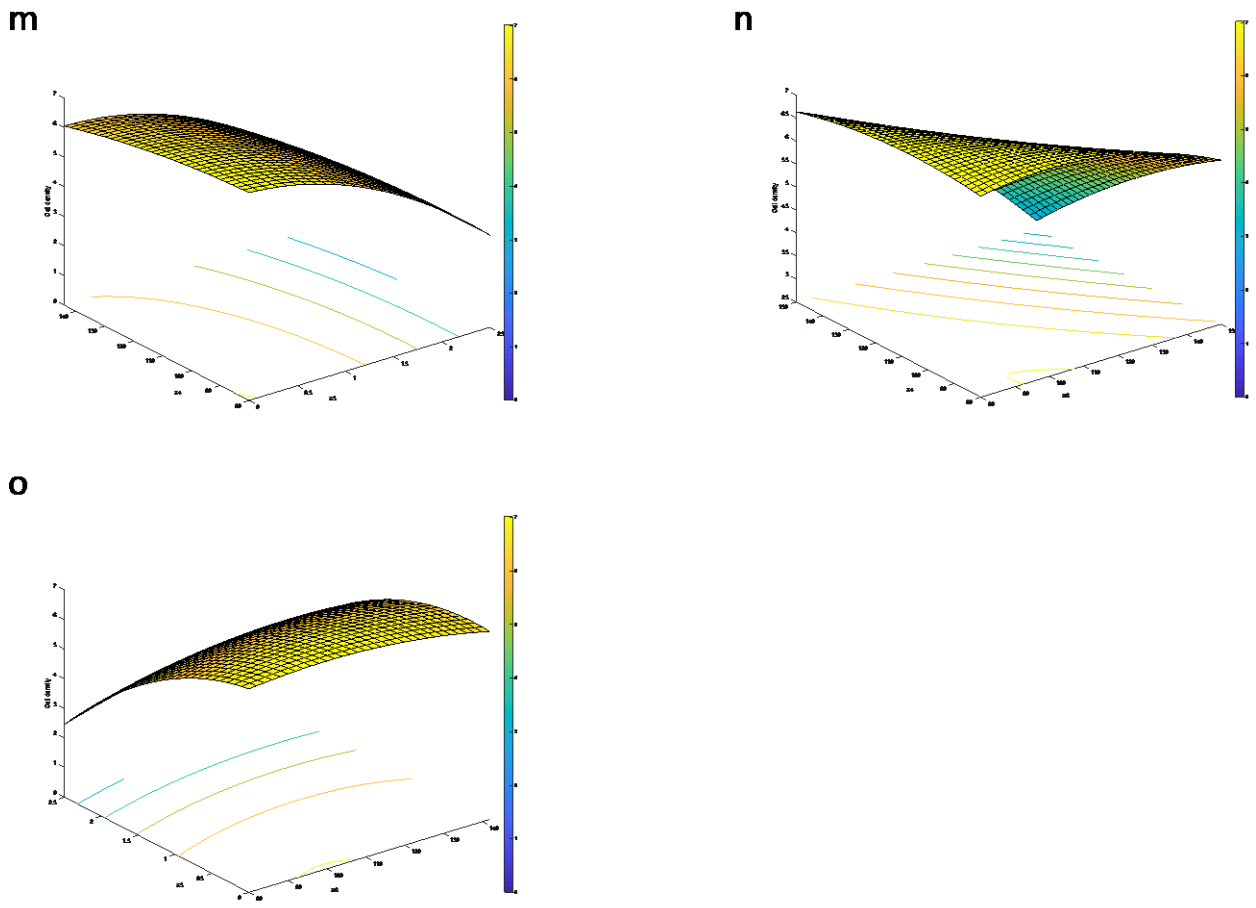

Figure 6.4. Response surface and contour plots showing the interaction effect of X_1 and X_2 (a); X_1 and X_3 (b); X_1 and X_4 (c); X_1 and X_5 (d); X_1 and X_6 (e); X_2 and X_3 (f); X_2 and X_4 (g); X_2 and X_5 (h); X_2 and X_6 (i); X_3 and X_4 (j); X_3 and X_5 (k); X_3 and X_6 (l); X_4 and X_5 (m); X_4 and X_6 (n); X_5 and X_6 (o) on cell density.

Cell density is normalized from 0 to 7.02% by the color bar. As can be seen in **Figure 6.4(a)**, cell density increased with decreasing X_1 while increasing X_2 from 3% to 4.67% or decreasing X_2 from 6% to 4.67%; in **Figure 6.4(b)**, cell density increased with decreasing X_1 while increasing X_3 from 1% to 3.37% or decreasing X_2 from 5% to 3.37%; in **Figure 6.4(c)** cell density

increased with the decrease of X_1 and X_4; in **Figure 6.4(d)** cell density increased with the decrease of X_1 and X_5; in **Figure 6.4(e)** cell density increased with decreasing X_1 while increasing X_6 from 80 rpm to 100 rpm or decreasing X_2 from 150 rpm to 100 rpm. X_2 and X_3 showed the maximum point in the response contour **Figure 6.4(f)**. In **Figure 6.4(g) and (h)**, cell density increased with decreasing X_4 and X_5 while increasing X_2 from 3% to 4.67% or decreasing X_2 from 6% to 4.67%, respectively. In **Figure 6.4(i)**, nearly the whole response surface is shown yellow, which indicates the combined impact of X_2 and X_6 on cell density is not large. In **Figure 6.4(j)** cell density increased with decreasing X_4 while increasing X_3 from 1% to 3.37% or decreasing X_2 from 5% to 3.37%; in **Figure 6.4(k)** cell density increased with decreasing X_5 while increasing X_3 from 1% to 3.37% or decreasing X_2 from 5% to 3.37%. X_3 and X_6 showed the maximum point in the response contour **Figure 6.4(l)**. As shown in **Figure 6.4(m)**, cell density increased gradually with increasing X_4 and X_5. **Figure 6.4(n)** showed some line contours of X_4 higher than 90 rpm while X_6 higher than 135 rpm.

6.3.5 Cell adaptation analysis

Fig. 6.3(b) shows the 3D plot of the proportion of living cells (%), live-cell average size (μm), and live-cell density ($\times 10^5$ cells/mL) for a total of 46 runs. Some runs showed low live-cell density, low live-cell percentage, and small live-cell average size, labeled by a circle. They were runs 2, 3, 4, 5, 6, 7, 12, 18, 28, 29, 30, 31, and 38. From the virtual observation result, runs 2, 3, 4, 5, 6, 18, 28, 29, 30, 31 and 38 were unable to be adapted to T-flask No. 3. Run 7 was unable to be adapted to shake flask No. 1. Run 12 was unable to be adapted to shake flask No. 3. In the controlled time, the cells did not adapt to the new flask/environment and stayed in the lag phase, resulting in low live cell density and low live cell percentage. Some debris caused small live-cell

average size.[25]

6.3.6 Validation of optimum condition

Predicted optimum cell adaptation conditions were confirmed by comparing the measured cell density with the predicted cell density through the model. Triplicate measurements of cell density under the predicted optimum conditions were carried out. Three cell density results were 7.21, 7.08, and 6.99×10^5 cells/mL. All measured cell densities were in the range of the predictive interval (95%) compared with the Y_{opt} 7.02×10^5 cells/mL, which shows the measured cell density matched the predicted cell density well. These results demonstrated that the RSM model and quadratic equations were reliable and could predict the optimal conditions to enhance cell density after the cell adapting serum-free suspension culture.

6.3.7 Validation of cell performance

As shown in **Figure. 6.5**, the CTLA-4-Ig-24 CHO cells successfully transferred from adhesion type (left) to suspension type (right) culturing in the serum-free medium. When transferring the cells from adhesion to suspension, adhesion and suspension cells co-occur under certain conditions.

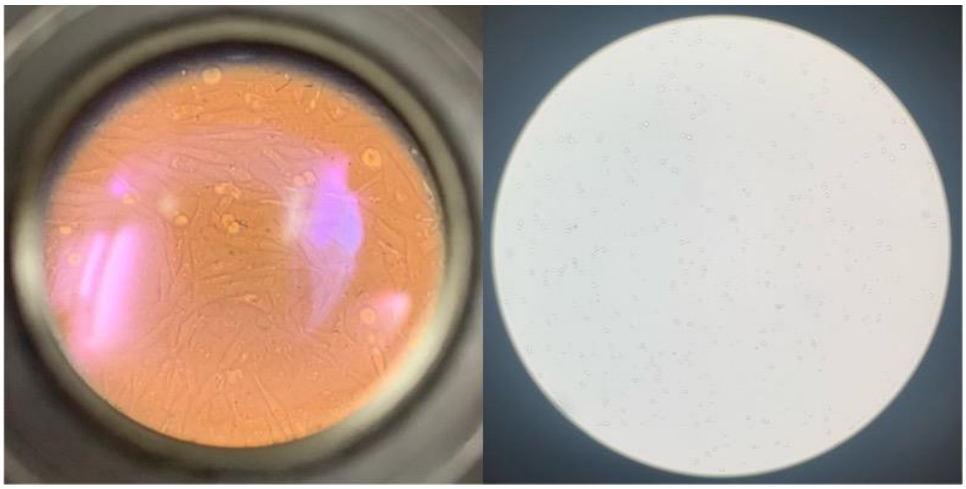

Figure 6.5. CTLA4 Ig-24 CHO cells morphology. Left: in adherent growth in T-flask in DMEM with 0.2 mM proline, 0.001 mM methotrexate + 10% FBS; magnification 2400×. Right: in suspension growth in Erlenmeyer flask in the serum-free medium (Right); magnification 100×.

To validate the suspension cell performance, we selected three fully adaptation cells (run 1-run 43, except run 2, 3, 4, 5, 6, 7, 12, 18, 28, 29, 30, 31 and 38) randomly to run in the bioreactor under fed-batch mode for 14 days. Inoculation cell density is 0.4-0.5 × 10^6 cells/mL. As can be seen in **Fig. 6.6 (a)**, all cell densities reached over 3 × 10^6 cells/mL on day 6, and then all decreased to over 2 × 10^6 cells/mL on day 14. Fusion protein increased gradually from day 1 to day 14 (**Fig. 6.6(b)**). Besides cell performance, we also compared the suspension cell with the original adherent cell. It maintained cell growth characteristics (cell doubling time, cell size, and production rate) before and after adaptation. Thus, the subcultured suspension cell is stable, and its ability to produce fusion protein is also stable. The adapted cells were tested. They support freezing and thawing cycles within a year. Cell growth profile after 30 passages under serum-free suspension conditions are tested with no obvious change.

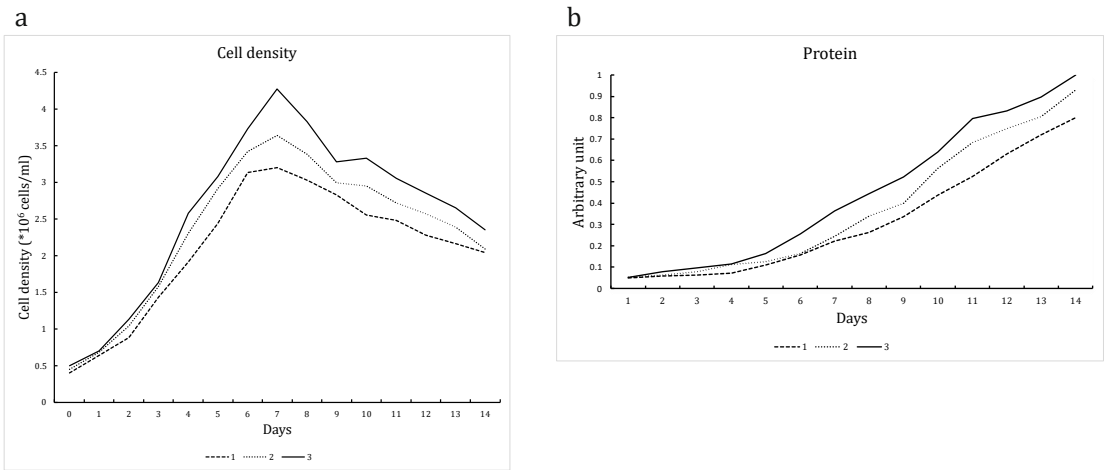

Figure 6.6. Growth profiles of fed-batch culture: (a) viable cell density and (b) arbitrary unit of protein versus culture time. 1, 2 and 3 represent three randomly selected suspension cells.

6.4 Conclusions

This study reports the first application of a new experimental design – SBD, with a quadratic model to optimize the cell density of CTLA-4-Ig-24 CHO cells in adherent culture to suspension serum-free culture. SBD is a seven-level quadratic response experimental design. Six factors were applied in this experimental design with 43 independent runs plus three more repeating center runs.

The corresponding quadratic response correlation coefficient R was 0.93, indicating the regression model represented the experimental data well. The medium and serum ratios were validated to be significant in the cell adaptation process. Cell adaptation optimization by applying RSM for cell density was investigated. The optimized cell adaptation process started from 90% DMEM with 0.2 mM proline, 0.001 mM methotrexate and 10% FBS in the T-flask, transferred to 54% DMEM, 40% serum-free medium with 6% FBS in the next T-flask, then transferred to 42.03% DMEM, 53.3% serum-free medium with 4.67% FBS in the next T-flask, then transferred to 30.33%

DMEM, 66.3% serum-free medium with 3.37% FBS in the shake flask on a rotary shaker at 80 rpm, then transferred to 100% serum-free medium in the next shake flask on a rotary shaker at 100 rpm, finally transferred to 100% serum-free medium in the next shake flask on a rotary shaker at 120 rpm. Accordingly, the optimized sequential cell adaptation strategy and cell performance were validated by additional experiments.

The process of cell adaptation affects cell proliferation in two ways: one is the rotation speed provided to mix the cells and medium. Under low rotation speed, even if the shear stress is low, oxygen may not be enough to support cell breath; while under high rotation speed, the shear stress is a severe problem[26, 27]. Another is media change causes a series of cell metabolism issues. FBS provides vital nutrients, attachment factors, toxin scavengers, and growth factors[28, 29]. The attachment factors include fibronectin and other adhesion-promoting molecules[30]. The decreases in FBS cause some adhesion cells to be unable to adapt to the suspension state. While some cells can adapt to suspension growth, their status is poor. The remaining cells were successfully transferred from the adherent state to the suspended state, and their performance was validated by fed-batch culture.

This study first uses SBD to solve actual problems. From the perspective of experimental design, SBD is a uniform design among all the distributed factors and levels, which are easy to generate the experimental conditions. The level of each factor in the experiment covers the whole design range, and the experimental level is unified with the factor. SBD is an innovative, conventional, and advanced experimental design that can be widely used in fermentation optimization, process development, medium development, etc. For example, the factors can be medium concentration, feed method, pH, DO, temperature, rotation speed, etc. This DoE solves the problem of time-consuming and labor-consuming issues transferring the adherent cells to

serum-free suspension culture.

6.5 References

1. Zhang, J., Mammalian cell culture for biopharmaceutical production. pp. 157-178. In *Manual of industrial microbiology and biotechnology*, A. T. Bull, B. J., L. Katz, L. R. Lynd, P. Masurekar, C. D. Reeves, and H. Zhao, Ed. ASM Press, Washington, USA: 2010.
2. Dumont, J.; Euwart, D.; Mei, B.; Estes, S.; Kshirsagar, R., Human cell lines for biopharmaceutical manufacturing: history, status, and future perspectives. *Critical reviews in biotechnology* **2016,** *36* (6), 1110-1122.
3. Jukić, S.; Bubenik, D.; Pavlović, N.; Tušek, A. J.; Srček, V. G., Adaptation of CHO cells in serum-free conditions for erythropoietin production: Application of EVOP technique for process optimization. *Biotechnology and applied biochemistry* **2016,** *63* (5), 633-641.
4. LeFloch, F.; Tessier, B.; Chenuet, S.; Guillaume, J.-M.; Cans, P.; Goergen, J.-L.; Marc, A., Related effects of cell adaptation to serum-free conditions on murine EPO production and glycosylation by CHO cells. *Cytotechnology* **2006,** *52* (1), 39-53.
5. Wu, S.; Rish, A. J.; Skomo, A.; Zhao, Y.; Drennen, J. K.; Anderson, C. A., Rapid serum-free/suspension adaptation: Medium development using a definitive screening design for Chinese hamster ovary cells. *Biotechnology progress* **2021,** *37* (4), e3154.
6. Brunner, D.; Frank, J.; Appl, H.; Schöffl, H.; Pfaller, W.; Gstraunthaler, G., The serum-free media interactive online database. *ALTEX-Alternatives to animal experimentation* **2010,** *27* (1), 53-62.
7. Rodrigues, M. E.; Costa, A. R.; Henriques, M.; Cunnah, P.; Melton, D. W.; Azeredo, J.; Oliveira, R., Advances and drawbacks of the adaptation to serum-free culture of CHO-K1 cells for monoclonal antibody production. *Applied biochemistry and biotechnology* **2013,** *169* (4), 1279-1291.
8. Zhang, J.; Robinson, D., Development of animal-free, protein-free and chemically-defined media for NS0 cell culture. *Cytotechnology* **2005,** *48* (1), 59-74.
9. Marigliani, B.; Balottin, L. B. L.; Augusto, E. d. F. P., Adaptation of mammalian cells to chemically defined media. *Current Protocols in Toxicology* **2019,** *82* (1), e88.
10. Caron, A. L.; Biaggio, R. T.; Swiech, K., Strategies to suspension serum-free adaptation of mammalian cell lines for recombinant glycoprotein production. In *Recombinant Glycoprotein Production. Methods in Molecular Biology, vol 1674*, Picanço-Castro, V., Swiech, K., Ed. Humana Press, New York, NY: 2018; pp 75-85.
11. Mandenius, C. F.; Brundin, A., Bioprocess optimization using design-of-experiments methodology. *Biotechnology progress* **2008,** *24* (6), 1191-1203.
12. Liu, S., *Bioprocess engineering: kinetics, sustainability, and reactor design*. Elsevier: 2020.
13. Weissman, S. A.; Anderson, N. G., Design of experiments (DoE) and process optimization. A review of recent publications. *Organic Process Research & Development* **2015,** *19* (11), 1605-1633.
14. Beg, S.; Swain, S.; Rahman, M.; Hasnain, M. S.; Imam, S. S., Application of design of experiments (DoE) in pharmaceutical product and process optimization. pp. 43-64. In

Pharmaceutical quality by design: principles and applications. Academic Press, Hasnain, S. B. a. M. S., Ed. London, United Kingdom: 2019.
15. Ferreira, S. L.; Dos Santos, W. N.; Quintella, C. M.; Neto, B. B.; Bosque-Sendra, J. M., Doehlert matrix: a chemometric tool for analytical chemistry. *Talanta* **2004,** *63* (4), 1061-1067.
16. Hibbert, D. B., Experimental design in chromatography: a tutorial review. *Journal of chromatography B* **2012,** *910*, 2-13.
17. Bezerra, M. A.; Santelli, R. E.; Oliveira, E. P.; Villar, L. S.; Escaleira, L. A., Response surface methodology (RSM) as a tool for optimization in analytical chemistry. *Talanta* **2008,** *76* (5), 965-977.
18. Giovanni, M., Response surface methodology and product optimization. *Food technology* **1983**.
19. Baş, D.; Boyacı, I. H., Modeling and optimization I: Usability of response surface methodology. *Journal of food engineering* **2007,** *78* (3), 836-845.
20. Takahashi, T.; Tagami, T.; Yamazaki, S.; Uede, T.; Shimizu, J.; Sakaguchi, N.; Mak, T. W.; Sakaguchi, S., Immunologic self-tolerance maintained by CD25+ CD4+ regulatory T cells constitutively expressing cytotoxic T lymphocyte–associated antigen 4. *The Journal of experimental medicine* **2000,** *192* (2), 303-310.
21. McCoy, K. D.; Le Gros, G., The role of CTLA-4 in the regulation of T cell immune responses. *Immunology and cell biology* **1999,** *77* (1), 1-10.
22. Fallarino, F.; Grohmann, U.; Hwang, K. W.; Orabona, C.; Vacca, C.; Bianchi, R.; Belladonna, M. L.; Fioretti, M. C.; Alegre, M.-L.; Puccetti, P., Modulation of tryptophan catabolism by regulatory T cells. *Nature immunology* **2003,** *4* (12), 1206-1212.
23. Wang, J.; Huang, J.; Guo, H.; Jiang, S.; Qiao, J.; Chen, X.; Qu, Z.; Cui, W.; Liu, S., Effects of different sodium salts and nitrogen sources on the production of 3-hydroxybutyrate and polyhydroxybutyrate by Burkholderia cepacia. *Bioresources and Bioprocessing* **2021,** *8* (1), 1-14.
24. Renner, W.; Jordan, M.; Eppenberger, H.; Leist, C., Cell–cell adhesion and aggregation: influence on the growth behavior of CHO cells. *Biotechnology and bioengineering* **1993,** *41* (2), 188-193.
25. Seewöster, T.; Lehmann, J., Cell size distribution as a parameter for the predetermination of exponential growth during repeated batch cultivation of CHO cells. *Biotechnology and bioengineering* **1997,** *55* (5), 793-797.
26. Hwang, K.-J.; Lin, S.-J., Filtration flux–shear stress–cake mass relationships in microalgae rotating-disk dynamic microfiltration. *Chemical Engineering Journal* **2014,** *244*, 429-437.
27. Choi, Y.; Morgenroth, E., Monitoring biofilm detachment under dynamic changes in shear stress using laser-based particle size analysis and mass fractionation. *Water Science and Technology* **2003,** *47* (5), 69-76.
28. Bieback, K.; Hecker, A.; Schlechter, T.; Hofmann, I.; Brousos, N.; Redmer, T.; Besser, D.; Klüter, H.; Müller, A. M.; Becker, M., Replicative aging and differentiation potential of human adipose tissue-derived mesenchymal stromal cells expanded in pooled human or fetal bovine serum. *Cytotherapy* **2012,** *14* (5), 570-583.
29. Honn, K. V.; Singley, J. A.; Chavin, W., Fetal bovine serum: a multivariate standard. *Proceedings of the Society for Experimental Biology and Medicine* **1975,** *149* (2), 344-347.

30. Hayman, E. G.; Pierschbacher, M. D.; Suzuki, S.; Ruoslahti, E., Vitronectin—a major cell attachment-promoting protein in fetal bovine serum. *Experimental cell research* **1985,** *160* (2), 245-258.

Chapter 7: Summary and Outlook

This dissertation researched adjusting the preparation pH, or temperature can resolve the issues with media precipitation. Also researched, an elevated preparation pH can maintain solubility when basal powder and AA concentrations are further increased. Two mechanisms have happened during the high-concentration media storage. One is precipitation, and the other is degradation. Medium preparation parameters are used to improve AA stability and mitigate precipitation issues. Raman and FTIR spectroscopy were used to compare and ascertain the quality of the cell culture medium under different treatment and different storage conditions. EEM spectroscopy was used to monitor fluorescent molecules' characteristics in a cell culture medium. Raman, EEM and FTIR were compared to evaluate the cell culture media quality by PCA. After that, the Raman and FTIR data were used to build two screen models for media quality evaluation. Cell culture performance results are the same as the PAT results. Besides cell culture media optimization, a new design of experiments – superlative box design, was adopted to optimize the adaptation of Chinese hamster ovary cells from adhesion culture to serum-free suspension culture. Experiments validated the predicted cell adaptation with the maximum cell density. This study provides an efficient method to transfer adherent cells to suspension cells and is the first to use SBD and successfully establish a parameter quadratic optimization model.

After this work, Raman and FTIR can be used for online monitoring of the concentration of important cell culture media components by PLS. Superlative box design can use for production process development. For example, the factors include medium concentration, feed method, pH, DO, temperature, rotation speed, etc.

Resume

WANYUE CUI

CONTACT INFORMATION
Email: wcui04@syr.edu Telephone number: 315-480-2015
LinkedIn: https://www.linkedin.com/in/wanyue-cui-542a60158/

EDUCATION

The State University of New York College of Environmental Science and Forestry
Syracuse, NY 8/2018 – 5/2023
Ph.D. Candidate - Chemical Engineering / GPA:3.7
Research project:

- Mammalian cell culture and production. Bioreactor, fermenter, shake tube and shake flask operation (5 years). (Manuscript under review)
- Fermentation process development and optimization of CHO cell production conditions (medium, pH, DO, temperature and rotation).
- Used multiple Process Analytical Technology (PAT) tools, including high-performance liquid chromatography (HPLC), nuclear magnetic resonance (NMR), ELISA and Fourier-transform infrared spectroscopy (FTIR) to test the metabolic of cell culture and production. Used SAS and MATLAB to analyze the data.
- Devised and applied a new design of experiments (DoE) – superlative box design for cell culture and production processes optimization, and subsequently wrote its quadratic model program in MATLAB and Excel file.

Achievements:

- Fellow Scholarship and Graduate Assistantship from 2018 to 2023
- Excellence in Research Award for the year 2022
- Excellence in Teaching Award for the year 2021
- Shastri Graduate Award for the year 2020

Dual BS Degrees 8/2014 – 5/2018
The State University of New York College of Environmental Science and Forestry, Syracuse, NY
BS - Bioprocess Engineering / GPA:3.7
Beijing University of Chemical Technology, Beijing, China
BS - Pharmaceutical Engineering

WORK EXPERIENCES

Project Intern, *Bristol Myers Squibb,* Devens, MA 6/2022 – 8/2022

- Upstream development. Prepared over 300 types of cell culture media under different conditions and developed a cell culture media screen model for the team to evaluate the quality of unknown media by FTIR and Raman spectroscopy. (Manuscript in preparation)

- Compared multiple PAT tools, including in situ Raman, excitation-emission matrix (EEM), and FTIR under different media preparation conditions on media stability by Principal component analysis (PCA) in MATLAB.
- Used Tecan subsequent CHO cell culture performance under fed-batch mode for over 200 reactions to validate the application of PAT.

Summer Intern, *Bristol Myers Squibb,* Remote 6/2021 – 8/2021

- Wrote a manuscript about perfusion media development for CHO cell culture manufacturing. (Manuscript under peer review)
- Summarized CHO cell culture media development in the past 20 years.

Project Intern, *Bristol Myers Squibb,* Devens, MA 6/2019 – 8/2019

- Upstream development. Including the use of shake flasks, wave bioreactors and perfusion bioreactors. Sampling by Cedex daily.
- Researched the impact of preparation conditions on amino acid (AA) stability of highly concentrated cell culture feed media. Used PCA to evaluate AA stability. (paper published)
- Used multiple assays to evaluate the stability of basal media and feed media, including dynamic light scattering (DLS), EEM, Raman, UV-Vis, HPLC, Roche Cedex, ICP, osmometer, and turbidimeter. All data were processed and analyzed by me.

Graduate Assistant – Chemical Engineering, *SUNY-ESF,* Syracuse, NY 8/2018 – 5/2023

Bioprocess Kinetics and Systems Engineering– Lecture course

- Teaching assistant (TA) to the undergraduate senior-level course BPE 421 Bioprocess Kinetics and Systems Engineering presented by Dr. Shijie Liu during Fall 2018.
- Held exam help-sessions and office hours to assist and mentor students with exam preparation and to tackle assignments.
- Assisted faculty members with classroom instructions, record keeping, and other projects.
- Prepared grading rubrics and graded exams and homework assignments.
- Skillfully apply the kinetics learned in this course to deal with the practical problems.

Bioprocess Kinetics and Systems Engineering Lab– Lab course

- Led TA for BPE 440 Bioprocess Kinetics and Systems Engineering Lab by Dr. Shijie Liu during Spring 2019.
- Designed and improved the five lab experiments, they are enzymatic hydrolysis of cellulose, batch enzyme reactor reaction, cell batch growth kinetics, catalytic reactor reaction, and biogas production.
- Independently prepared and delivered all classroom and lab experiments.
- Led a team of teaching assistants to organize and execute lab classes and fostered a respectful lab environment.

Cell Culture – Lab course

- Taught undergraduate students and graduate students CHO cell culture and production technology.
- Guided student use DoE to optimize the parameters of cell culture.

PROFESSIONAL SKILLS

- Expert user of Excel, Word, and PowerPoint.
- Working knowledge to use instruments and detection methods: FTIR, Tecan, EEM, Raman, ELISA, PCR, RT-PCR, UV-Vis, SEM, HPLC and NMR.

- Working knowledge to use data analytics methods such as: ANOVA, MANOVA, PCA, PLS, Hotelling T^2 test and PARAFCA.
- Software: Proficient in MATLAB, SIMCA, Solo, Origin, SAS and Minitab. Highly professional in coding.

PUBLICATIONS AND PRESENTAION

- Cui, Wanyue, et al. "Impact of preparation pH and temperature on amino acid stability of highly concentrated cell culture feed media." *Journal of Chemical Technology & Biotechnology* (2022).
- The American Institute of Chemical Engineering (AIChE) at the Phoenix Convention Center, Phoenix, AZ (2022). Oral presentation: Transferring CHO cells from monolayer to suspension culture by a new design of experiments – superlative box design. Presenter: Wanyue Cui.